Mixed Forest plantation: managing complexity under climate change and innovative silvicultural approaches.

By

Andrea Rabbai

A thesis submitted to
the University of Birmingham
for the degree of
DOCTOR OF PHILOSOPHY

Water science research group
School of Geography, Earth and Environmental Sciences
College of Life and Environmental Sciences
University of Birmingham
March 2024

Abstract

Mixed forests are receiving increased attention globally. Their potential to contribute to adaptation and mitigation of climate change by improving resilience is considered an opportunity to highlight the role of tree species diversity within complex socio-ecological systems. However, there is a lack of a theoretical framework for effectively managing mixed forests. This thesis aims to advance our understanding of mixed forest management in the face of climate change while investigating active methods to improve forest productivity and carbon sequestration. In the initial study, the hydrological functions of a young mixed forest were compared to those of a mature forest over a five-year period, focusing on their responses to drought conditions. Results revealed that drought events can trigger adaptive responses in a young mixed forest, potentially driven by the diverse water acquisition strategies of different trees, resulting in significant changes in soil moisture levels. These findings also highlight the challenges of climate change-induced droughts for newly planted forests in temperate regions, emphasizing the need for careful management strategies. We further investigate alternative management practices for a four-year old mixed forest plantation, with the combined application of fertilizer and irrigation though to reduce drought susceptibility while enhancing carbon sequestration. Findings indicate an overall increment in tree growth after applying fertilizer and irrigation, although significant variations across species are attributable to the complex site hydrological conditions. In addition, evaluation of the influence of fertilizer application revealed significant alteration of soil greenhouse gas emissions such as carbon dioxide (CO_2), nitrous oxide (N_2O), and methane (CH_4). This assumes critical importance within the context of afforestation and reforestation initiatives aimed at mitigating climate change. It also underscores the uncertainties of long-term viability of irrigation and fertilization, indicating that these intensive management practices may need to be temporary or site-specific. In summary, these results advance our understanding of managing mixed-forest plantations considering the influence of drought and active management. Findings highlight the substantial impact of intensive fertilization and irrigation on tree

growth and the GHG balance within mixed-forest ecosystem, emphasizing the need for sustainable management practices.

Dedication

This work is dedicated to all the curios minds driven by passion for the fascinating world of forests.

May you read the acknowledgements and then show interest – read the abstract, introduction, and conclusions- or plunge into the complexity of forest management and read all.

Acknowledgements

First of all, I would like to thank Stefan Krause, Nicholas Kettridge, and Sami Ullah for their supervision. Many thanks for the encouraging meetings, patience, and feedback on my work and dedication to the research. I would also like to thank Giulio Curioni, Adriane, and Bruno for their help and guidance along the way in GEES.

The last four years have been more than challenging, with the pandemic, the loneliness, and the continuous thought of achieving the PhD. But I've been lucky. Along the way, I discovered not only the pleasure of working as a scientist but also a few people that I can properly call friends. I would like to thank Fabio, Ilaria, Yiannis, Marco C., Khuram, Eleonora, Giulia, Anna, Alessandra, Enrico, Davide, Marco, Filippo who became my second family here in Birmingham, helping me through many difficult times that they did not even imagine. I would like to thank Matt O'Callaghan, my Irish friend always being present with good words and thoughts. A person of rare kindness who, with his allotment, knowledge, friends, and stories, made me appreciate any moment in England. I owe another thank you to Kris Hart, who sustained me along the path of my PhD, becoming my mentor and, most importantly, my friend.

I'd also like to thank all my peers in Gees, knowing that the pandemic did limit our possibility of enjoying this adventure together. Adriá, Doris, Manon, Aaron, Grace, Dom, Alex, and all the people with whom I had lovely moments in the last four years. A special thanks to Ben who helped me a lot during the first few months in Birmingham through many talks and walks.

A big thanks to my Italian friends, especially the ones who visited!! A warm hug to Francesco and Eleonora, and the new arrived Edoardo, to whom I wish a life full of wonder.

I want to express my heartfelt gratitude to my family Luigi, Marcella, Sergio, Silvia, Ethan, and Victoria who gave me the possibilities to achieve something that I would never imagine possible. And I cannot forget to give a profound thanks to Tamara who bravely stood by my side all these years. My love and devotion go entirely to her. Despite the challenges of the organization and long-tiring travels, she has always taught to me how to find the beauty in every little thing.

I am grateful for the financial support of JABBS Foundation and the University of Birmingham

List of papers

The following three papers form the basis of this thesis:

Chapter Two:

Rabbai, A., Wendt, D.E., Curioni, G., Quick, S.E., MacKenzie, A.R., Hannah, D.M., Kettridge, N., Ullah, S., Hart, K.M., Krause, S., (2023). Soil moisture and temperature dynamics in juvenile and mature forests as a result of tree growth, hydrometeorological forcings, and drought. *Hydrological Processes*, 37(6), e14919, doi: 10.1002/hyp.14919

Chapter Three:

Rabbai, A., Curioni, G., Kettridge, N., Ullah, S., Krause, S.: Fertigation management of forest plantations: key aspects, challenges, and future perspectives". *In submission.*

Chapter Four:

Rabbai, A., Barba, J., Canducci, M., Hart, M.K., MacKenzie, A.R., Kettridge, N., Curioni, G., Ullah, S., Krause, S.: Fertilization-induced greenhouse gas emissions may partially offset carbon sequestration during afforestation. *In submission.*

Contents

List of Figures

List of Tables

Chapter One

Introduction

1.1 Background

Nearly one-third of the earth land area is covered by forests. Natural forests represent 93% of the total global forest area, with an annual decrease of 1.3 million hectares observed between 2010 and 2015. The remaining 7% of the forest area is occupied by planted forests, which have shown from 1990 to 2015 an average annual expansion of 3.1 million hectares (FAO 2015). Thus, the reduction in global forest cover is partially offset by an increase in the area of planted forests, which have also contributed to meeting the demand for timber worldwide over the past three decades (Warman, 2014). Planted forests have become a significant source of roundwood, accounting for 33% of the total timber supply chain. Projections suggest that by 2040, they will meet 50% of global timber demand (Kanninen, 2010; Jurgensen et al., 2014). However, forests encompass a wider range of benefits for human societies beyond timber production. The concept of ecosystem services (ES) has gained prominence over the past years, shaping the public perception of forests. The increased awareness of the inherent value of forests has led to a growing demand for regulatory services such as carbon sequestration and water quality, along with cultural services such as recreation and spiritual values (FAO, 2010). In this context, forest plantations emerge as a viable

option, capable of providing a diverse range of goods and sustainable ecosystems that may contribute to biodiversity preservation, soil health, and the well-being of local communities (Wang et al., 2022; TEEB, 2010). Consequently, international policies such as the Bonn Challenge and the New York Declarations, along with national initiatives like the UK pledged to plant 30.000 hectares of new woodland as part of its net-zero strategy (Burton et al., 2018; Committee on Climate Change, 2020), have underscored the importance of forests ecosystems. The Reducing Deforestation and Forest Degradation (REDD+) programme of the United Nations Framework Convention on Climate Change (UNFCC) and the Clean Development Mechanism (CDM) of the Kyoto Protocol further highlighted the potential role of native and plantation forests to curb anthropogenic greenhouse gas emissions (GHG) (Gullison et al., 2007). Therefore, afforestation and reforestation initiatives hold significant promise in mitigating climate change by capturing and storing atmospheric carbon, while also providing essential ecological services to society and the environment (Baral et al., 2016, Bauhus et al., 2010). However, several trade-offs and caveats should be considered while managing this natural capital in a sustainable way. Competition with agricultural land, tree species selection, historical land use, high potential water demand, globalised tree disease, and climate change (Lewis et al., 2019; Smith et al., 2016; Smith et al., 2019) represent only a part of the challenges that managing forest plantations may face. The different forms of afforestation and reforestation then introduce an additional layer of complexity. Monocultures are the most common types of forest plantations and are largely employed for timber and fibre production, as well as for restoring watersheds or degraded landscapes to improve water quality (Minhas et al., 2015). Monocultures, which are frequently composed of fast-growing exotic species, are characterized by rapid carbon accumulation and easy management due to their uniform structures (Liu et al., 2018). Tree species are mostly even aged and planted at high density in accessible areas, facilitating treatment and harvesting operations. However, despite their widespread adoption, mounting criticisms highlighted the inherent problems associated with their management. Monocultures, primarily driven by economic interests, pose various environmental concerns, including loss of soil fertility, disruption of hydrological cycles, introduction

of non-native species, loss of biodiversity, and vulnerability to biotic and abiotic stress such as windthrow and bark beetles (Millar et al., 2007; Bowyer, 2006; Hurley et al., 2017; Liu et al., 2018).

On the other hand, a growing body of research suggests that forests with greater species diversity can provide more social and environmental advantages (Warner et al., 2023; Forrester et al., 2005; Hartley, 2002). This awareness has already led to significant shifts from monoculture to “climate-smart” mixed forests, especially in temperate regions (Palacios-Agundez et al., 2015; Liu et al., 2018). Evidence shows that greater tree species diversity can enhance stand-level productivity and carbon sequestration (Werner et al., 2024; Warner et al., 2023; Feng et al., 2022; Liu et al., 2018). The enhanced productivity compared to monocultures in similar environments often referred to as “overyielding” (Ammer, 2019; Lwila et al., 2021), is driven by several mechanisms. These include *competitive reduction* (when inter-specific competition is lower than intra-specific competition), *facilitation* (wherein one or multiple species within the mixed-species stand facilitate the survival or growth of other species), and *growth-stabilizing effects* (when the growth of one species compensates for productivity loss of other species due to abiotic or biotic stresses) (Forrester & Pretzsch, 2015; Schnabel et al., 2021). For instance, intraspecific competition may limit crown expansion in monocultures (Pretzsch and Schütze, 2016), whereas mixed species stands encourage complementarity and better space utilization due to the different phenological and adaptive growth patterns of the various species (Martin-Blangy et al., 2023; Seidel et al., 2011). Belowground, mixed species stands promote root stratification, which may promote higher nutrient acquisition capacity along with complementarity, root physiology, and interactions with mycorrhizal symbionts (Lwila et al., 2021; Kinzinger et al., 2024). Mixed forests exhibit also greater resistance and resilience to changing climate (FAO, 2023) and damages caused by severe weather events, insects, or disease (Pardos et al., 2021; Lewis et al., 2019; Hartley, 2002).They represent a clear example of complex adaptive systems, where the interactions among various species create feedback loops, allowing for adaptability to changing environmental conditions (Messier et al., 2019; Puettmann et al., 2009). Aesthetic and

recreational values (Carnol et al., 2014), along with increased biodiversity, are only a few of the other advantages offered by mixed plantations. Therefore, recommendations for providing essential ES while addressing climate change through forest management emphasize the avoidance of monocultures, favouring restoration and forest diversification (del Río et al., 2022; Di Sacco et al., 2021).

Nevertheless, despite the potential for social and environmental benefits, the adoption of mixed-species plantations by companies and landowners remained particularly limited. While expanding species portfolio can act as an insurance against the uncertainties of climate change (Bolte et al., 2009; Keenan, 2015), perceived higher costs continue to hamper the widespread design of mixed species stands (Coll et al., 2018). The greater diversity of tree species increases the complexity of silvicultural systems and forest management, leading to differentiated production cycles and a wider range of wood products that need specific market focus. Despite these challenges and the need for immediate solutions, a consistent theoretical framework for managing mixed stands remains largely lacking (Bravo-Oviedo et al., 2018; Coll et al., 2018). Overcoming these barriers requires a concerted effort to develop a comprehensive understanding of mixed-plantation management. This involves bridging existing knowledge gaps through research and experimentation while simultaneously raising awareness of the advantages associated with mixed species stands. These benefits extended beyond the timber supply chain, including crucial contributions to carbon storage and ecosystem resilience in the face of climate change. In this context, the objective of this thesis is to advance the understanding of mixed plantation management amidst climate change and investigate innovative methods which include the combined application of fertilizer and irrigation aimed to improve forest productivity while reducing limitations due to abiotic factors. Focusing on local-scale management strategies and their outcomes may provide crucial insights for scaling up sustainable afforestation and reforestation practices globally. Given the key role of forests in global climate mitigation, the study of these novel management practices is of paramount importance.

In particular, Chapter One analyses the changes over time in the hydrological function of a young mixed plantation in comparison to a mature forest ecosystem in response to drought conditions. Results indicate that droughts can trigger adaptive responses within the mixed forest plantation, resulting in soil moisture levels that align with those observed in the mature forest. Furthermore, the chapter highlights the significance of drought in influencing the hydrological functions in young mixed plantations, representing a new challenge in the context of climate change in temperate regions. This is a crucial aspect to consider when predicting the outcome of afforestation and reforestation schemes. Chapter Two, on the other hand, provides several recommendations for managing mixed-species plantations under intensive practices involving irrigation and fertilization. The relationship between site suitability, irrigation, and species selection is explored, highlighting how hydrological complexities can play a key role in shaping the overall response of the forest system to active management. The outcomes emphasize the importance of careful site assessment to optimize the effectiveness of afforestation initiatives. Finally, Chapter Three, analyses the possible adverse effects of fertilizer application through irrigation system on soil GHG emissions, which assumes critical importance given the role that mixed-forest plantations play in mitigating climate change. The findings show how the combined use of irrigation and fertilizer significantly altered CO_2, N_2O, and CH_4 emissions, thereby offsetting carbon sequestration during afforestation. This study emphasizes the importance of considering appropriate management of mixed-species plantations according to the site history to ensure the provision of appropriate ecosystem services and optimise C sequestration potential.

References

Ammer, C. (2019). Diversity and forest productivity in a changing climate. *The New Phytologist*, 221, 50-66, doi: 10.1111/nph.15263.

Baral, Himlal, Guariguata, Manuel R., Keenan, Rodney J. (2016). A proposed framework for assessing ecosystem goods and services from planted forests. *Ecoystem services*, Volume22, Part B, 260-268, doi: 10.1016/j.ecoser.2016.10.002.

Bauhus, J., Pokorny, B., Van der Meer, P., Kanowski, P.J., Kanninen, M (2010). Ecosystem goods and services – the key for sustainable plantations. Ecosystem Goods and Services from Plantation Forests, Earthscan, London, UK (2010).

Bolte, A., Ammer, C., Löf, M., *et al* 2009. Adaptive forest management in central Europe: climate change impacts, strategies and integrative concept. *Scandinavian Journal of Forest Research*, 24, 73-482, doi: 10.1080/02827580903418224.

Bowyer, J.L., 2006. Forest plantations threatening or saving natural forests? *Arborvitae (IUCN/WWF Forest Conservation Newsletter)*, 31, 8-9.

Bravo-Oviedo, A., Pretzsch, H., del Río, M. (2018). Dynamics, Silviculture and Management of Mixed Forests. *Spring Cham*, 1568-1319, doi:10.1007/978-3-319-91953-9.

Burton, V., Moseley, D., Brown, C., Metzeger, M.J., Bellamy, P., 2018. Reviewing the evidence base for the effects of woodland expansion on biodiversity and ecosystem service in the United Kingdom. *Forest Ecology Management*, 430, 366-379, doi:10.1016/j.foreco.2018.08.003.

Carnol, M., Baeten, L., Branquart, E., Grégoire, J.C., Heughebaert, A., Muys, B., Ponette, Q., Verheyen, K., 2014. Ecosystem services of mixed forest stands and monocultures: comparing practicioners' and scientists' perceptions of with formal scientific knowledge. *Forestry: An International Journal of Forest Research*, 87, 639-653, doi:10.1093/forestry/cpu024.

Coll, L., Ameztegui, A., Collet, C., Magnus, L., Mason, B., Pach, M., Verheyen, K., Abrudan, I., Barbati, A., Barreiro, S., Bielak, K., Bravo-Oviero, A., Ferrari, B., Govedar, Z., Kulhavy, J., Lazdina, D., Metslaid, M., Mohren, F., Pereira, M., Peric, S., Rasztovits, E., Short, I., Spathelf., P., Sterba, H., Stojanovic, D., Valsta, L., Tzvetan, Z., Ponette, Q., 2018. *Forest Ecology and Management*, 407, 106-115, doi:10.1016/j.foreco.2017.10.055.

Del Río, M., Pretzsch, H., Ruiz-Peinado, R., Jactel, H., Coll, L., Löf, M, Aldea, J., Ammer, C., Avdagić, A., Barbeito, I., Bielak, K., Bravo, F., Brazaitis, G., Cerny, J., Collet, C., Condés, S., Drössler, L., Fabrika, M., Heym, M., Holm, S., Hylen, G., Jansons, A., Kurylyak, V., Lombardi, F., Matović, B., Metslaid, M., Motta, R., Nord-Larsen, T., Nothdurft, A., den Ouden, J., Pach, M., Pardos, M., Poeydebat, C., Ponette, Q., Pérot, T., Reventlow, D.O.J., Sitko, R., Sramek, V., Steckel, M., Svoboda, M., Verheyen, K., Vospernik, S., Wolff, B., Zlatanov, T., Bravo-Oviedo, A., 2022. Emerging stability of forest productivity by mixing two species buffers temperature destabilizing effect. *Journal of Applied Ecology*, 1-12, doi:10.1111/1365-2664.14267.

Di Sacco, A., Hardwick, K.A., Blakesley, D., Brancalion, P.H.S., Breman, E., Cecilio Rebola, L., Chomba, S., Dixon, K., Elliot, S., Ruyonga, G., Shaw, K., Smith, P., Smith, R.J., Antonelli, A., 2021. Ten golden rules for reforestation to optimize carbon sequestration, biodiversity recovery and livelihood benefits. *Global Change Biology*, doi:10.1111/gcb/15498.

FAO, 2023. Towards more resilient and diverse planted forests. Rome: FAO.

FAO, 2015. Global forest resource assessment 2015. How are the world's forests changing? FAO, Rome

FAO, 2010a. Global Forest Resources Assessment 2010.Terms and Definitions. FRA Working Paper 144. Rome, Italy, 27p.

Feng, Y., Schmid, B., Loreau, M., Forrester, D.I., Fei, S., Zhu, J., Tang, Z., Zhu, J., Hong, P., Ji, C., Shi, Y., Su, H., Xiong, X., Xiao, J., Wang, S., Fang, J., 2022.

Multispecies forest plantations outyield monocultures across a broad range of conditions. *Science*, 376, 865-868, doi: 10.1126/science.abm6363.

Forrester, D.I., Pretzsch, H., 2015. Tamm Review: On the strength of evidence when comparing ecosystem functions of mixtures with monocultures. *Forest Ecology Management*, 356, 41–53, doi: 10.1016/j.foreco.2015.08.016.

Forrester, D.I., Bauhus, J., Cowie, A.L., 2005. On the success and failure of mixed-species tree plantations: lessons learned from a model system of *Eucalyptus globulus* and *Acacia* mearnsii. *Forest Ecology Management*, 209, 147-155, doi: 10.1016/j.foreco.2005.01.012.

Freer-Smith, P., Muys, B., Bozzano, M., Drössler, L., Farrelly, N., Jactel, H., Korhonen, J., Minotta, G., Nijnik, M., Orazio, C. 2019. Plantation forests in Europe: challenges and opportunities. From Science to Policy 9. European Forest institute, 53, doi:10.36333/fs09.

Gullison, R.E., Frumhoff, P.C., Canadell, J.G., Field, C.B., Nepstad, D.C., Hayhoe, K., Avissar, R., Curran, L.M., Friedlingstein, P., Jones, C.D., Nobre, C., 2007. Tropical Forests and Climate Policy. *Science*, 316, 985-986, doi:10.1126/science.1136163.

Hartley, M.J. 2002. Rationale and methods for conserving biodiversity in plantation forests. *Forest Ecology and Management*, 155, 81-95, doi:10.1016/S0378-1127(01)00549-7.

Hurley, B.P., Slippers, B., Sathyapala, S. *et al*., 2017. Challenges to planted forest health in developing economies. *Biological Invasions*, 19, 3273-3285, doi:10.1007/s10530-017-1488-z.

Jürgensen, C., Kollert, W., Lebedys, A., 2014. Assessment of industrial roundwood production from planted forests. Working Paper FP/48/E/, FAO Planted Forests and Trees Working Paper Series, Food and Agriculture Organization of the United Nations, Rome.

Kanninen, M., 2010. Plantation forests: global perspectives. The Earthscan Forest Library in: Bauhus, J., Van der Meer, P., and Kanninen, M. (eds.). Ecosystems Goods and Services from Plantation Forests, 1-15. London, UK, Earthscan. ISBN: 9781849711685.

Keenan, R.J., 2015. Climate change impacts and adaptation in forest management: a review. *Annals of Forest Science*, 72, 145-167, doi: 10.1007/s13595-014-0446-5

Lewis S.L., Wheeler C.E., Mitchard E., Koch A., 2019. Restoring natural forests is the best way to remove atmospheric carbon storage in subtropical forests. *Nature*, 568(7750), 25-28, doi: 10.1038/d41586-019-01026-84.

Liu, C.L.C., Kuchma, O., Krutovsky, K.V. (2018). Mixed-species versus monocultures in plantation forestry: Development, benefits, ecosystem services and perspectives for the future. *Global Ecology and Conservation*, 15, doi: 10.106/j.gecco.2018.e00419.

Lwila, A.S., Mund, M., Ammer, C., Glatthorn, J. (2021). Site conditions more than species identity drive fine root biomass, morphology and spatial distribution in temperature pure and mixed forests. *Forest Ecology and Management*, 499: 119581, doi: 10.1016/j.foreco.2021.119581.

Martin-Blangy, S., Meredieu, C., Jactel, H., Bonal, D., Charru, M. (2023). Species-mixing effects on crown dimensions and canopy packing in a young pine-birch plantation are modulated by stand density and irrigation. *European Journal of Forest Research*, 142, 197-216, doi: 10.1007/s10342-022-01511-2.

Millar, C.I., Stephenson, N.L., Stephens, S.L. (2007). Climate change and forest of the future: managing in the face of uncertainty. *Ecological Applications*, 17, 2145-2151, doi:10.1890/06-1715.1.

Minhas, P.S., Yadav, R.K., Lal, K., Chaturvedi, R.K., 2015. Effect of long-term irrigation with wastewater on growth, biomass production and water use by eucalyptus

(Eucalyptus tereticornis Sm.) planted at variable stocking density. *Agricultural Water Management*, 152, 151-160, doi: 10.1016/j.agwat.2015.01.009.

Palacios-Agundez, I., Onaindia, M., Barraqueta, P., Madariaga, I. (2015). Provisioning ecosystem services supply and demand: the role of landscape management to reinforce supply and promote synergies with other ecosystem services. Land Use Policy, 47, 145-155, doi: 10.1016/j.landusepol.2015.03.012.

Pardos, M., del Río, M., Pretzsch, H., Jactel, H., Bielak, K., Bravo, F., Brazaitis, G., Defossez, E., Engel, M., Godvod, K., Jacobs, K., Jansone, L., Jansons, A., Morin, X., Nothdurft, L., Oreti, L., Ponette, Q., Pach, M., Riofrío, R. Ruíz-Peinado, Tomao, A., Uhl, E., Calama, R., 2021. The greater resilience of mixed forests to drought mainly depends on their composition: Analysis along a climate gradient across Europe. *Forest Ecology and Management*, 481, doi: 10.1016/j.foreco.2020.118687.

Pretzsch, H., Schütze, G., 2016. Effect of tree species mixing on the size structure, density, and yield of forest stands. *European Journal of Forest Research*, 135: 1-22, doi: 10.1007/s10342-015-0913-z.

Puettmann, K.J., Parrot, L., Messier, C. (2009). A critique of silviculture: managing for complexity. Island Press, Washington.

Schnabel, F., Liu, X., Kunz, M., Barry, K.E., Bongers, F.J., Bruelheide, H., Fichtner, A., H¨ardtle, W., Li, S., Pfaff, C., Schmid, B., Schwarz, J.A., Tang, Z., Yang, B., Bauhus, J., H¨avon Oheimb, G., Ma, K., Wirth, C., 2021. Species richness stabilizes productivity via asynchrony and drought-tolerance diversity in a large-scale tree biodiversity experiment. *Science Advances*, 7, 11–13, doi: 10.1126/sciadv.abk1643.

Seidel, D., Leuschner, C., Müller, A., Krause, B., (2011). Crown plasticity in mixed forests quantifying asymmetry as a measure of competition using terrestrial laser scanning. *Forest Ecology and Management*, 261, 2123-2132, doi: 10.1016/j.foreco.2011.03.008.

Smith, P., Davis, S., Creutzig, F. et al (2016). Biophysical and economic limits to negative CO_2 emissions. *Nature Climate Change*, 6, 42-50, doi:10.1038/nclimate2870.

TEEB, 2010. A synthesis of the approach, conclusion and recommendations of TEEB The Economics of Ecosystems and Biodiversity: Mainstreaming the Economics of Nature: UNEP, Geneva.

Wang, C., Zhang, W., Li X., Wu, J. (2022). A global meta-analysis of the impacts of tree plantations on biodiversity. *Global Ecology and Biogeography*, 31, 576-587, doi:10.1111/geb.13440.

Warman, R.D., 2014. Global wood production from natural forests has peaked. *Biodiversity and Conservation*, 23, 1063–1078, doi: 10.1007/s10531-014-0633-6.

Warner, E., Cook-Patton, S., Lewis Owen, T., Brown, N., Koricheva, J., Eisenhauer, N., Ferlian, O., Gravel, D., Jefferson, H., Jactel, H., Mayoral, C., Meredieu, C., Messier, C., Paquette, A., Parker, W.C., Potvin, C., Reich, P., Hector, A., 2023. Young mixed planted forest store more carbon than monocultures-a meta-analysis. *Frontiers in Forest and Global Change*, 6, doi:10.3389/ffgc.2023.1226514.

Werner, R., Gasser, L.T., Steinparzer, M., Mayer, M., Ahmed, I., Sanden, H., Godbold, D.L., Rewald, B. (2024). Early overyielding in a mixed deciduous forest is driven by both above-and below-ground species-specific acclimatization. *Annals of Botany*, 1-19, doi:10.1093/aob/mcae150.

Chapter Two

Soil moisture and temperature dynamics in juvenile and mature forest as a result of tree growth, hydrometeorological forcings, and drought.

Authors: Andrea Rabbai, Doris E. Wendt, Giulio Curioni, Susan E. Quick, A. Robert MacKenzie, David M. Hannah, Nicholas Kettridge, Sami Ullah, Kris M. Hart, Stefan Krause

Running head: Dynamic of forest soil moisture in response to external disturbances.

Word count: 5.505

Corresponding author:

Andrea Rabbai

School of Geography, Earth and Environmental Sciences

University of Birmingham,

Edgbaston

West Midlands

United Kingdom

B15 277

Email: axr1049@student.bham.ac.uk

Abstract

Afforestation, as one of the major drivers of land cover change, has the potential to provide a wide range of ecosystem services. Aside from carbon sequestration, it can improve hydrological regulation by increasing soil water storage capacity and reducing surface water runoff. However, afforested areas are rarely studied at the appropriate time scale to determine when changes in soil hydrological processes occur as the planted (mixed) forests establish and grow. This study investigates the seasonal soil moisture and temperature dynamics, as well as the event-based responses to precipitation events and dry periods, between a mature and juvenile forest ecosystem over a 5-year time period. Generally, soil moisture was higher in the juvenile forest than in the mature forest, suggesting a lower physiological water demand. Following the 2018 drought, soil moisture dynamics in the growing juvenile plantation began to match those of the mature forest, owing to canopy development and possibly also to the internal resilience mechanisms of the young forest to these external hot weather perturbations. Soil temperature dynamics in the juvenile plantation followed air temperature patterns closely, indicating lower thermal regulation capacity compared to the mature forest. While our findings show that an aggrading juvenile plantation achieves mature forest shallow soil moisture storage dynamics at an early stage, well before maturity, this was not the case for soil temperature. Our results shed light on long-term trends of seasonal and event-based responses of soil moisture and temperatures in different-aged forest systems, which can be used to inform future assessments of hydrological and ecosystem responses to disturbances and forest management.

Keywords: soil moisture; forest hydrology, drought, microclimate, afforestation, BIFoR.

2.1 Introduction

Forests represent a key global carbon store and afforestation is an important tool for sequestering atmospheric carbon (Lewis et al., 2019). The increased awareness of the mitigating role that forests could play is supported by global initiatives including The Bonn Challenge (*The Bonn Challenge, accessed Sept. 2020. https://www.bonnchallenge.org/*), the UN's "Decade on Ecosystem Restoration" (2021-30), and the UN's REDD+ initiative. In the UK, the restoration of forests in agricultural settings helps to achieve the targets set by Net Zero by 2050, as stipulated in Environmental Land Management Policy (Land use: Policies for a Net Zero UK, 2020). Forests have a significant impact on hydrological processes, and well-planned afforestation has the potential to mitigate water management challenges in the context of global change (Ellison et al., 2012; Levia et al., 2020, Cao et al., 2011). Mature forests act as important modulators of water, nutrients and energy fluxes across the soil-vegetation-atmosphere interface (Ellison et al., 2017). Through their different water storage mechanisms from canopy down to deep root system, forests provide hydrological buffering capacity that is critical to moderate overland flow paths and thus, flood risk, as well as mitigating drought impacts through increased catchment storage (Choat et al., 2012). Consequently, afforestation influences runoff generation processes (Levia et al., 2020) and regulates soil moisture that provides the catchment template for flooding and hydrological drought (Brodribb et al., 2020) that are expected to be exacerbated under climate change. In addition, afforestation impacts (micro)meteorological conditions and boundary layer energy balances (Hannah et al., 2008), biogeochemical cycling in soils (Levia et al., 2020) and the landscape resilience to fire (Spence et al., 2020) as well as affecting soil habitat conditions, including the spread of soil and plant pathogens (Krause et al., 2013).

Forest soil moisture content directly impacts the system's capacity to absorb precipitation, preventing or reducing surface runoff generation during storm events, with infiltration rates varying significantly by soil type, tree species and forest

management practice (Zimmermann et al., 2006). Additionally, spatial patterns of soil moisture deficit directly control the intensity of root water uptake to satisfy the photosynthetic water demand and growth of trees and sub-canopy vegetation (Seneviratne et al., 2010). Concurrently, tree physiology features such as canopy architecture, leaf area index, and stand age can have a direct impact on water inputs by controlling interception, throughfall, and stemflow (Levia et al., 2020), thereby influencing infiltration processes. Physiology features also affect water outputs through root water uptake, decreased runoff and evapotranspiration (ET). The balance and interactions between these governing processes determines the spatial patterns and temporal dynamics of forest soil moisture (Naithani et al., 2013).

Soil moisture also influences plant nutrient availability, carbon sequestration by plants and soils, gaseous exchanges, including greenhouse gases, the leaching of nutrients into groundwater (Schlesinger et al., 2016), as well as plant-microbe interactions processes and nutrient cycling that ultimately affect the health and resilience of forests under climate change (Braganza et al., 2013). Changes in soil moisture dynamics, ranging from saturation to water deficit, affect the balance between aerobic and anaerobic microbial metabolism in soils. Water-saturated forest soils, for example, have lower nitrogen mineralization rates (Ullah and Moore, 2009) and can also act as a source for atmospheric methane (CH_4), whereas lower moisture conditions result in higher CH_4 absorption (Ullah and Moore, 2011). The establishment of aggrading juvenile forests is expected to exert increasing influence on soil hydrological processes at various spatial and temporal scales. This complex relationship is expected to stabilize once fully-grown trees can effectively regulate the forest stand microclimate, as well as the nutrient and site hydrology (Douglas, 2018). However, inadequate consideration of the inherent relationship between abiotic factors and trees can limit afforestation success. For instance, the selection of unsuitable tree species combined with inappropriate high initial planting density accelerates soil drying, thus threatening the overall tree survival rate (Nan et al., 2020). Yang et al. (2012) also reported soil moisture depletion following a change in land cover to forest plantation in the semi-arid Loess Plateau in China, where warming and drying trends increased the overall

moisture stress (Pu et al., 2006, Yao et al., 2005). Similarly, forest plantation failures were reported in Mediterranean drylands (Del campo et al., 2020; Rey Benayas et al., 2015). Successes in afforestation are found when reforested areas following ideal planting criteria, and lead to higher infiltration rate and improved soil moisture retention (Ilsted, 2016; Mapa, 1995). Given these challenges in afforestation, characterizing soil moisture dynamics on afforested sites is crucial in identifying techniques that may optimize tree growth processes and, thus, carbon sequestration from the atmosphere (Lewis et al., 2019, Pérez-Silos et al., 2021), as well as forest water-related ecosystem services. As reviewed by Jones et al. (2022), our understanding of the interplay between afforestation, soil moisture, and temperature dynamics, particularly in the long term, remains limited. This knowledge gap is primarily attributed to the different impacts of different stages of forest growth on soil moisture dynamics which result from variation in tree water use, evapotranspiration (Liang et al., 2018, Porporato et al., 2002) and the co-evolution of roots and soil structure (Carminati, 2012). Multi-annual observations are critical for properly addressing this knowledge gap. By making multi-annual observations, it also becomes possible to capture the effect of external disturbances, such as drought events, on the internal resilience of young forests (Au et al., 2022). Integrating this valuable information will aid in bridging the existing knowledge gap, which is crucial for supporting efforts to better understand afforestation and restoration approaches enhancing their efficacy.

This paper presents the findings of a study that compared soil moisture and temperature dynamics between a juvenile forest and a neighbouring mature forest ecosystem. While the initial focus was to understand the different hydrological processes in the two forest ecosystems, a drought event impacted the internal dynamics of the forests. As a result, this study presents not only different hydrological processes in two forest systems, but also investigates the hydrological evolution of a juvenile forest ecosystem following external perturbations. The multi-annual observations facilitated this opportunity, enabling a comprehensive understanding of how differently juvenile forest stand responded to external disturbances like drought

and how it could provide water ecological functions similar to those of a mature woodland, such as flood regulation.

2.2 Material and Methods

2.2.1 Field site description

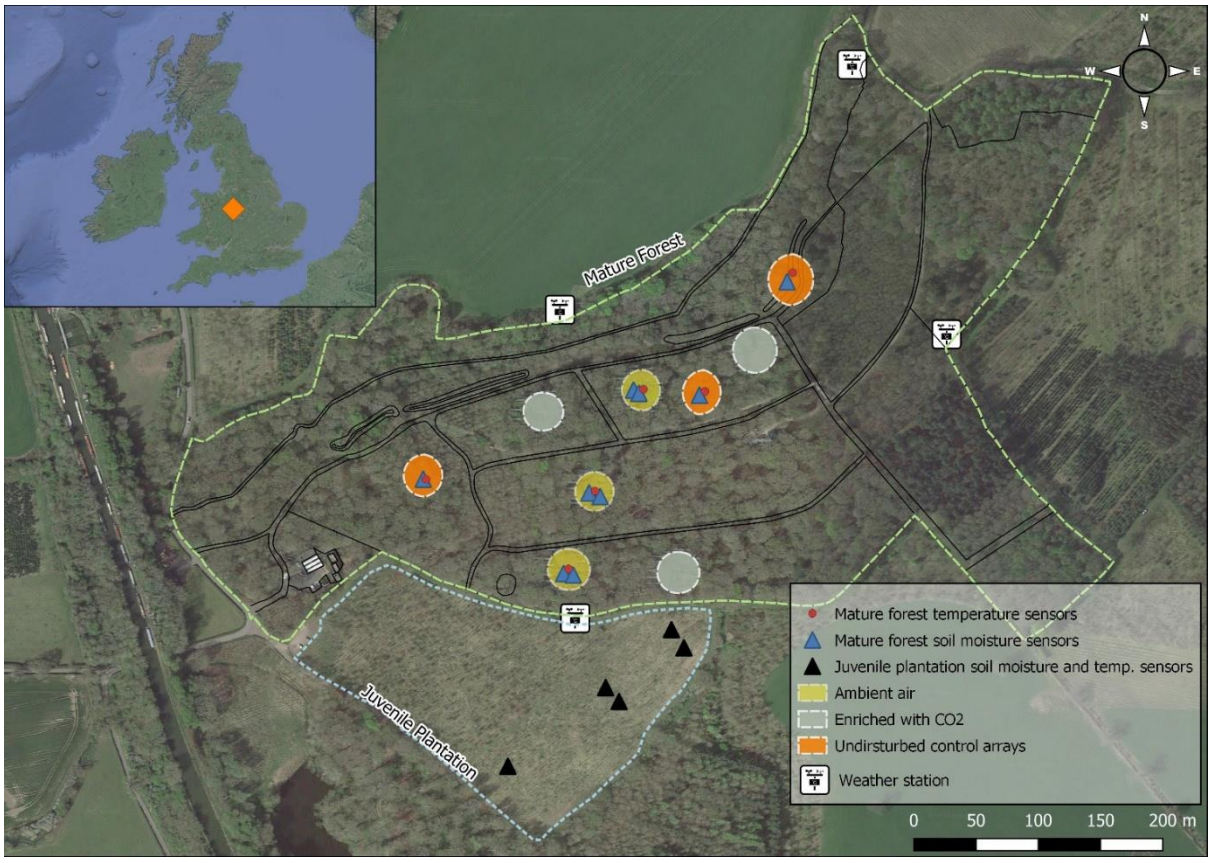

Figure 2.1: Field site map. Paired plots of juvenile plantation (blue dotted outline) and mature forest (green dotted outline) with the latter placed within the BIFoR FACE facility, as well as sensor locations in the FACE facility's control arrays (treated with ambient air, in yellow).

The study site is located in rural Staffordshire, Central England, UK and consists of a mature temperate deciduous forest patch hosting the Birmingham Institute of Forest

Research Free-Air Carbon Dioxide Enrichment (BIFoR FACE) facility (MacKenzie et al., 2021; Hart et al., 2019) and an adjacent juvenile forest plantation established in 2014 over previous arable farmland (52° 48' 3.6" N, 2° 18' 0" W, 106 m above mean sea level (amsl)). The annual average above-canopy temperature was 10.6 (± 0.8) ºC; using 1 min average from 2016 to 2019, with a maximum of 24.3 º C and a minimum of - 4.6 º C. The annual rainfall averaged 676 (± 66) mm. The BIFoR FACE facility consists of six approximately circular experimental arrays of 15 m radius with an open infrastructure 2-3 m taller than the tree canopy (Hart et al., 2019). Three arrays are treated with CO_2-enriched air to maintain +150 ppmv above ambient CO_2 (eCO_2) during daytime and growing season, and three are treated with ambient air only (control, shown in yellow in Figure 2.1). In addition, the facility includes three additional arrays with no physical infrastructure (undisturbed, shown in orange in Figure 2.1). The FACE infrastructure was built in 2015 causing minimal disturbance to the forest (Hart et al., 2019). The eCO_2 treatment started in April 2017 and has been active during leaf out daylight hours April to October, inclusive, each year since. The BIFoR FACE forest (from now on called the “mature forest”, Figure 2.1) is a mature deciduous woodland covering approximately 19 ha (Hart et al., 2019), dominated by *Quercus robur* (English oak) planted around 1850, coppiced for *Corylus avellana* (common hazel) and remaining largely unmanaged for the last three decades until 2015. Other native tree species including *Crataegus monogyna* (common hawthorn), *Acer pseudoplatanus* (sycamore maple) and *Ilex aquifolium* (holly) have self-set sporadically (Hart et al., 2019). The average height of the oak trees is 25 m, while the other sub-dominant species usually reach approximately 10 m, creating a dense and complex multi-layered canopy structure. The soil depth of the mature forest presents a generally sandy loam layer at a depth of 40 cm, and mostly loamy sand and sand conditions until 1 m (Hollis et al., 2021). The underlying geology is composed of superficial till deposits with a limited area of glaciofluvial deposits overlying sandstone of the Helsby Sandstone formation (BGS, 2020). The adjacent plantation (Figure 2.1), is a 4.66 ha aggrading mixed-species deciduous woodland (named “juvenile plantation”, Figure 2.1) planted in spring 2014 over a previously ploughed field (plough depth 0.4 m), characterized by a soil depth of approximately 1 m with mostly sandy

loam characteristics. The estimated available water holding capacity (AWC) at both sites is 1.2 mm per cm depth of soil, based on the predominant sandy loam conditions (Table 2.1).

Table 2.1: Available water holding capacity (mm/cm depth of soil) for both sites. Figures are reference averages and vary with soil structure and organic matter content (Blencowe et al., 1960).

Texture	Field capacity (FC)	Wilting point (PWP)	Available water (AWC)
sandy loam	2.0 mm/cm depth of soil	0.8 mm/cm depth of soil	1.2 mm/cm depth of soil

The juvenile plantation was afforested with 75% *Quercus robur* (English oak), 8% *Betula pendula* (silver birch), 7% *Prunus avium* (wild cherry), 5 % *Corylus avellana* (common hazel), and smaller saplings amounts of other deciduous tree species (detail in Appendix 2-S1). Saplings less than 1 m tall were planted at a density of 2500 trees ha^{-1} in rows approximately 2-2.5 m apart, with 1.8 m distance between trees within the same row.

2.2.2 Experimental setup

The data analysed in this study cover the period from 4th April 2016 until 1st March 2020. Air temperature, precipitation, soil moisture and soil temperature were taken at a sub-hourly resolution and were aggregated into hourly and daily data before analysis. Prior to March 2019, weather data was collected from the "Weather Underground" sensor network (https://www.wunderground.com/) using a range of weather stations in the village of Gnosall, approximately 3.5 km from the site. In early 2019, four heavily instrumented meteorological towers were installed outside the boundary of the mature forest and equipped with rain gauges (TR-525M, Texas Electronics) and air temperature sensors (HMP155, Vaisala) at 25 m. Furthermore, 30-year average precipitation and temperature data for climatological normal (CN)

calculation were acquired from the MET office weather station at Shawbury (MET office, 2020), located nearly 20 km from the research site. Soil moisture was measured by two different sets of probes. In the mature forest, CS655 probes, Campbell Scientific (0.12 m) were inserted diagonally from the surface inside the control and undisturbed BIFoR FACE arrays (Figure 2.1; the CO_2-enriched arrays were not used in this study to avoid potential interferences of the elevated CO_2 regime on the soil moisture dynamics). Each location currently hosts 3 sensors in triangular formation spaced approximately 1 m apart about 2 m from the nearest mature *Q. robur*. A group of 2-3 sensors in close proximity were averaged and considered as a single point measurement. The number of sensors was gradually expanded over time, with six locations recorded since October 2016, seven since March 2017 and nine since December 2018. Soil temperature was measured by 107 thermistors, Campbell Scientific, buried horizontally at 0.1 m since early 2018 (one location per array). Soil moisture sensors were installed in the juvenile plantation in the summer of 2015. Soil moisture and soil temperature were measured with 5TM probes, Decagon Devices (now METER group), buried at five locations at 0.1 m (one sensor per location; Figure 2.1). One of these locations was permanently damaged in winter 2017 leaving four locations active for the remaining period. The soil moisture data analysed in this study covers the period from 4th April 2016 until 1st March 2020. For this specific period, data from 64 observations (from 28th March 2019 to 23rd May 2019) were missing in the juvenile plantation dataset and were filled using linear interpolation (detail in Appendix 2-S2) to allow the time series decomposition.

2.2.3 Juvenile plantation monitoring

Understanding the interactions between climatic and hydrological conditions, site conditions, general forest dynamics, and relative land use changes relies strongly on knowledge of tree growth. Diameter at breast height (DBH) and tree height represent the key measurements for describing forest stand growth and density, as well as

suggesting appropriate management strategies. We collected data on the DBH at 1.35 m and tree height using a combination of an extensible height stick and clinometer for the tallest trees during two surveys in 2019 and 2021. Using these measurements, we calculated the basal area as a sum of the transversal areas at 1.35 m of all the trees surveyed within the plantation. Finally, by comparing data from the two surveys, we estimated the mortality rates across species.

2.2.4 Time series analysis

Analysing the dynamics of soil moisture over time is essential for determining the relationship between forest development and hydrological processes. Soil moisture patterns vary annually and seasonally due to changes of precipitation regime, forest phenology (i.e., leaf-on vs. leaf-off), forest growth, and soil properties. In this context, time series decomposition method has become an important tool for identifying the main drivers of hydrological processes change by isolating the data into key sub-series. The statistical approach used for time series decomposition is detailed in section 2.2.7.1

2.2.5 Event analysis

To characterize the mature forest and juvenile plantation response to single meteorological events we selected four two-day periods with precipitation events of contrasting magnitude (5 and 20 mm) for 2016 and 2019. Detailed information on the distribution of the precipitation data can be found in Appendix 2-S3. The precipitation events were chosen based also on their occurrence during similar seasons, ensuring comparable average air temperature and vegetation period. This approach allowed us to focus on the forest ecosystems' response to meteorological events themselves. In addition, two two-month summer periods from mid-June to mid-August in 2016 and

2019 were selected and analysed using the statistical methods described in Section 2.2.7.

2.2.6 Temperature regulation

We investigated the canopy cover thermoregulation capacity in both the mature forest and juvenile plantation by monitoring the mean daily air (25 m) and soil temperatures of topsoil (10-12 cm) from 2018 to 2020. The temperature difference (ΔT) was calculated between air temperature and topsoil temperature.

2.2.7 Statistical methods

We used two statistical methods to determine the effects of the dry periods on soil moisture dynamics. Firstly, to evaluate the difference between soil moisture observations in both mature forest and juvenile plantation we applied the two-sample Kolmogorov-Smirnov test (KS; Hazelwinkel, 2019) using the *stats* package in R. This approach compares two samples determining whether they are from the same distribution (null hypothesis, H_0), or distinct ones (alternative hypothesis, H_1). The test is carried out at a predefined statistical significance level *α* of 5%. Given a first sample of size *m* with an observed cumulative distribution function *F(x)* and a second sample of size *n* with an observed cumulative distribution function of *G(x)*, the Kolmogorov-Smirnov statistic *D* is given by:

$$D_{n,m} = max\,|F(x) - G(x)| \qquad [2.1]$$

If $D_{n,m}$ is greater than $D_{n,m,\alpha}$, the null hypothesis at significance level *α* is rejected where $D_{n,m,\alpha}$ is the critical value. For sufficiently large *m* and *n*:

$$D_{n,m,\alpha} = c(\alpha)\sqrt{\frac{m+n}{mn}} \quad [2.2]$$

Secondly, we applied the piecewise linear regression (PLR) method, also known as segmented linear regression, to investigate the difference in the system's temporal response to the dry periods. In ecological studies, this analysis has been widely used (Toms et al., 2003, Ficetola and Denoel, 2009, Shea and Vecchione, 2002, Toms and Villard, 2015) to identify thresholds that reflect step changes in the studied variable dynamics or the processes governing them. The statistical model for only one breakpoint at $t = \varphi$ is given by:

$$y_i = \begin{cases} \beta_0 + \beta_1 t_i + e_i & for\ t_i \leq \varphi \\ \beta_0 + \beta_1 t_i + \beta_2 (t_i - \varphi) + e_i & for\ t_i > \varphi \end{cases} \quad [2.3]$$

Where y_i is the value for the *i*th observation of soil moisture, t_i is the corresponding value for the independent variable, φ is the breakpoint (the threshold), and e_i are assumed to be the independent, additive errors with mean zero and constant variance. The slopes of the lines are respectively β_1 and $\beta_1 + \beta_2$, so β_2 can be considered as the difference in slopes. The *strucchange* package in R (Zeileis A. et al., 2002) has been used to determine the optimal number of breakpoints and their temporal location

2.2.7.1 Time series decomposition

For time series decomposition we transformed the soil moisture dynamics of the mature forest and juvenile plantation using the seasonal and trend decomposition using the LOESS (STL) procedure (Cleveland et al., 1990) over a 5-year time period (2016-2020). This method performs an additive decomposition that allows the trend

(T_T), seasonal (S_T) and remainder components (R_T) (Harvey and Peters 1990) to be isolated and analyzed (Equation 2.1):

$$Y_T = T_T + S_T + R_T \quad [2.4]$$

The core of the process is the Loess smoother application which defines the explanatory variables, the value closest to the point whose response is being estimated by fitting a locally weighted polynomial regression over several observations. The STL procedure is carried out via an iterative cycle consisting of an inner and outer loop. Each passage of the inner loop applies a moving average smoother to the seasonal and trend components while the subsequent outer loop calculates the remainder component. Finally, the Loess process is used to compute the weight of the remainder component's extreme values. Further iterations of the inner cycle use the calculated weights to reduce the effects of extreme values identified by the previous outer loop. For more detailed information about the STL method, see Cleveland et al. (1990). The STL function from the *stats* package (R Core Team 2022) used for time-series analysis required the definition of the seasonal component smoothing parameter n_s which should be an odd integer number corresponding to the years of observation. In our case, given the study period from 2016 to 2020, n_s was set to 5.

2.3 Results

2.3.1 Juvenile plantation survey

The first tree survey in the juvenile plantation was carried out in January 2019, with a tree density of 1340 tree ha^{-1} estimated. Because of the limited dimension of tree diameter, only the heights were measured during this survey. The average height of *Quercus robur* was 1.6 m, ranging from a maximum of 2.5 m to a minimum of 1 m. *Betula pendula* and *Prunus avium* had higher average height values of 3.4 and 3.2 m with maximum values of 5 and 4.5 m respectively. During the second tree survey, which took place in 2020, the estimated density was 975 trees ha^{-1} with a basal area of 1.2 m^2 ha^{-1}. *Quercus robur* and *Prunus avium* had higher death rates, losing 33 percent and 16 percent of their respective population (Table 2.2).

Table 2.2: Average, maximum, minimum heights, as well as mortality rates across all species within the juvenile plantation following a tree survey in 2010.

Common name	Latin name	Average height (m)	Maximum height (m)	Minimum height (m)	Mortality rates from 2019 survey
English Oak	*Quercus robur*	2	4.50	1	33%
Silver Birch	*Betula pendula*	5	6.50	3	3%
Wild Cherry	*Prunus avium*	4	6	1.50	16%
Hazel	*Corylus avellana*	2.50	4.50	1	5%
Hornbeam	*Carpinus betulus*	3	4.50	1.50	0%
Rowan	*Sorbus aucuparia*	3.5	4.50	1	8%
Field Maple	*Acer campestre*	3	4	1	0%
Chestnut	*Castanea sativa*	2	4	1	22%

Whitebeam	*Sorbus aria*	2	2.50	0.70	0%
Wild Pear	*Pyrus communis*	3	3.50	1.50	0%
Crab Apple	*Malus sylvestris*	2.7	3	2.50	33%

In comparison, the average oak height increased to 2 m, with some individuals reaching 3.3 m. Similarly, *Betula pendula* and *Prunus avium* reached an average height of 5 and 4 m, respectively, with maximum values of 6.50 and 6 m. Figure 2.2 shows the growth of juvenile plantation from 2014 to 2019.

Figure 2.2: Juvenile plantation stages from planting in 2014 (A) to further development in 2016 (B), 2017 from a different camera angle showing both the mature forest in BIFoR (top) and juvenile forest

(bottom) (C), and 2019 (D) respectively. In panels B and C early tree morality can be observed in the foreground.

2.3.2 Soil moisture dynamic and hydrometeorological conditions

Average daily soil moisture at the juvenile plantation and mature forest from 2016 to 2020 is shown in Figure 2.3, in which two distinct phases are identified. The first period, from April 2016 to June 2018, was characterized by a similar seasonal pattern for both sites (Figure 2.3C). From September to April, soil moisture levels generally increased, with minimum and maximum values of 8-32% and 20-36% in mature and juvenile forests, respectively.

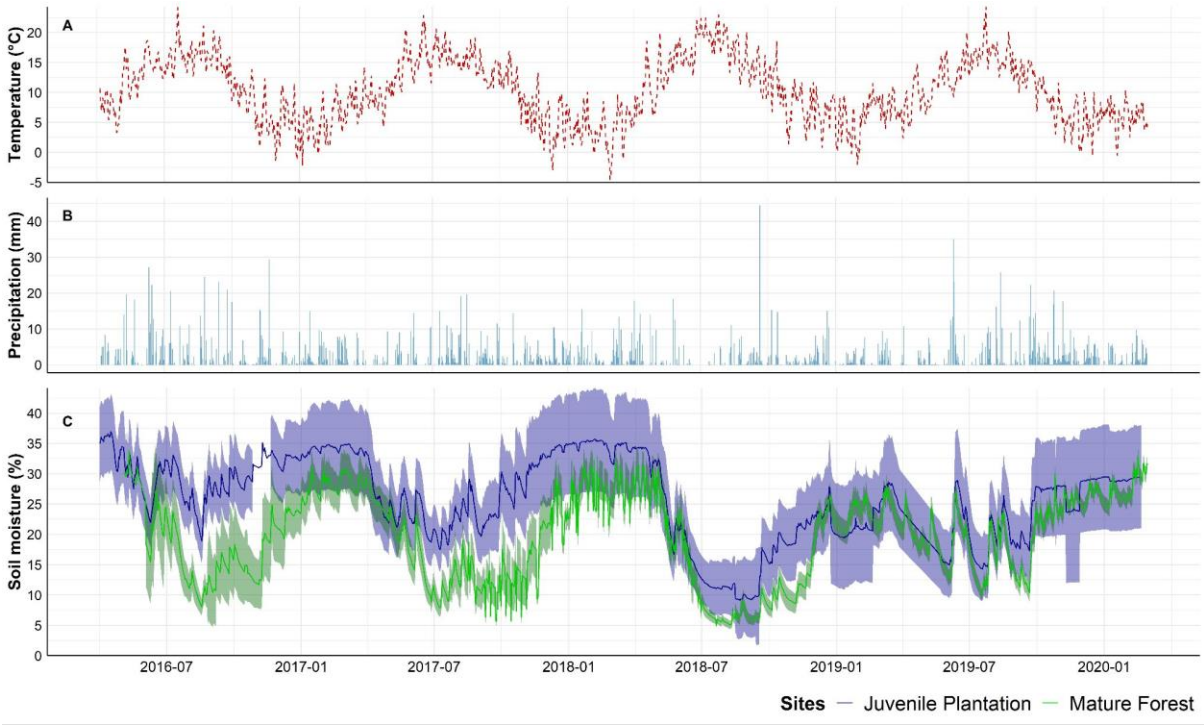

Figure 2.3: Daily air temperature (A), precipitation (B), and soil moisture (C) observations for the juvenile plantation and mature forest. Daily mean soil moisture plots (C) for both plots include the relative standard error of the mean (SE). Note that soil moisture observations at BIFoR FACE are only used for control and undisturbed arrays.

Peak soil moisture values synchronized for all years with some minor delays in the mature forest compared to the juvenile plantation (Figure 2.3C). When considering seasonal variability, the largest absolute difference in soil moisture is observed from early summer to mid-autumn (e.g. Δ_{sm} = 15%) compared to more similar soil moisture observations in winter and spring. This seasonal pattern is also reflected in the standard error (SE) that shows a larger range in summer compared to winter. Substantial precipitation events in 2016 and 2017 resulted in a soil moisture increase, but the absolute difference between the forests remained consistently larger over this first period. Note that the SE for the mature forest is smaller due to the larger aggregated samples in the studied arrays. The second identified period starts in June 2018 and co-coincides with a dry period. In the following months, soil moisture in the mature and juvenile plantation declined to minimum of 5 and 10%, respectively. This extended drought ended with heavy precipitation events (1 August and 30 September), which only partially restored seasonal soil moisture levels. The absolute difference in soil moisture was altered after this dry stage, resulting in similar soil moisture conditions in both forest types, both on seasonal and annual time scales. For example, soil moisture in 2019 varied only 3-4% on average from January to July, based on a total rainfall of 338 mm, which is nearly the same amount that fell during the same period in 2018 (341 mm). The SE for the juvenile plantation increased during this period peaking at nearly 22% in late 2019. In the mature forest, however, the SE decreased over time due to installation of additional soil moisture probes overtime (MacKenzie et al., 2021).

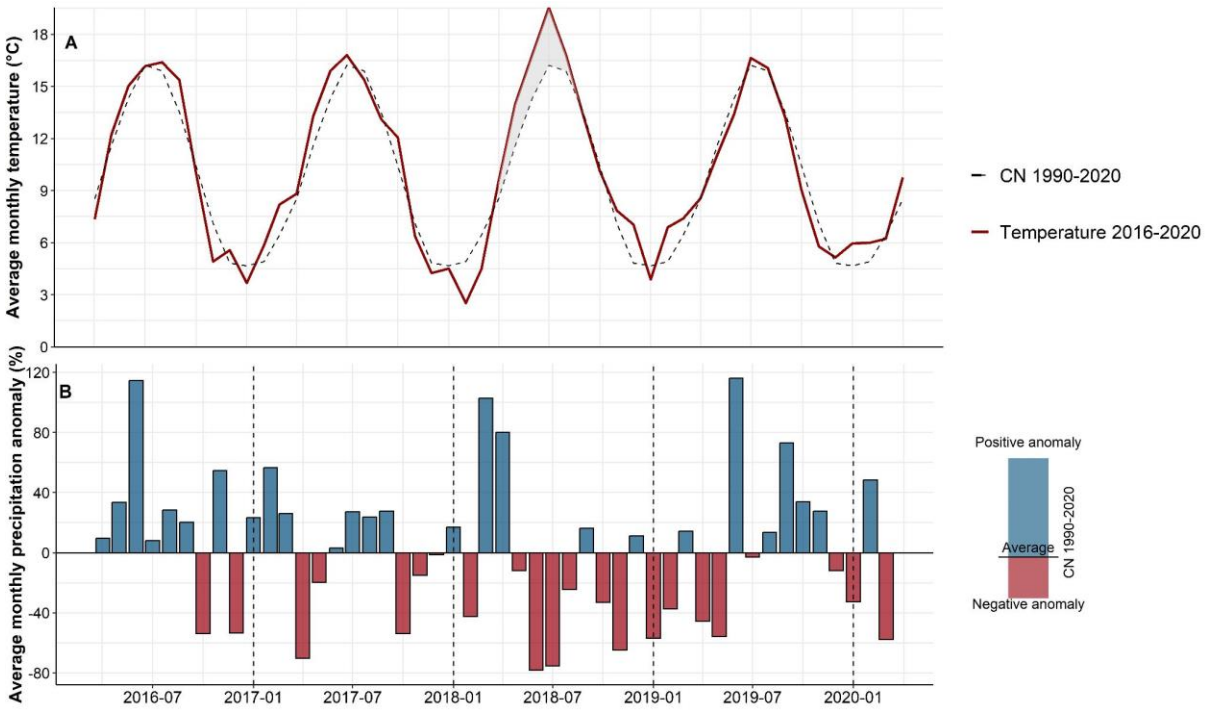

Figure 2.4: Monthly averages of air temperature (A) and precipitation (B) in the research area from 2016 to 2020 in relation to the monthly climatological normal (CN) calculated for the period 1991-2020. 30 years weather data acquired from a weather station located at Shawbury, 15 km away (UK Met office, 2020).

Figure 2.4 depicts the monthly average temperature and percentage precipitation anomalies from 2016 to 2020 in relation to the 1990-2020 climatological normal (CN). In particular, 2018 differed more from the other years of the series (Figure 2.4A), with below-average temperature (-1.5 °C) winter months followed by a 10-month period characterized by several positive thermal anomalies (peaking in July with + 3.3 °C) that ended in early 2019. Related to this, Figure 2.4B highlights how summer months of 2018 were affected by a severe drought, measuring -1.7 SPI across the UK (UKCEH, 2022), with annual rainfall being reduced to 79% in July. Despite the period 2018-2019 being drier and warmer than normal, the start of 2019 represented a shift to generally wetter and colder conditions. In 2019, the mean annual air temperature dropped to +9.75 (± 4.28) °C, in line with the CN, while a mean annual precipitation of 775 (± 35.4) mm represented an estimated 19% increase compared to 2018. However,

when focusing on the summer months of 2018 and 2019, the difference in precipitation is estimated to be 60% with 148.6 mm and 368 mm respectively.

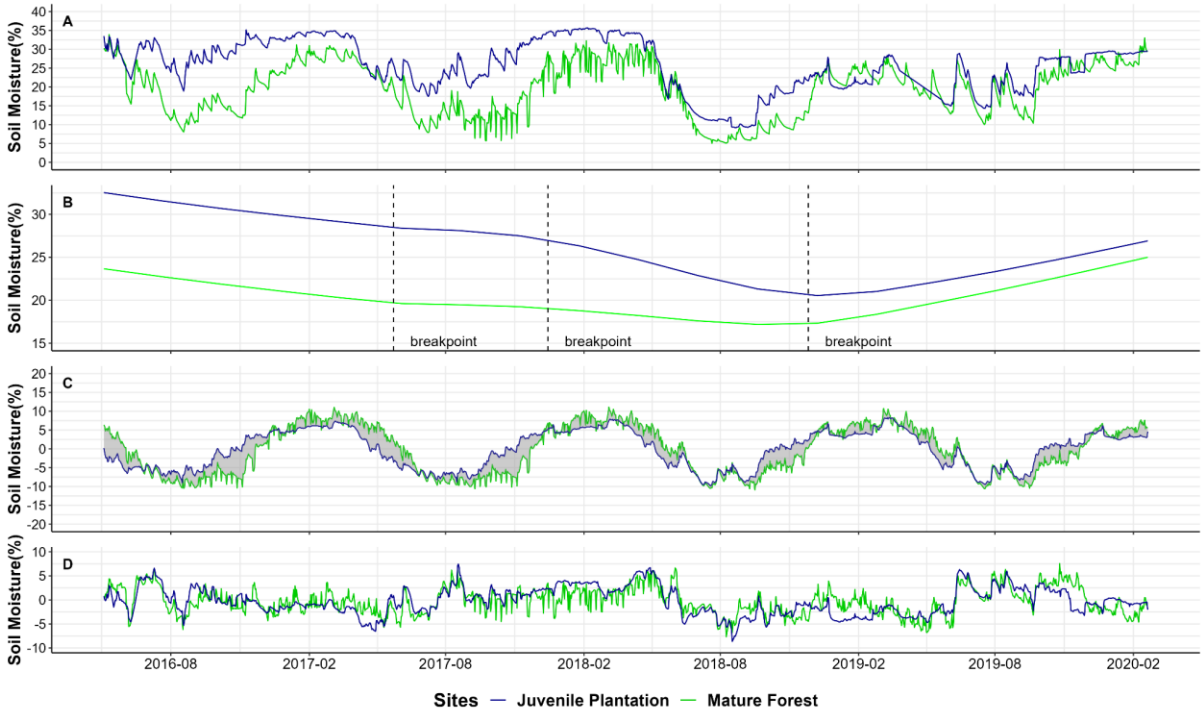

Figure 2.5: Soil moisture time series decomposition over the period 2016-2020. Daily mean soil moisture at mature and juvenile forest (A); long-term trend in soil moisture with dashed lines representing the breakpoints (B); soil moisture seasonal component with grey filling area highlighting the difference between both forest ecosystems (C); soil moisture residual component (D).

Decomposition of soil moisture time series revealed significant differences between the juvenile plantation and the mature forest (Figure 2.5A). Although soil moisture decreased for both forest systems from 2016 to 2018 (Figure 2.5B), the decline was greater in the juvenile plantation than in the mature forest (KS test: $D = 0.590$, $p < 0.05$). In 2019, soil moisture in the mature forest returned to pre-drought levels in less than 1.5 years, whereas soil moisture in the juvenile plantation reached a 10% lower value than before (Figure 2.5B). The application of piecewise linear regression (details can be found in Appendix 2-S4) to soil moisture trends identified three major breakpoints that occurred in May 2017, December 2017, and November 2018 (dashed line in Figure 2.5B). The slopes of linear regression calculated between December

2017 and November 2018 are -0.030 ad 0.020, respectively, indicating multiple distinct soil moisture dynamics that coincide with the identified two periods in Figure 2.3. Figure 2.5C also depicts the progressive synchronization of seasonal soil moisture dynamics, as evidenced by the reduction of the summer soil moisture difference between juvenile and mature forest from 2016 (KS test: D = 0.46, p-value < 0.05) to 2019 (KS test: D = 0.15, p-value = 0.2435). Residual components (Figure 2.5D) of soil moisture in both forest sites confirm these findings, with their dynamics aligning more during the summer of 2019.

2.3.3 Event based analysis of temporal difference in soil moisture responses.

Figure 2.6 shows hourly mean soil moisture in juvenile and mature forest measurements in response to selected precipitation events (Pr >= 20 mm and Pr = 5 mm) during the summers of 2016 and 2019. Regardless of precipitation magnitude, juvenile plantation had higher soil moisture values in 2016 compared to the mature forest (KS test: D = 0.54, p-value < 0.05), with an average difference ranging from 12% to 15%. In 2019, however, this dissimilarity between the two sites is no longer significant (KS test: D = 0.12, p-value > 0.05) with the soil moisture differences reduced to 5% or less.

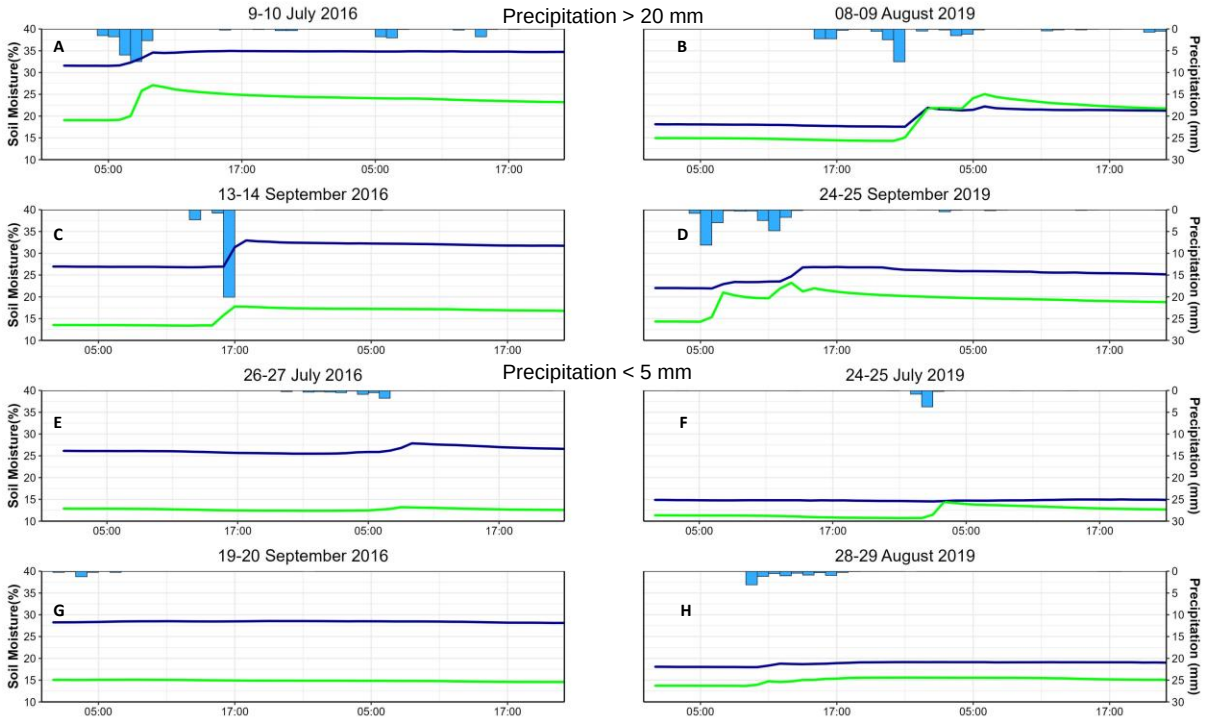

Figure 2.6: Effect of selected precipitation events on soil moisture. Panels show hourly soil moisture at the mature forest and juvenile plantation after precipitation events of different intensity (Pr >= 20 mm and Pr = 5 mm) in summers 2016 and 2019.

Additionally, mature forest soil moisture is generally lower than that in the juvenile plantation, but this pattern was reversed on 8-9 August (Figure 2.6). Soil moisture exceeded that of the plantation by approximately 3%, following a 23.5 mm rainfall event. Overall, soil moisture in the mature forest increases more compared to the plantation following heavy rain events. On the other hand, it appears that smaller events (Pr = 5 mm) cause negligible soil moisture response at the monitored soil depths in all cases (Figure 2.6). To further characterize the two identified periods that show pre-and post-drought responses of soil moisture dynamics in both forest ecosystems, we selected two summer periods in 2016 and 2019. The first summer period, which lasted from 20 June to 20 August 2016 had total rainfall of 90.7 mm and an average temperature of +15.3 (± 1) °C. During this time, both the mature forest and

juvenile plantation showed a progressive soil moisture decline of 16% and 14%, respectively, reaching lows of 10% and 20% (Figure 2.7A).

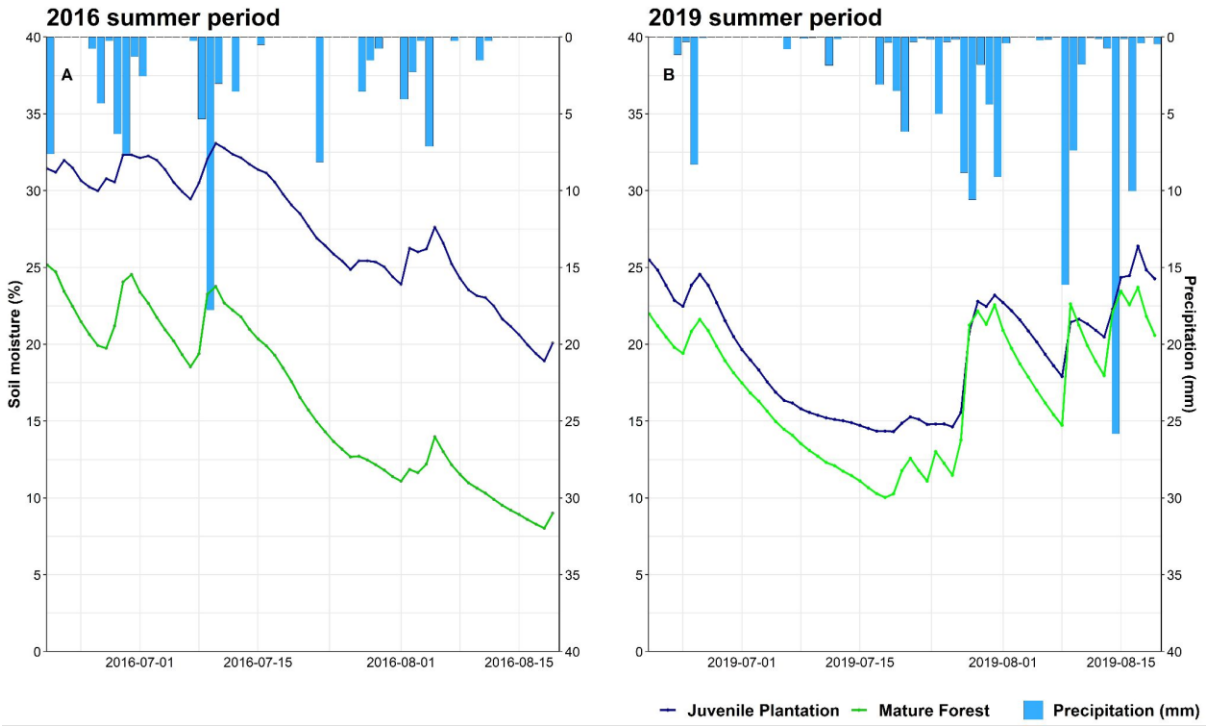

Figure 2.7: Soil moisture in mature forest and juvenile plantation relative to the summer 2016 (panel A) and summer 2019 (panel B).

The second selected summer period in 2019 (from 20 June to 20 August) had higher precipitation (total of 130.2 mm) and slightly warmer conditions than 2016 (mean temperature of 16.03 °C). The soil moisture showed an interesting dynamic here, as the first month was characterized by drier conditions (19.6 mm) resulting in a 12% and 10% decrease for both mature forest and juvenile plantation, respectively (Figure 2.7B). Following this initial period, increased precipitation (104.4 mm) resulted in a similar sharper soil moisture response in both forest ecosystems, nearly restoring the initial conditions. Despite forest soil moisture dynamics continuing to differ significantly, there is a shift toward a new distinct period, with the stark difference between systems becoming minimal (KS test: $D(2016) = 0.71$, $D(2019) = 0.34$, $p\text{-value} < 0.05$).

2.3.4 Buffering impact on air temperature.

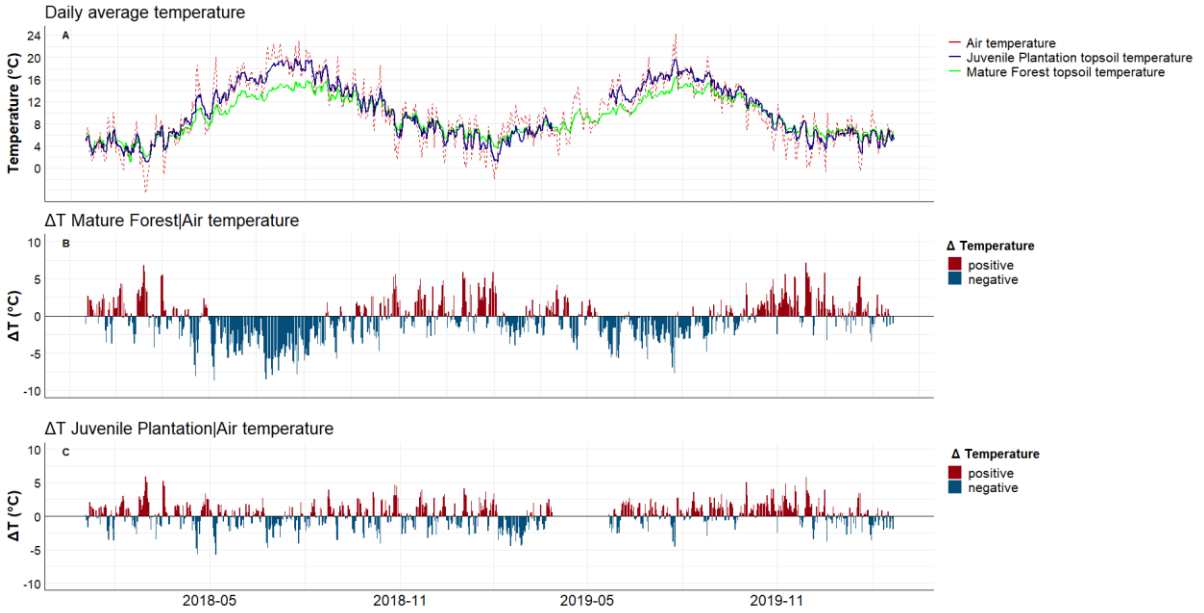

Figure 2.8: Difference between topsoil temperature and air temperature observed at the mature forest and juvenile plantation (2016-2020). Panel A shows daily air temperature and topsoil temperature collected at the control and undisturbed arrays within BIFoR FACE, panels B and C show the daily difference between topsoil and air temperature for both sites.

From 2018 to 2020, the average daily dynamics of air and topsoil temperatures show that the mature forest buffers large temperature differences. Its microclimate is effectively modulated with topsoil temperature showing decreasing by only 0.2% over this period. This is remarkable given that 2019 had nearly one degree below the mean annual air temperature of + 9.77 ℃ (Figure 2.8A). Seasonally, the mature forest topsoil temperature is characterized by higher temperature during the colder periods and lower temperatures in warmer ones compared to air temperature (KS test: D= 0.18, p-value < 0.05). The extent of the mature forest buffering effect is clearest between 1 May and 1 September 2018, when there is 4 °C average difference between the topsoil and air temperature (Figure 2.8B). For the same period, the buffering effect of the juvenile plantation is far inferior, with average differences between topsoil and air temperature less than 1°C (KS test: D = 0.06, p-value > 0.05; Figure 2.8C).

2.4 Discussion

2.4.1 Increasing similarity in soil moisture dynamics between juvenile plantation and mature forest.

Based on the presented soil moisture observations, the juvenile plantation showed a more conservative water balance, less fluctuation between soil moisture contents, than the mature forest (Figure 2.3). Soil moisture conditions depend on different water fluxes that relate to vegetation type, hydrometeorological conditions, and soil properties (Seneviratne et al., 2012). Despite having comparable soil textures (Table 2.1), the mature forest and juvenile plantation exhibit variations in soil properties and soil moisture dynamics due to their different histories. In particular, the juvenile plantation, which was only 6 years old at the time of the drought reported in this study, is characterized by an open canopy (Figure 2.2) and possibly low levels of organic matter in the soil. In fact, afforestation efforts often take several decades to improve various soil properties (Yao et al., 2023, Manso et al., 2022, Korkanç, 2014). As a result, the variation in soil moisture observed within the juvenile plantation is most likely caused by the increased physiological water demand of the trees after the drought, as well as differences in forest structure compared to the mature forest.

The developed canopy structure of an undisturbed forest ecosystem, for example, plays an important role in regulating soil moisture oscillation due to increased rainfall interception and reduced throughfall, as well as shade that influences the understory microclimate and the evaporation from the soil (He et al., 2013). Similarly, water consumption to meet photosynthetic water demand in the mature forest is likely to result in higher ET losses and soil water deficits due to a more developed root network (Landsberg et al., 2017). Interestingly, the developed ground cover vegetation in the juvenile plantation does not appear to cause additional soil water uptake, as our results show over the period preceding the drought, which would reduce soil moisture to a similar level as in the mature forest (3C). This relates to the principal difference in

functional rooting depth between trees and grasses, implying that trees respond primarily to deeper soil moisture availability (10-20 cm) compared to grasses that have a larger presence in the shallow soil layers (Weltzin and McPherson, 1997). This interpretation is coherent with the moisture dynamics at the different depths within the juvenile plantation during the dry stress period, where similar dynamics in soil moisture can be detected (details in the Appendix 2-S5). In this context, the drought acted effectively as a “renewal event”, eliminating previous moisture dynamics (Viola et al., 2008). Although vertical moisture profile dynamics is critical for understanding the overall response and adaptation to drought, the 10 cm depth is a reliable indicator of the hydrological processes in action. Furthermore, the 10 cm depth provides valuable information on the development of flood capacity regulation by the juvenile plantation (Figure

2.6, 2.7), which is a valuable water ecological service provided by forest ecosystems (Jenkins and Schaap, 2018). This effect of functional root depth is also reflected in the analysis of high rainfall events, where the mature forest shows a greater adaptability to uptake soil moisture. This could be related to retaining soil moisture in deeper soil layers and/or a more extensive root network (Holdo et al., 2015), although this falls outside the direct scope of this research.

Notably, Figure 2.5 shows how soil moisture changes highlight differences in resilience (Lloret et al., 2011) between the two forest ecosystems, with the mature forest showing higher resistance and recovery. Nevertheless, differences in soil moisture between the mature forest and juvenile plantation became smaller beginning in September 2018. This pattern becomes more evident analysing the soil moisture trends (Figure 2.5B) and the progressive alignment of seasonal soil moisture (Figure 2.5C) which suggests that the hydrological functionality of both forest ecosystems becomes similar after the 2018 drought. One explanation might be the rapid growth of trees observed within the juvenile plantation, which was 6 years old in 2018 (Figure 2.2). This increases overall the associated water photosynthetic needs with greater contribution from the fast-growing species (Cao et al., 2011) such as *Betula pendula, Prunus avium*, and *Corylus*

avellana accounting for 20% of the total population. A mixed species plantation is likely to exhibit higher growth rates and carbon storage even during dry periods compared to monoculture due to their different water and nutrient acquisition strategy (Liu et al., 2018). Furthermore, the change in soil moisture dynamics could relate to dry and warm conditions, which forced the trees to adapt their belowground surface to maintain plant water and nutrient uptake. Trees can use one of two strategies to overcome periods of water stress: either increase fine root biomass (FRB) formation to maintain absorbing surface (extensive approach) or modify root morphology and physiology to maximize uptake efficiency per root mass (intensive approach) (Lõhmus et al., 2006). It has been shown before that drought-induced decreases in FRB can be compensated by higher growth rates (Joslin et al., 2000) during favourable periods, resulting in soil moisture dynamic changes as shown, for instance, by the juvenile plantation seasonal dynamics. Related to these studies, it could be that the meteorological drought in 2018 (SPI -1.7. UKCEH, 2022) and persistent higher topsoil temperature in the juvenile plantation (Figure 2.8A) could be driving root growth (Salazar et al., 2020, Kwatcho Kendo et al., 2022, Joslin et al., 2000). Similarly, mycorrhizal network growth pulses may play an important role in forest ecosystem resilience (Simard et al., 2011). Tree C allocation to mycorrhizal fungi represent an essential strategy in sustaining nutrient and water uptake over stress periods (Wang et al., 2021, Hawkes et al., 2011, Simard et al., 2011). In fact, during a drought an extensive hyphal network that allows for water movement and redistribution (Bingham and Simard, 2011) can be critical to plant survival (Querejecta et al., 2007, Neumann et al., 2012) and resilience. Finally, more research is required to understand how severe perturbations, such as droughts, can erode natural soil structure resilience, potentially leading to an alternative stable state in an ecosystem for either mature forests or juvenile plantations. Hydrological extremes, such as droughts, can alter soil hydraulic parameters, resulting in different soil moisture trajectories with a domino effect on all terrestrial ecosystems processes like soil respiration, nutrient cycling, and net primary productivity (Robinson et al., 2016). Overall, a closer correlation of the water dynamics between the juvenile plantation and the mature forest over time suggests that key aspects of a mature forest hydrological functionality can be achieved

on shorter times scales compared to other ecological goals, and likely in response to the drought period. This is an important finding for areas where reforestation is introduced to restore local water resources. It is also worth noting that trees in both forests are suffering from water stress. Unfavourable climatic conditions, most notably a lack of precipitation, rising air temperatures, and increasingly frequent and extended dry periods, have serious, but varying, long-term implications for mixed forest ecosystems (Niinemets & Valladares, 2006; Češljar et al., 2022). In particular, juvenile plantations tend to be more sensitive to water stress due to high tree density and the adoption of genetic provenance with low drought tolerance, resulting in lower planting vigor and higher mortality ratio when compared to a naturally regenerated forest (Navarro-Cerrillo et al., 2018). For example, tree oak mortality has been known to occur approximately 2 years after dry stress, which may explain their high mortality rates observed in the juvenile plantation during the 2020 tree survey (Table 2.2). With this work, we show that long-term observation of soil moisture dynamics in different forest types and management conditions shows differences in drought resilience, but more research is needed to provide guidance to forest management under climate change conditions where dry spells and droughts are expected to occur more often and with increased severity (Dai, 2013; Stagge et al., 2017; Hari et al., 2020).

2.4.2 Differences in forest soil moisture responses to wetting and dry events.

The similarity in soil moisture response is also echoed when focusing on both storm events and dry spells in 2016 and 2019. The 2016 events show that the juvenile plantation had 12% to 15% wetter conditions compared to the mature forest and soils were close to fully saturated at times (Figure 2.6). In 2019, soil moisture responses in the juvenile plantation were more similar to those of the mature forest after storm events, indicating an initial buffer effect of the young trees (Figure 2.6). Summer periods in 2016 and 2019 showed overall higher values for the juvenile plantation indicating inferior water uptake of growing trees when compared to the mature forest (Figure 2.7). In 2016 the decline in soil moisture is similar in both forest ecosystems considering an absolute difference between systems. This compared to the soil

moisture in 2019 that shows several overlapping dynamics in response to precipitation events (Figure 2.7B). The observed response to wetting and drying events provides further evidence in support of the prior interpretation that the growth (Figure 2.2) of trees has led to increased water balance buffering capacity. Moreover, it indicates that the juvenile plantation exhibits recovery mechanisms that allow it to recover from water stress. In fact, when compared to a mature forest, the altered response of juvenile plantation soil moisture to storm events in 2019 may indicate increased infiltration due to the growth of the root network (Jones et al., 2022, Ilstedt et al., 2016; Lange et al., 2013; Zhang et al., 2014). This may lead to a change in water storage in shallow soil and relative flood capacity regulation, which is one of the most important water-ecosystem services provided by a forest stand in a watershed (Crossman, et al., 2019).

2.4.3 Buffering impact on air temperature.

Given the low fluctuations in topsoil temperature, the mature forest's thermal buffering capacity is evident (Figure 2.8A). However, the larger fluctuations of the juvenile plantation reveal a significantly lower thermal regulation capacity during the monitored period. This is due to the less developed forest and canopy structure of the juvenile plantation (Figure 2.2), which also explains the higher (close to the air temperature) soil temperature (Figure 2.8A), as opposed to the observed reduced summer topsoil temperature and temperature anomalies in the mature forest. In fact, as illustrated in Figure 2.8B, the mature forest cools summer air and warms the cold winter air, thereby buffering temperature changes (Jin et al., 2019). As a result of extreme climate conditions, temperature differences between inside and outside forests increase (De Frenne et al., 2013). Despite the growing canopy cover, the juvenile plantation has not (yet) attained similar thermal buffering capacity (Figure 2.8C).

2.4.4 Limitations and uncertainty in data.

While the mature forest investigated here has been thoroughly studied, the neighboring juvenile plantation lacks detailed tree physiology observations, which limits a detailed interpretation of the role of forest conditions on soil moisture and temperature differences. To move beyond the empirical findings presented here, towards causal mechanistic understanding of the effect of tree growth and forest management on hydrological processes, additional research within the juvenile plantations such as rooting depth, sap flow, and interception losses will be required.

2.5 Conclusion

In this work, we compared soil moisture and temperature observations of a juvenile and mature forest that revealed significant differences in seasonal patterns as well as event. The ongoing monitoring shows a transition in hydrological trends, as well as changes in precipitation response, particularly within the juvenile forest. These alterations suggest that there has been a change in water storage in shallow soil as a result of increased infiltration, and subsequently improvement in the ability of the juvenile plantation to control flooding. We found that shallow soil moisture dynamics of the juvenile plantation match those of the mature forest in less than 10 years (8 years after planting), which is most likely due to adaptation strategies of the plantation following the 2018 drought. This event may have promoted modification of the tree root structure (i.e. biomass and morphology) to maintain adequate water and nutrient uptake. Additionally, the impact of drought on the hydrological function of the juvenile plantation highlights a new challenge of climate change in temperate regions which needs to be considered when predicting outcome of reforestation schemes. The observed effects on the soil moisture and hydrological function of the juvenile plantation may be due to the complementarity nutrient and water acquisition strategies of mixed species, which might not be case in traditional monoculture forestry system. Finally, thermal regulation capacity remained dissimilar between juvenile plantation and mature forest suggesting how other forest ecosystem functions take longer to

establish. This study highlights the value and the challenges of continuous long-term observation at high frequency to complement the analysis of seasonal and interannual behavior with investigating the trends in event-based responses. Further research on this long-term observatory will continue to facilitate analyses in ecosystem and hydrological responses to forest management practices, as well as provide invaluable insights into the complex relationship between land use changes, such as reforestation, and drought.

2.6 References

Ainslie, W.B., Smith, R.D., Pruitt, B.A., Roberts, T.H., Sparks, E.J., West, L., Godshalk, G.L. & Miller, M.V., (1999). A regional guidebook for assessing the functions of low gradient, riverine wetlands in Western Kentucky. *Technical report, WRP-DE-17*, US Army corps of Engineers, Waterways Experiment Station, Vicksburg, Mississippi, USA.

Au, T.F., Maxwell, J.T., Robeson, S.M. et al., (2022). Younger trees in the upper canopy are more sensitive but also more resilient to drought. *Nature Climate Change*, 12, 1168-1174, doi:10.1038/s41558-022-01528-w.

BGS, Geology of Britain viewer | British Geological Survey (BGS) (2020).

Bingham, M.A., Simard, S.W., (2011). Do mycorrhizal network benefits to survival and growth of interior Douglas-fir seedling increase with soil moisture stress? *Ecology and Evolution*, 1, 306-316, doi:10.1002/ece3.24.

Blencowe, J.P.B., Moore, S.D., Young, G.J., Shearer, R.C., Hagerstrom, R., Conley, W.M., Potter, J.S., 1960. U.S Soil Department of Agriculture Bulletin 462, pp (1960).

Braganza, K., Hennessy, K., Alexander, L., & Trewin, B., (2013). Changes in extreme weather. Four degrees of global warming: Australia in a hot world. *Routledge, Abingdon*, 33-60.

Brodribb, T. J., Powers, J., Cochard, H., & Choat, B., (2020). Hanging by a thread? Forests and drought. *368*(6488), 261-266, doi:10.1126/science.aat7631 %J Science.

Cao, S., Chen, L., Shankman, D., Wang, C., Wang, X., Zhang, H., (2011). Excessive reliance on afforestation in China's arid and semi-arid regions: Lessons in ecological restoration. *Earth-Science Reviews*, 104, 240-245, doi: 10.1016/j.earscirev.2010.11.002.

Carminati, A., Vetterlein, D., Koebernick, N., Blaser, U., Vogel, W., Vogel, H.J., (2013). Do roots mind the gap. *Plant and Soil*, 367 issues 1, 651-661, doi: 10.1007/s11104-012-1496-9.

Climate Change Committee. "Land use: Policies for a Net Zero UK", 23 Jan (2020). Available at: https://www.theccc.org.uk/publication/land-use-policies-for-a-net-zero-uk/.

Češljar, G., Jovanović, F., Brašanac-Bosanac, L., Đorđević, I., Mitrović, S., Eremija, S., Ćirković-Mitrović, T., Lučić, A., (2022). Impact of an Extremely Dry Period on Tree Defoliation and Tree Mortality in Serbia. *Plants*, *11*, 1286, doi:10.3390/plants11101286.

Choat, B.,Jansen, S., Brodribb, T. J., Cochard, H., Delzon, S., Bhaskar, R.,Bucci, S. J., Feild, T. S.,Gleason, S. M., Hacke, U. G., Jacobsen, A. L.; Lens, F.; Maherali, H.; Martínez-Vilalta, J.; Mayr, S.; Mencuccini, M.; Mitchell, P. J., Nardini, A., Pittermann, J., Pratt, R. B., Sperry, J. S., Westoby, M., Wright, I. J., Zanne, A. E. (2012). Global convergence in the vulnerability of forests to drought. *Nature,* 491, 752-755, doi:10.1038/nature11688.

Crossman, N.D., Nedkov, S., Brander, L., (2019). Water flow regulation for mitigating river and coastal flooding. SEEA EEA, *Revision* 15.

Dai, A., (2013). Increasing drought under global warming in observations and models *Nature Climate Change, 3, 52-58*, doi:10.1038/nclimate1633.

De Frenne, P., Rodríguez-Sánchez, F., Coomes, D.A., et al., (2013). Microclimate moderates plant responses to macroclimate warming. *PNAS*, 110, 18651-18565, doi:10.1073/pnas.1311190110.

Del Campo, A.D., Segura-Orenga, G. Ceacero, C.J., Gonzalez-Sanchis, M., Molina, A.J., Reyna, S., Hermoso, J., (2020). Reforesting drylands under novel climates with extreme drought filters: the importance of trait-based species selection. *Forest Ecology Management*, 467, doi:101016/jforeco2020118156.

Douglas, S., (2018). Forests, atmospheric water and an uncertain future: the new biology of the global water cycle. *Forest Ecosystem,* 5, 19, doi:10.1186/s40663-018-0138-y.

Ellison, D., N. Futter, M., & Bishop, K., (2012). On the forest cover–water yield debate: from demand- to supply-side thinking. *Global Change Biology*¸18(3), 806-820, doi:10.1111/j.1365-2486.2011.02589.x.

Ellison, D., Morris, C. E., Locatelli, B., Sheil, D., Cohen, J., Murdiyarso, D., Sullivan, C. A., (2017). Trees, forests and water: Cool insights for a hot world. *Global Environmental Change, 43*, 51-61, doi:10.1016/j.gloenvcha.2017.01.002.

Ficetola, G.F., Denoël, M., (2009). Ecological thresholds: An assessment of methods to identify abrupt changes in species-habitat relationships. *Ecography*, 32, 1075-1084, doi:10.1111/j.1600-0587.2009.05571.x.

Hannah, D. M., Malcolm, I. A., Soulsby, C., & Youngson, A. F., (2008). A comparison of forest and moorland stream microclimate, heat exchanges and thermal dynamics. *Hydrological Processes*, *22*(7), 919-940, doi:10.1002/hyp.70037.

Hart, K. M., Curioni, G., Blaen, P., Harper, N. J., Miles, P., Lewin, K. F., MacKenzie, A. R., (2019). Characteristics of free air carbon dioxide enrichment of a northern

temperate mature forest. *Global Change Biology*, *26*(2), 1023-1037, doi:10.1111/gcb.14786.

Hari, V., Rakovec, O., Markonis, Y., Hanel, M. & Kumar, R., (2020). Increased future occurrences of the exceptional 2018-2019 Central European drought under global warming. *Scientific Reports,* 10, (12207), doi:10.1038/s41598-020-68872-9.

Harvey, A.C., Peters, S., (1990). Estimation procedures for structural time series models. *Journal of Forecasting*, 9, 89-108, doi:10.1002/for.3980090203.

Hawkes, C.V., Kivlin S.N., Rocca J.D., Huguet V., Thomsen M.A., Suttle K.B., (2011). Funga community responses to precipitation. *Global Change Biology*, 17, 1637-1645.

Hazewinkel, M., (2001). Kolmogorov-smirnov test. In *Encyclopedia of Mathematics*. New York: Springer.

He, L., Ivanov, V.Y., Bohrer, G.,Thomsen, J.E., Vogel, C.S., Moghaddam, M., (2013). Temporal dynamics of soil moisture in a northern temperate mixed successional forest after a prescribed intermediate disturbance. *Agriculture and Forest Meteorology*, 180, 22-33, doi: 10.1016/j.agrformet.2013.04.014.

Holdo, R.M. and Nippert, J.B., (2015). Transpiration dynamic support resource partitioning in Africa savanna trees and grasses. *Ecology*¸ 96: 1466-1472, doi:10.1890/14-1986.1.

Hollis, J., Jones, B., Ullah, S., MacKenzie, R., Hart, K., (2021). Soil Profile Pit at BIFoR-FACE, Norbury Junction, Staffordshire, doi: https://edata.bham.ac.uk/706/.

Holmes, E. E., M. D. Scheuerell, and E. J. Ward, (2020). Applied time series analysis for fisheries and environmental data. NOAA Fisheries, Northwest Fisheries Science Center, 2725 Montlake Blvd E., Seattle, WA 98112, https://nwfsc-timeseries.github.io/atsa-labs/.

Ilstedt, U., Bargués Tobella, A., Bazié, H., Bayala, J., Verbeeten, E., Nyberg, G., Sanou, J., Benegas, L., Murdiyarso, H., Laudon, H., Sheil, D., Malmer, A., (2016).

Intermediate tree cover can maximize groundwater recharge in the seasonally dry tropics. *Scientific Report,* 6, 21930, doi:10.1038/srep21930.

Jenkins, M., Schaap, B. (2018). Forest ecosystem services. *United Nations Forum on Forests*, p. 41.

Jin, Z., Guo, L., Fan, B., Lin, H., Yu, Y., Zheng, H., Chu, G., Zhang, J., Hopkins, I. Effect of afforestation on soil and ambient air temperature in a pair of catchments on the Chinese Loess Plateau. *Catena*, 175, 356-366, doi: 10.1016/j.catena.2018.12.036.

Jones, J., Ellison, D., Ferraz, S., Lara, A., Wei, X., Zhang, Z, (2022). Forest restoration and hydrology. *Forest Ecology and Management*, 520, 120342, doi:10.1016/j.foreco.2022.120342.

Joslin, J.D., Wolfe, M.H., Hanson, P.J., (2000). Effects of altered water regimes on forest root systems. *New Phytologist*, 147, 117-129, doi:10.1046/j.1469-8137.2000.00692.x.

J.P.B. Blencowe, S.D. Moore, G.J. Young, R.C. Shearer, R. Hagerstrom, W.M. Conley, J.S. Potter, U.S. Soil Department of Agriculture Bulletin 462, (1960), pp. 1960.

Kahle, P., Baum C., Boelcke, B., (2005). Effect of Afforestation on Soil Properties and Mycorrhizal Formation. *Pedosphere*, 15, 754-760.

Krause, S., Taylor, S. L., Weatherill, J., Haffenden, A., Levy, A., Cassidy, N. J., & Thomas, P. A., (2013). Fibre-optic distributed temperature sensing for characterizing the impacts of vegetation coverage on thermal patterns in woodlands. *Ecohydrology*, *6*(5), 754-764, doi:10.1002/eco.1296.

Korkanç, S.Y., (2014). Effect of afforestation on soil organic carbon and other soil properties. *Catena*, 123, 62-69, doi:10.1016/j.catena.2014.07.009.

Kwatcho Kengdo, S., Peršon, D., Schindlbacher, A., Heinzle, J., Tian, Y., Wanek, W., & Borken, W., (2022). Long-term soil warming alters fine root dynamics and morphology, and their ectomycorrhizal fungal community in a temperate forest soil. *Global Change Biology*, 28, 3441-3458, doi:10.1111/gcb.16155.

Landsberg, J., Waring, R., & Ryan, M., (2017). Water relations in tree physiology: where to from here? *Tree Physiology*, 37(1), 18-32, doi:10.1093/treephys/tpw102 %J Tree Physiology.

Lange, B., Germann, P.F., Lüscher, P., (2013). Greater abundance of *Fagus sylvatica* in coniferous flood protection forests due to climate change: impact of modified root densities on infiltration. *European Journal Forest Research*, 132, 151-163, doi:10.1007/s10342-012-0664-z.

Levia, D. F., Creed, I. F., Hannah, D. M., Nanko, K., Boyer, E. W., Carlyle-Moses, D. E., Bruen, M., (2020). Homogenization of the terrestrial water cycle. *Nature Geoscience, 13*(10), 656-658, doi:10.1038/s41561-020-0641-y.

Liang, H., Xue, Y., Zongshan, L., Wang, S., Xing, W., Guangyao, G., Guohua, L., Bojie, F., (2018). Soil moisture decline following the plantation of Robinia pseudoacacia forests: Evidence from the Loess Plateau. *Forest Ecology and Management*, 412, 62-69, doi: 10.1016/j.foreco.2018.01.041.

Liu, X., Trogisch, S., He, J.S., Niklaus, P.A., Bruelheide, H., Tang, Z., Erfmeier, A., Scherer-Lorenzen, M., Pietsch, K.A., Yang, B., Kuhn, P., (2018). Tree species richness increases ecosystem carbon storage in subtropical forests. *Proceedings of The Royal Society B.*, 285, doi:10.1098/rspb.2018.1240.

Lewis, S. L., Wheeler, C. E., Mitchard, E., Koch, A., (2019). Restoring natural forests is the best way to remove atmospheric carbon. *Nature*, 568(7750), 25–28, doi:10.1038/d41586-019-01026-8.

Lõhmus, K., Truu, J., Truu, M., Kaar, E., Ostonen, I., Alama, S., Kuznetsova, T., Rosenvald, K., Vares, A., Uri, V., et al., (2006). Black alder as a promising deciduous species for the reclaiming of oil shale mining areas. *Browfield Sites III – Prevention, Assessment, Rehabilitation and Development of Browfield Sites*, 87-97, ISBN 1845640411, doi:10.1007/978-3-540-36763-5_24.

MacKenzie, A.R., Krause, S., Hart, K.M., Thomas, R.M., Blaen, P.J., Hamilton, R.L., Curioni, G., Quick, S.E., Kourmouli, A., Hannah, D.M., Comer-Warner, S.A.,

Brekenfeld, N., Ullah, S., Press, M.C, (2021). Water-soil-vegetation-atmosphere research in a temperate deciduous forest catchment, including under elevated CO_2. *Hydrological Processes*, 35:e14096, doi: 10.1002/hyp.14096.

Mapa, R.B., (1995). Effect of reforestation using Tectona grandis on infiltration and soil water retention. *Forest Ecology and Management*, 77, 119-125, doi:10.1016/0378-1127(95)03573-S.

McCormack, M. L., & Iversen, C. M., (2019). Physical and functional constraints on viable below-ground acquisition strategies. *Frontiers in Plant Science*, 10, 1215, doi:10.3389/fpls.2019.01215.

Met Office, (2020). MIDAS Open: UK hourly weather observation data, v202007. Centre For Environmental Data Analysis, doi:10.5285/8d85f664fc614ba0a28af3a2d7ef4533.

Mongil-Manso, J., Navarro-Hevia, J., San Martin, R., (2022). Impact of Land Use Change and Afforestation on Soil Properties in a Mediterranean Mountain Area of Central Spain. *Land*, 11, 1043, doi:10.3390/land11071043.

Naithani, K.J., Baldwin, D.C., Gaines, K.P., Lin, H., Eissenstat, D.M., (2013). Spatial distribution of tree species governs the spatio-temporal interaction of leaf area index and soil moisture across a forested landscape. *PLoS One*, 8(3):e58704, doi:10.1371/journal.pone.0058704.

Nan, W., Tat, F., Meng, X., Dong, Z., Xiao, N., (2020). Effects of age and density of *Pinus sylvestris* var. *mongolica* on soil moisture in the semiarid Mu Us Dunefield, northern China. *Forest Ecology and Management*, 473, 118313, doi: 10.1016/j.foreco.2020.118313.

Navarro-Cerrillo, RM, Rodriguez-Vallejo C, Silveiro E, Hortal A, Palacios-Rodríguez G, Duque-Lazo J, Camarero JJ, (2018). Cumulative Drought Stress Leads to a Loss of Growth Resilience and Explains Higher Mortality in Planted than in Naturally Regenerated *Pinus pinaster* Stands. *Forests*, 9(6):358, doi:10.3390/f9060358.

Neumann, R.B., Carbon, Z.G., (2012). The magnitude of hydraulic redistribution by plant roots: a review and synthesis of empirical and modeling studies. *New Phytologist*, 194, 337-352, doi: 10.1111/j.1469-8137.2012.04088.x.

Niinemets, Ü., & Valladares, F., (2006). Tolerance to shade, drought, and waterlogging of temperate Northern Hemisphere trees and shrubs. *Ecological Monographs,* 76(4), 521-547, doi: 10.1890/0012-9615(2006)076[0521: Ttsdaw]2.0.Co;2.

Pérez-Silos, I., Alvarez-Martinez, J.M. & Barquin, J., (2021). Large-Scale afforestation for ecosystem service provisioning: learning from the past to improve the future. *Landscape Ecology*, 36, 3329-3343, doi:10.1007/s10980-021-01306-7.

Porporato, A., D'Odorico, P., Laio, F., Ridolfi, L., Rodriguez-Iturbe, I., (2002). Ecohydrology of water-controlled ecosystems. *Advances in Water Resources*, 25, Issues 8-12, 1335-1348, doi:10.1016/S0309-1708(02)00058-1.

Pu, J.Y., Yao, X.Y., Den, Z.Y., Zhang, C.J., Zhang, M.C., Wang, W.T., (2006). Impact of climate change on soil water content in Loess Plateau, Gansu. *Journal of Soil Science*, 37(6), 1086-1090.

Qiu, H., Blaen, P., Comer-Warner, S., Hannah, D. M., Krause, S., & Phanikumar, M. S., (2019). Evaluating a Coupled Phenology-Surface Energy Balance Model to Understand Stream-Subsurface Temperature Dynamics in a Mixed-Use Farmland Catchment. *Water Resources Research*, *55*(2), 1675-1697, doi:10.1029/2018wr023644.

Querejeta J.I., Egerton-Warburton L.M., Allen M.F., (2007). Hydraulic lift may buffer rhizosphere hyphae against the negative effects of severe soil drying in a California oak savanna. *Soil Biology and Biogeochemistry*, 39, 409-417, doi: 10.1016/j.soilbio.2006.08.008.

Rey Benayas, J.M., Martinez-Baroja, L., Perez-Camacho, L., Villar-Salvador, P., Holl, K.D, (2015). Predation and aridity slow down the spread of 21-year-old planted woodland islets in restored Mediterranean farmland. *New Forest*, 46, 841-853, doi: 10.10007/s11056-015-9492-6.

Richter, R., Ballasus, H., Engelmann, R.A. *et al*, (2022). Tree species matter for forest microclimate regulation during the drought year 2018: disentangling environmental drivers and biotic drivers. *Nature Scientific Report*, 12, 17559, doi: 10.1038/s41598-022-22582-6.

Robinson, D.A., Jones, S.B., Lebron, I., Reinsch, S., Domínguez, M.T., Smith, A.R., Jones, D.L., Marshall, M.R., Emmet, B.A., (2016). Experimental evidence for drought induced alternative states of soil moisture. *Nature Scientific Report*, 6, 20018, doi:10.1038/srep20018.

Salazar, A., Rousk, K., Jónsdóttir, I. S., Bellenger, J.-P., & Andrésson, Ó. S., (2020). Faster nitrogen cycling and more fungal and root biomass in cold ecosystems under experimental warming: A meta-analysis. *Ecology*, 101(2), e02938, doi:10.1002/ecy.2938.

Shea, E., Vecchione, M., (2002). Quantification of ontogenetic discontinuities in three species of oegopsid squids using model II piecewise linear regression. *Marine Biology*, 140, 971-979, doi:10.1007/s00227-001-0772-7.

Schlesinger, W. H., Dietze, M. C., Jackson, R. B., Phillips, R. P., Rhoades, C. C., Rustad, L. E., & Vose, J. M., (2016). Forest biogeochemistry in response to drought. *Global Change Biology*, 22(7), 2318-2328, doi:10.1111/gcb.13105.

Seneviratne, S., Nicholls, N., Easterling, D., Goodess, C., Kanae, S., Kossin, J., Zhang, X., (2012). Changes in climate extremes and their impacts on the natural physical environment: An overview of the IPCC SREX report. In (pp. 12566).

Seneviratne, S. I., Corti, T., Davin, E. L., Hirschi, M., Jaeger, E. B., Lehner, I., Teuling, A. J., (2010). Investigating soil moisture–climate interactions in a changing climate: A review. *Earth-Science Reviews*, 99(3), 125-161, doi:10.1016/j.earscirev.2010.02.004.

Simard, S., Beiler, K., Bingham, M., Deslippe, J., Philip, L., Teste, F., (2012). Mycorrhizal networks: Mechanisms, ecology and modelling. *Fungal Biology Reviews*, 26, 39-60, doi: 10.1016/j.fbr.2012.01.001.

Spence, C., Hedstrom, N., Tank, S. E., Quinton, W. L., Olefeldt, D., Goodman, S., & Dion, N. (2020). Hydrological Resilience to Forest Fire in the Subarctic Canadian Shield. *Hydrological Processes*, 34:4940-4958, doi:10.1002/hyp.13915.

Stagge, J. H.; Kingston, D. G.; Tallaksen, L. M. & Hannah, D. M., (2017). Observed drought indices show increasing divergence across Europe. *Nature Scientific Reports,* 7, 14045, doi:10.1038/s41598-017-14283-2.

Tansey, C. J., Hadfield, J. D., & Phillimore, A. B., (2017). Estimating the ability of plants to plastically track temperature-mediated shifts in the spring phenological optimum. *Global Change Biology*, 23(8), 3321-3334, doi:10.1111/gcb.13624.

Toms, J.D., Lesperance, M.L., (2003). Piecewise Regression: a tool for identifying ecological thresholds. *Ecology*, 84, 2034-2041, doi:10.1890/02-0472.

Toms, J., Villard, M., (2015). Threshold detection: Matching statistical methodology to ecological questions and conservation planning objectives. *Avian Conservation and Ecology*, 10, 2, doi:10.5751/ACE-00715-100102.

UKCEH, UK Centre for Ecology & Hydrology, (2022): https://eip.ceh.ac.uk/hydrology/water-resources

Ullah, S., & Moore, T., (2009). Soil drainage and vegetation controls of nitrogen transformation rates in forest soils, southern Quebec. *Journal of Geophysical Research*, 114, doi:10.1029/2008JG000824.

Ullah, S., & Moore, T. R., (2011). Biogeochemical controls on methane, nitrous oxide, and carbon dioxide fluxes from deciduous forest soils in eastern Canada. *Journal of Geophysical Research,* 116, G03010, doi:10.1029/2010jg001525.

Viola, F., Daly, E., Vico, G., Cannarozzo, M., Porporato A., (2008). Transient soil-moisture dynamics and climate change in Mediterranean ecosystems. *Water Resources Research*, 44, 11, doi:10.1029/2007WR006371.

Vitasse, Y., (2013). Ontogenic changes rather than difference in temperature cause understory trees to leaf out earlier. *New Phytologist*, *198*(1), 149-155, doi:10.1111/nph.12130.

Wang, R., Cavagnaro, T.R., Jiang, Y., Keitel, C., Dijkstra, F.A., (2021). Carbon allocation to the rhizosphere is affected by drought and nitrogen addiction. *Journal of Ecology*, 109, 3699-3709, doi:10.1111/1365-2745.13746.

Weltzin, J. F., & McPherson, G. R., (1997). Spatial and temporal soil moisture resource partitioning by trees and grasses in a temperate savanna, Arizona, USA. *Oecologia, 112*(2), 156-164, doi:10.1007/s004420050295.

Wynn, H. P., (1985). The advanced theory of statistics, Vol. 3, 4th Edition, Kendall, Sir Maurice, Stuart, A. and Ord, J. K., High Wycombe: Charles Griffin, 1983. Pages: 780. *4*(3), 315-315, doi:10.1002/for.3980040310.

Yang, L., Wei, W., Chen, L., Mo, B., (2012). Response of deep soil moisture to land use and afforestation in the semi-arid Loess Plateau, China. *Journal of Hydrology*, 475, 111-122, doi: 10.1016/j.jhydrol.2012.09.041.

Yao, Y.B., Wang, Li, Y.H., Zhang, X.Y., (2005). Climate warming and drying and its environmental effects in the Loess Plateau. *Resour.Sci.*, 27(5), 146-152.

Yao, W., Nan, F., Li, Y., Li, Y., Liang, P., Zhao, C., (2023). Effects of Different Afforestation Years on Soil Properties and Quality. *Forests*, 14(2):329, doi:10.3390/f14020329

Zeileis, A., Leisch, F., Hornik, K., Kleiber, C., (2002). “Strucchange: An R Package for Testing for Structural Change in Linear Regression Models. *Journal of Statistical Software, 7(2)*, 1-38, doi:10.18637/jss.v007.i02.

Zhang, X., Qiang, G., Zhan, B., Peng, L., (2014). Experimental Study on Slope Runoff, Erosion and Sediment under Different Vegetation Types. *Water Resources Management*, 28, 2415-2433, doi:10.1007/s11269-014-0603-5.

Zimmermann, B., Elsenbeer, H., & De Moraes, J. M., (2006). The influence of land-use changes on soil hydraulic properties: Implications for runoff generation. *Forest Ecology and Management, 222*(1), 29-38, doi:10.1016/j.foreco.2005.10.070.

2.7 Appendix

2-S1: Juvenile plantation trees species composition

Common name	Latin name	Trees population composition
English Oak	*Quercus robur*	75
Silver Birch	*Betula pendula*	7.4
Wild Cherry	*Prunus avium*	6.7
Hazel	*Corylus avellana*	4.9
Hornbeam	*Carpinus betulus*	3.1
Rowan	*Sorbus aucuparia*	2.8
Field Maple	*Acer campestre*	2.3
Chestnut	*Castanea sativa*	1.8
Whitebeam	*Sorbus aria*	1.3
Wild Pear	*Pyrus communis*	0.8
Crab Apple	*Malus sylvestris*	0.5

2-S2: Data Filling

Filling of missing data in the juvenile plantation dataset. The data series contained 64 missing observations in the 4-year dataset (from 4-5-2016 to 2-2-2020). Missing observations were interpolated linearly for two periods (in red) prior to the decomposition analysis.

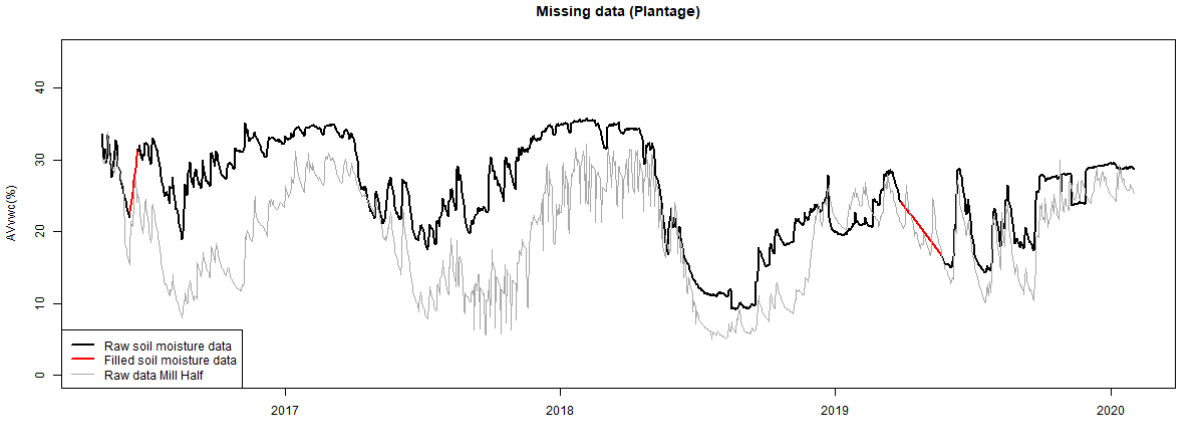

2-S3: Precipitation data distribution

The distribution of precipitation data allows for an emphasis on both the lower and upper extremes. The chosen thresholds of 5 mm (1.89%) and 20 mm (0.89%) highlight critical extremes in the rainfall distribution that are ecologically significant. Although these events occur infrequently, their rarity may underscore their significance, as atypical or extreme rainfall events often provoke notable responses in ecosystems.

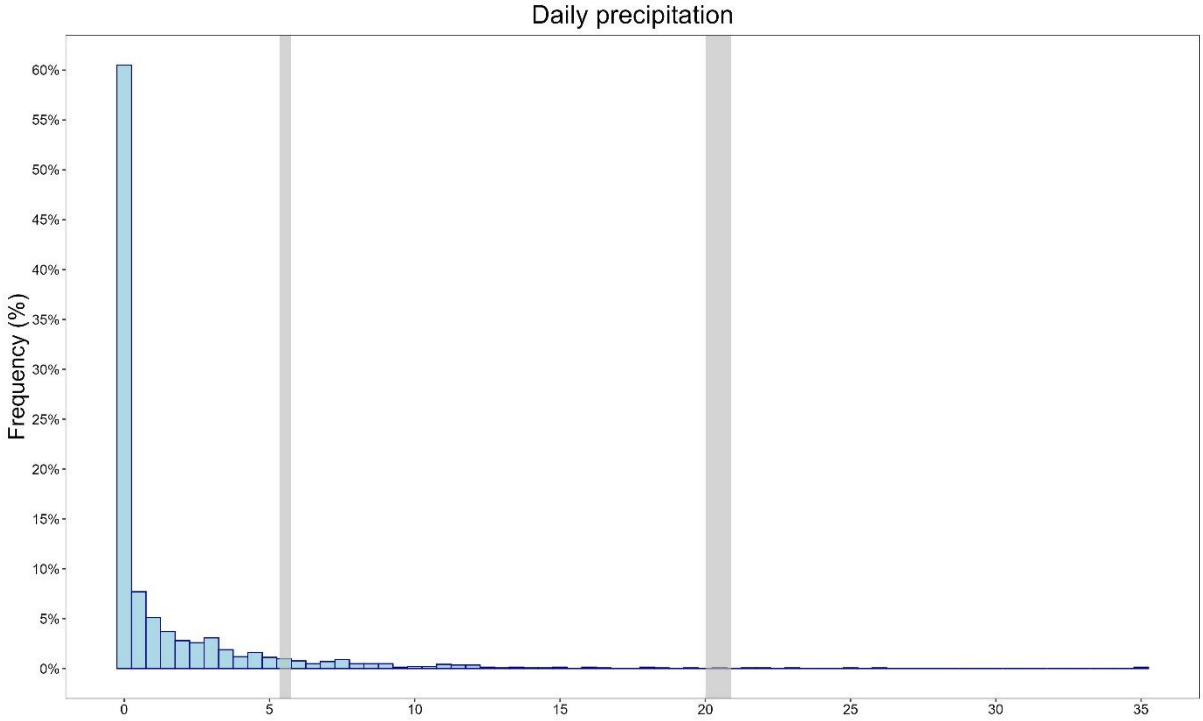

2-S4: Breakpoint analysis

Breaking point analysis for the trend dynamic of juvenile plantation water volumetric content. The three breakpoints, which were defined in R using the package "Strucchange", are on 24-05-2017, 15-12-2017, and 26-11-2018 respectively.

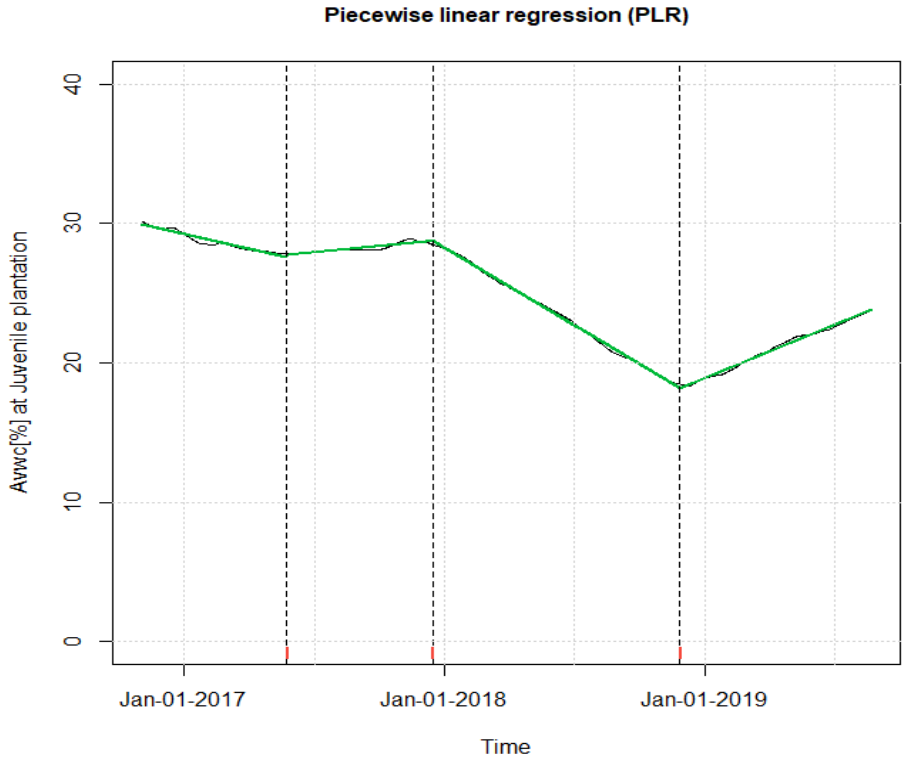

2-S5-A

Daily precipitation (A) and soil moisture dynamics (B) within the juvenile plantation. The three depths visualized in this graph are 10, 25, and 40 cm respectively. After the 2018 drought, where rainfall values decreased noticeably, comparable trends and absolute value changes can be observed.

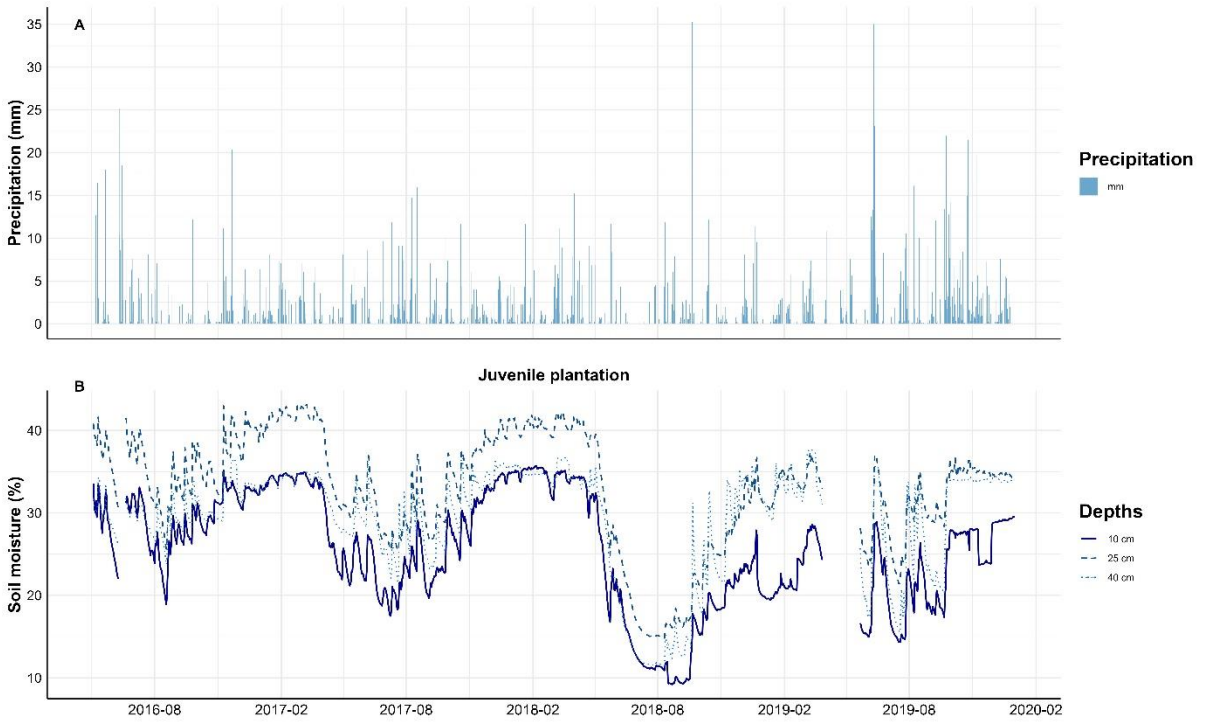

2-S5-B:

a zoom of daily precipitation (A) and soil moisture (B) within the juvenile plantation for the year 2018 is shown for clarity.

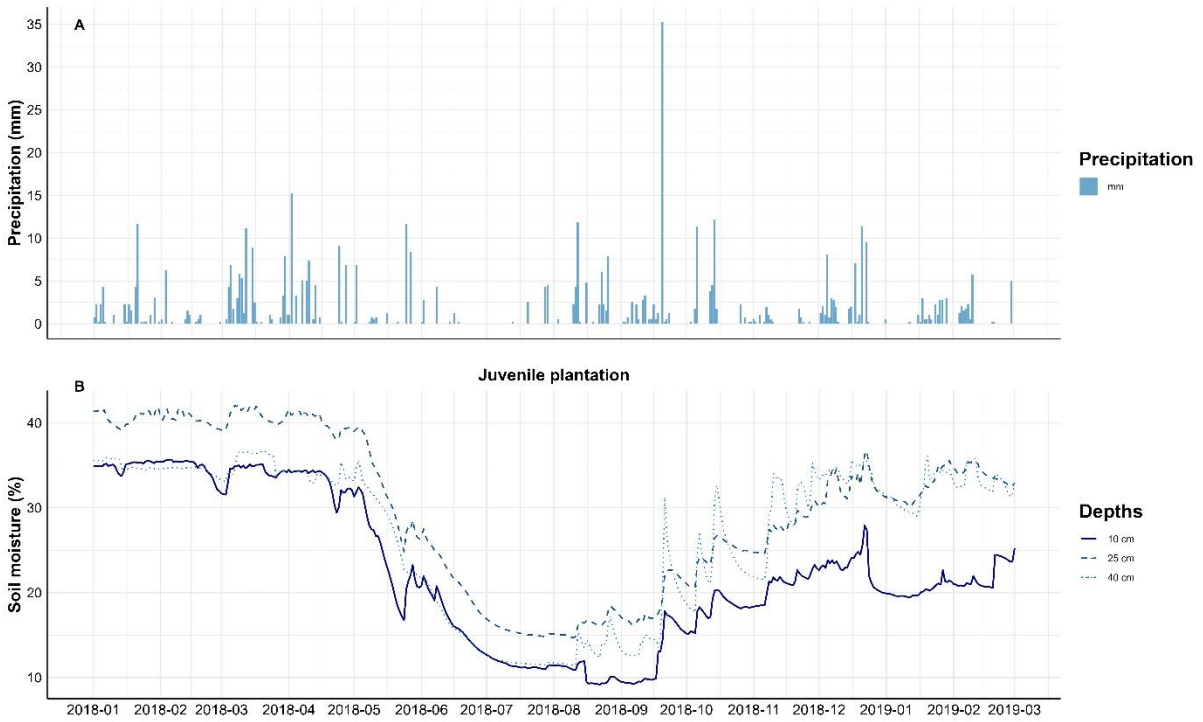
A
Precipitation (mm)
35
30
25
20
15
10
5
0
Precipitation
mm
Juvenile plantation
B
Soil moisture (%)
40
30
20
10
2018-01
2018-02
2018-03
2018-04
2018-05
2018-06
2018-07
2018-08
2018-09
2018-10
2018-11
2018-12
2019-01
2019-02
2019-03
Depths
10 cm
25 cm
40 cm

Chapter Two summary

In summary, this chapter evaluates the influence of a drought event on the hydrological function of juvenile forest, highlighting the transition towards conditions similar to those of a mature forest ecosystem. The case study examined changes in precipitation responses and hydrological patterns within the juvenile plantation, emphasizing the critical need for prolonged monitoring of soil hydrological processes in afforested areas. The study also spotlights the differential responses of young forest ecosystems to external stressors, such as drought, which significantly influence the uneven development of ecological functions, including temperature regulation due to canopy closure. These findings highlight the challenges posed by climate change-induced droughts in temperate regions and their potential implications for afforestation and reforestation initiatives. Understanding these dynamics is paramount for short-term and long-term management strategies in forest conservation and restoration efforts amidst changing environmental conditions. Further implications of these findings are discussed in the Conclusion and Outlook of the thesis (Chapter Five). Prior to that, we examine the relationship among mixed-species plantation management, site hydrological complexity, and intensive fertilization and irrigation (Chapter Three), while Chapter Four analyses the impact of fertilization on greenhouse gas emissions.

Chapter Three

Fertigation management of forest plantations: key aspects, challenges, and future perspective.

Authors: Andrea Rabbai, Giulio Curioni, Nicholas Kettridge, Sami Ullah, Stefan Krause.

Running head: Fertigation management of mixed species plantation

Word count: 5.760

Corresponding author:

Andrea Rabbai

School of Geography, Earth and Environmental Sciences

University of Birmingham,

Edgbaston

West Midlands

United Kingdom

B15 2TT

Email: axr1049@student.bham.ac.uk

Abstract

In the effort to limit global climate change to drive the average temperature increase to 2 °C above pre-industrial levels, ambitious goals for tree planting have been established as a crucial component of climate change mitigation strategies. Afforestation initiatives are recognized as a viable Natural Climate Solution (NCS) capable of capturing and storing large amounts of atmospheric CO_2. However, many challenges emerge when considering where and how to effectively manage new forest plantations. To mitigate climate change, future forests will have to meet targets for both productivity and carbon sequestration, while also being resilient to biotic and abiotic disturbances, including increased frequencies and magnitudes of hydrometeorological extremes such as drought. In this context, innovative silvicultural approaches, including combined fertilization and irrigation (fertirrigation), may have the potential to play a crucial role in meeting the established climate targets. Although many studies have focused on fertirrigation management in areas with water and nutrient limitations, there is a lack of research exploring the relationship between site suitability, fertirrigation management, and tree growth. Therefore, the aim of this study is to assess the growth and gross carbon uptake capacity (GCU) of a four-year-old mixed forest plantation in response to fertirrigation management, while considering the influence of soil texture and site hydrology. Our findings showed that fertirrigation increased overall tree growth and relative GCU by 70% and 56%, respectively, on sandy loam and loamy soil types. However, distinct deviations from this trend were observed, highlighting the significant role of complex site hydrology and soil characteristics in shaping the forest system response. Geospatial analysis of degree of saturation (SR) at shallow and 30 cm depths revealed consistent patterns that negatively influenced tree growth in specific areas of the site, despite fertirrigation. The outcomes of this study emphasize the need for a comprehensive understanding of the interplay between site-specific hydrological conditions, soil properties, and intensive forest management practices such as fertirrigation to optimize the effectiveness of afforestation initiatives in mitigating climate change.

Keywords: climate change mitigation, Forest management, Land suitability, Fertirrigation, BIFoR.

3.1 Introduction

Ensuring that the global average temperature remains 2 °C below pre-industrial levels requires a major societal and economic shift (Paris Agreement 2015). Achieving this target entails a significant reduction of anthropogenic carbon dioxide (CO_2) emissions and an increase in the biosphere carbon (C) sink capacity (Rockström et al., 2017). In this challenging context, forests management and forestry can play a crucial role. Forest ecosystems are the largest terrestrial C sink with nearly 45% of the organic carbon on land in their biomass and soils (Bonan et al., 2008). They are acknowledged as one of the main Natural Climate Solutions (NCS), with the potential to offset 27% (15.8 Pg CO_2-eqv yr^{-1}) of the required global emissions reduction by 2030 (Griscom et al., 2017). Therefore, the increased awareness of the role of forests as a C sink amid climate change resulted in a greater emphasis on their protection and restoration. The United Nations Framework Convention on Climate Change (UNFCCC), established in the early 1990s, has supported forestry-based emission reduction according to well-known policy frameworks: the Reduction of Emissions from Deforestation and Forest Degradation (REDD +), designed to preserve existing forest ecosystems, and Afforestation and Reforestation (A/R) projects under the Clean Development Mechanisms (CDM), which support forest surface expansion on non-forested or degraded forest land (UNFCCC, 2013).

According to Pugh et al. (2019), old growth and natural regenerating forests absorb nearly 2 Gigatonnes of carbon (Gtc) annually. However, a recent analysis suggests that forest plantations could capture up to 205 GtC (Bastin et al., 2019), accounting for approximately one-third of the total anthropogenic emissions (~ 600 GtC). This has drawn increased attention to forest plantations due to their significant capacity for carbon sequestration (Popkin, 2019). Other studies considered these initial C capture

projections to be overly optimistic (Lewis et al., 2019; Veldman et al., 2019), suggesting more conservative estimates with large-scale afforestation and reforestation efforts capable of removing between 40 and 100 GtC from the atmosphere when forests reach maturity. Considering a general C wood allocation of 2 t of C ha^{-1} $year^{-1}$ (Bonan et al., 2008) for newly planted forests, this approach serves as a long-term strategy (Ameray et al., 2021). Furthermore, land and water suitability were questioned for successful afforestation and reforestation initiatives (Lewis et al., 2019a). Thus, when considering forest plantations as an important part of the NCS, several factors need to be considered. These include logistical problems (seedling availability; Mataruga et al., 2023), biophysical limitations (e.g., site conditions, water availability, inadequate tree species selection, globalization of tree disease; Smith et al., 2016; Ramsfield et al., 2016), and climate change (Pawson et al., 2013), all of which may reduce the potential for C sequestration. Climate change in particular poses serious challenges to forest ecosystems, as the frequency, duration, and severity of droughts are expected to increase in the next century (DeSoto et al., 2020), with a consequent important shift in woodland composition (Yu et al., 2021). Mitigating the negative effects of climate change while increasing the C storage capacity of forest plantations requires the forestry sector to be innovative and forward-thinking (Bolte et al., 2010). In this context, the combination of drip irrigation and nitrogen (N) fertilization, commonly referred to as fertirrigation, could be part of effective drought-resilience techniques while enhancing forest stand productivity (Grant et al., 2013). The soil water and N status are closely linked to biomass production, and several studies highlight the role of fertigation in enhancing forest stand C sequestration capacity (Albaugh et al., 2004; Campoe et al., 2013). This explains the increasing interest in the adoption of fertigation in forest plantations, where the emphasis on productivity and efficient resource management aligns with the core principles of precision forest restoration (PFR; Castro et al., 2021). Fertigation has already found widespread application in the short-rotation forestry sector (SRF), where fast growing trees including poplar, aspen, willow, and sycamore are intensively managed for wood production (Schulze et al., 2017).

Cobb et al. (2008) found that sycamore trees exhibited 132% increase in total aboveground biomass, as well as nitrogen use efficiency under fertigation management. Similarly, Coyle et al. (2016) found a 26% increase in Net Primary Productivity (NPP) in Sycamore and Loblolly Pine when irrigation and fertilizer were applied together. Albaugh et al. (2004) reported that fertigation doubles the annual stem mass increment (8.5 Mg ha^{-1}) in a loblolly pine plantation in Scotland. These findings suggest that fertigation may represent a valuable tool in afforestation and reforestation initiatives that contribute to net-zero strategies (Land Use: Policies for a Net Zero UK, 2020) by increasing the total ecosystem atmospheric carbon sequestration (Lewis et al., 2019b). Despite these promising outcomes, a limited number of studies have focused on site-specific water and nutrient management or explored the intricate relationship between site suitability, fertigation, and tree growth (Castro et al., 2021; Khamzina, 2006; Dubovyk et al., 2013; Veldman et al., 2019). Traditionally, the relationship between forest plantations and fertigation management has been framed in terms of fertirrigation beneficial effects on forest productivity within sites characterized by water and nutrient deficits. There is therefore a pressing need for further understanding of the impact of fertirrigation on tree performance, especially in areas characterised by hydrological complexities resulting from the interaction among soil types, slopes, and shallow groundwater. Recent studies, exemplified by Bateman et al. (2023), questioned about the benefits of large-scale planting, especially when inappropriate species and environments are selected. Consequently, identifying, and characterizing areas suitable for afforestation within fertirrigated landscapes pose significant challenges. A crucial aspect in addressing these challenges is the spatial analysis of moisture patterns, which forms the basis for optimal land resource allocation and effective environmental interventions.

Therefore, this study aims to evaluate how intensive fertigation management affects the growth patterns, productivity, and gross carbon uptake (GCU) capacity of a four-year-old plantation forest. We hypothesize that that interplay among fertigation practices, soil textures, and site hydrology leads to diverse soil moisture conditions, thereby influencing the growth performance of the forest plantation. To investigate this,

we utilize geostatistical analysis techniques to analyse the spatial distribution of soil moisture expressed as soil saturation (SR) across the site. Specifically, we differentiate between shallow saturation (sSR) and deep saturation (dSR) to capture the variation in moisture at different soil depths. Our objective is to provide insights that inform decisions regarding the design and management of forest plantations, aiming to enhance productivity, biodiversity, economic viability, and overall forest health.

3.2 Material and methods

3.2.1 Field site description

The research site is located in rural Staffordshire, central England, UK, and is hosted by the Norbury Park Estate. It is a forest plantation planted in 2019, on a former agricultural land, where sunflowers were farmed until 2018 (52º 80' 43" N, 2º 29' 62", 95 m above mean sea level (AMSL). The forest plantation is located near the Birmingham Institute of Forest Research Free-Air Carbon Dioxide Enrichment (BIFoR FACE) facility (Mackenzie et al., 2021; Hart et al., 2019). The climate is temperate maritime, with a total rainfall over 2021, since April, of 648.47 mm, while in 2022 it was 867.9 mm. The annual average temperature above-canopy based on the daily average were 11.77 (± 0.13 SE) °C in 2021 from April onwards, and 11.73 (± 0.12 SE) °C for 2022. The highest temperature was registered in July 2022 at 28.7 °C (Figure 3.1).

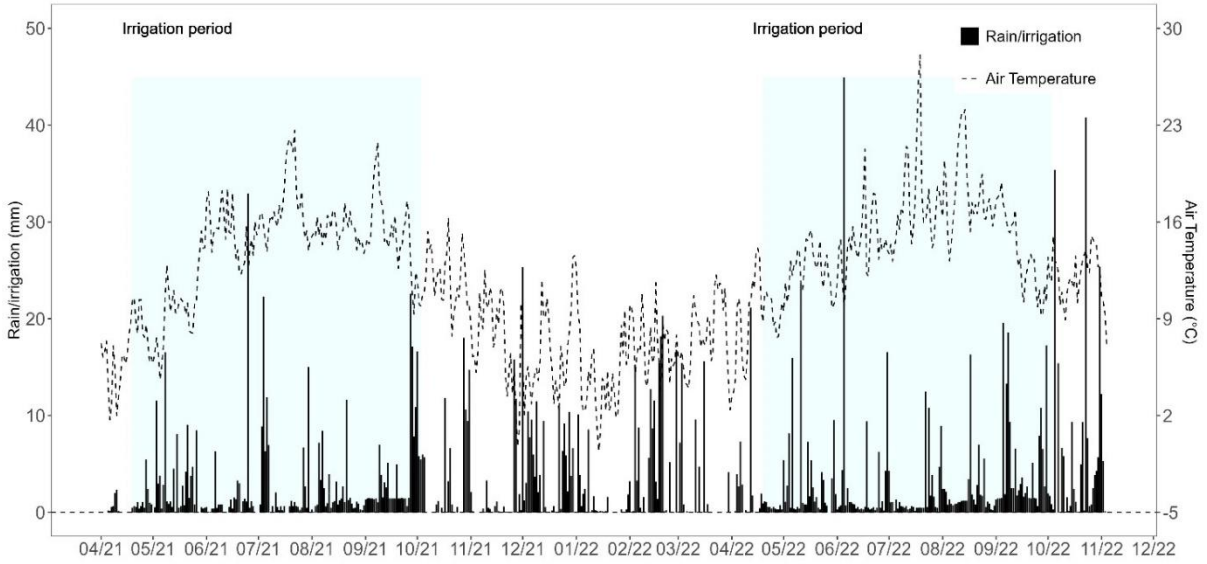

Figure 3.1: Daily mean air temperature (grey line), and precipitation/irrigation (black bars). The azure box indicates the period of irrigation and fertilizer application from April-October 2022.

The forest plantation is a 4.3 ha aggrading complex mixture of broadleaves and conifers (intimate mixture rather than compartments or lines) of nine different species distributed across zones LFt2-LFt3, SFt1-SFt3, SCt and with few parcels of oak monoculture in zones LFt1, and LCt1 (Figure 3.2). *Quercus robur* (English oak) from various geographical origins (England, Netherlands, and France) constitutes 60% of the entire forest plantation population. Other native UK species, including *Betula pendula* (silver birch), *Picea abies* (Norway spruce), *Pinus sylvestris* (Scots pine), *Alnus incana* (grey alder), *Acer pseudoplatanus* (European sycamore), and *Carpinus betulus* (hornbeam), combined with some American native species like *Abies fraseri* (fraser fir) and *Thuja plicata* (western red cedar), were planted in a 1:4 ratio with oaks, serving as “nurse trees”. Saplings, measuring less than 1 m in height, were planted at a density of 2600 trees per hectare. The rows were spaced approximately 2.4 m apart, with a distance of 1.6 m between individual trees within the same row. The geological composition includes surface till deposits, with limited presence of glaciofluvial deposits overlying the Helsby Sandstone Formation (BGS, 2020).

3.2.2 Experimental design

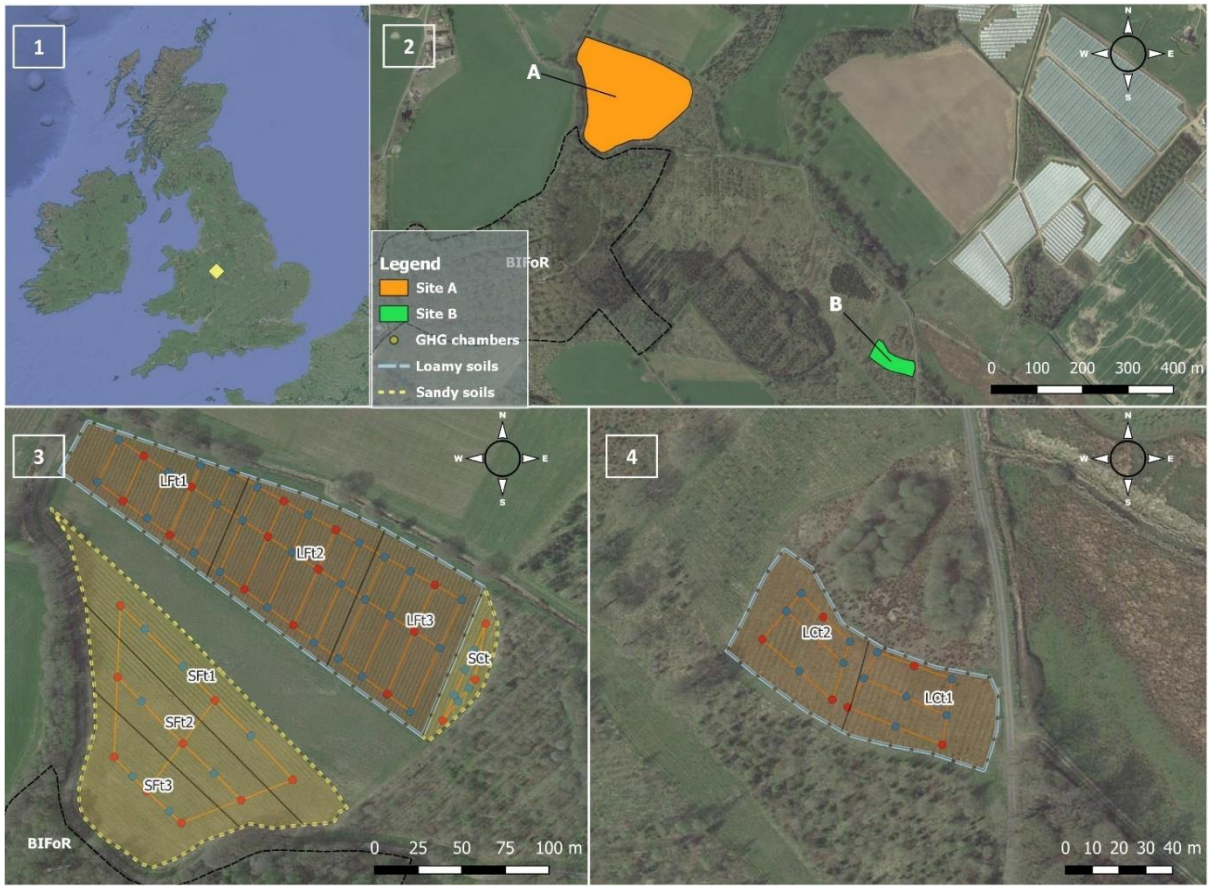

Figure 3.2: Field site map. In panel 1, the UK research site is shown. Panel 2 illustrates the various research areas within the Norbury Park Estate, with the main site A in orange and the control site B in green. Panel 3 provides details of the main site A, which covers zone LFt1-LFt3, SFt1-SFt3 and SCt, while panel 4 shows site B with LCt1 and LCt2 controls. Soil texture zone groupings are represented by blue-dashed lines for loamy conditions and yellow-dashed lines for sandy loam conditions. The moisture sampling grid is also illustrated, with blue and red points corresponding to shallow and deep & shallow soil moisture measurement, respectively.

The study site consists of two afforested locations: the main site A of 3.5 ha, located on a hill with a gentle slope with elevation spanning from 95 to 92 m, and site B of 0.8 ha, located 650 m south-east with elevation between 94 and 93 m (Figure 3.2). Site A includes the fertilized and irrigated zones LFt1-LFt3, SFt1-SFt3, and the SCt control, while site B includes control zones LCt1 and LCt2. As shown in Table 3.1, the eight zones within the two sites were grouped according to their soil type, following the

USDA soil classification. Zones LFt1-LFt3 and LCt1-LCt2 are representative of loamy conditions, while zones SFt1-SFt3 and SCt exhibit sandy loamy characteristics. Irrigation water is drawn from a water reservoir through a pump station and conveyed via pressured PVC pipelines with a total length of 387.5 m. The water supplied for zones LFt1-LFt3 and SFt1-SFt3 relies on surface drip irrigation. This method utilizes polyethylene tubes with emitters spaced 50 cm apart, aligned with the rows of trees (details in Appendix 3-S1). The forest plantation is irrigated from mid-April to early October each year (Figure 3.1). Soil moisture levels are monitored weekly by the estate managers at 10 and 30 cm depths using an SM150t probe (Delta-T Devices Ltd., UK) across settled points within the sites. Aiming to maintain a soil moisture level of 35%, the irrigation management involves two daily irrigations scheduled for early morning and late afternoon, seven days a week. The irrigation system applies an estimated annual water supply of 145 ± (3.9 SE) mm per zone. Nitrogen-based fertilizer Hortimix Extra (Hortifeeds©, Park Farm, Park Farm Road, Kettlethorpe, Lincoln, UK) was also applied every Tuesday and Friday. A malfunction of the irrigation system in zones LFt2 and LFt3 was reported in June 2022. During spring and summer, intensive weed control management was carried out through glyphosate applications.

Table 3.1: soil texture characterization and grouping of each specific zone based on the USDA soil classification (USDA). Soil characteristics are the mean of n = 5 samples for each zone. Also reported are the average value of bulk density (BD) for each zone and the number of samples (n) used for soil characterization.

Zone	Management	n (samples)	Sand (%)	Silt (%)	Clay (%)	Soil texture	BD
	Group 1						
LFt1	Fertirrigation	5	36.2	38.3	25.5	Loam	1.06
LFt2	Fertirrigation	5	38.6	37.4	24.6	Loam	1.04
LFt3	Fertirrigation	5	39.9	36.1	24.0	Loam	0.95

LCt1	Control	5	39.4	38.3	22.3	Loam	1.05
LCt2	Control	5	39.4	38.3	22.3	Loam	1.05
	Group 2						
SFt1	Fertirrigation	5	52.7	28.3	19.0	Sandy Loam	1.22
SFt2	Fertirrigation	5	51.3	29.5	19.2	Sandy Loam	1.40
SFt3	Fertirrigation	4	44.1	34.6	21.3	Sandy Loam	1.42
SCt	Control	4	45.2	32.9	21.8	Sandy Loam	1.12

3.2.3 Soil physical properties

To assess the soil texture, forty undisturbed soil samples were collected using a soil corer with a 68-cm diameter and 70-cm tube length. The sampling was conducted following a random approach, with five samples collected in each designed zone. The soil texture composition was analysed utilizing laser diffraction particle size analysis via Mastersizer 2000 with the Hydro Mu attachment (Malvern Ltd., UK). For this analysis, 1 gramme of soil subsamples underwent digestion with 30% hydrogen peroxide (H_2O_2), followed by a chemical dispersion in sodium hexametaphosphate ($(NaPO_3)_6$). Instrument parameters were configured based on the recommendations of Ryzak & Bieganoswky (2011) to ensure reliable soil texture measurements. Furthermore, to determine the bulk density (BD), an additional forty soil samples were collected using the same random approach. A custom-made soil corer with a diameter of 4.2 cm and a length of 15 cm was employed for sample collection. Soil samples were placed in a plastic bag, labelled according to progressive number and zones,

and transferred to the laboratory. Soil samples were air-dried for 72 h for determination of BD, total porosity, and void volume.

3.2.4 Soil moisture monitoring

To investigate the hydrological influence of irrigation practices and rainfall on site, data about the spatial and temporal dynamics of volumetric water content (VWC) of. the soils were gathered over a 16-month campaign, from July 2021 to October 2022. Shallow and profile measurements of VWC were collected weekly during the spring and summer seasons, and monthly during the autumn and winter seasons.

Shallow soil moisture at 5 cm depth was measured with a ML3 Theta Probe (Delta T-Device LTD, UK) at high spatial resolution, according to 86 sampling points evenly distributed in a regular grid of 30 x 25 m across all zones (Figure 3.2). To monitor the soil moisture profile, 34 sampling points were established according to a 30 x 100 m regular grid (Figure 3.2). All data points locations within the study area were recorded using a handheld global positioning system (GPS; Garmin Etrex 10). Hand-auger equipment was used to bore holes at the sampling points for installing the 40-cm-long access tubes compatible with the PR2/4 Profile Probe (Delta T-device Ltd., UK). Each tube was then equipped with a cap and collar to prevent water flow into and along the outside wall of the access tubes. After the installation, all the access tubes were left for a few weeks to ensure the consolidation of soil around the tubes. Continuous measurement of VWC was made by inserting a PR2/4 profile probe (a multi-level capacitance probe with 4 sensors at depths of 10, 20, 30, and 40 cm) into the access tubes. The measurements were taken using a handheld HH2 moisture meter (Delta-T Device Ltd., UK) along with the PR2/4. For each location, for both shallow and deep moisture, three replicates of the measurements were taken. The VWC data were converted into the corresponding degree of saturation (SR), representing the soil water saturation. This conversion was achieved by using the ratio of volumetric water content to the total volume of voids, as defined in the following equation:

$$SR = \frac{\Theta_v}{\Theta_s} = \frac{\Theta_v}{\frac{\mathrm{p}-BD}{\mathrm{p}}} \quad [3.1]$$

where Θ_v represents the volumetric water content (VWC), Θ_s the volumetric saturation, p the particle density equal to 2.75 g/cm^3 for mineral particles (Blake, 1965) and BD the bulk density (g/cm^3) measured across each zone.

3.2.5 Tree growth monitoring within the mixed plantations

Tree growth is an essential indicator of the relationship between climate, hydrology, and site characteristics. A total of 1764 trees across nine species were surveyed, respectively in October 2021 and October 2022. Within each zone, 25 specimens per species were tagged and georeferenced to ensure measurement consistency over time. To account for the spatial variability of tree performances, a random sampling strategy was applied. Measurements of the diameter at breast height (DBH) were taken at 1.3 m aboveground and at the root collar, according to the tree heights. To ensure measure consistency across the two-year survey, the measure spots were marked with biodegradable paint. Tree heights for all species were recorded through a combination of an extendible height stick and a clinometer, specifically for the tallest trees. By comparing the height and DBH data obtained from the two surveys, we calculated the growth rates across species and soil types. The estimation of tree biomass was conducted using species-specific generalized allometric equations proposed by Forrester et al. (2017). The Total biomass, including both above- and below-ground biomass, was determined using a root-shoot ratio of 0.3, as recommended by Mokany (2006). To calculate the tree carbon stock, a Carbon Content (CC) fraction of 0.47 was applied based on the 2006 IPCC guidelines. Finally, from the CC the net C_2O uptake was derived.

3.2.6 Statistical analysis

3.2.6.1 Spatial interpolation for the degree of saturation (SR)

Analysing the spatial distribution of the soil degree of saturation (SR) is a crucial step for understanding the site hydrological complexities and their relationship with forest plantation growth, potentially helping to design and manage the irrigation system according to the site characteristics. In this study, two geospatial interpolation techniques, Ordinary Kriging (OK) and Inverse Distance Weighting (IDW), were applied to compute the complex geospatial information of soil SR. The OK was selected to capture the spatial variability of shallow SR according to high-resolution sampling point grid of 30 x 25 m (Figure 3.2). Conversely, IDW was applied for SR measurements at depths of 10, 20, 30, and 40 cm, based on a lower resolution grid of 30 x 100 m (Figure 3.2). IDW is well known for its reduced sensitivity to limited spatial data compared to the OK method, where the semivariogram may struggle to capture the spatial correlation structure (Mueller et al., 2001). Our specific emphasis was on examining the spatial variations in soil SR at a depth of 30 cm, as trees primarily respond to moisture availability in deeper soil layers (Weltzin and McPherson, 1997; Tromp-van Meerveld et al, 2006).

3.2.6.2 Ordinary Kriging for shallow degree of saturation spatial patterns (sSR).

OK is an interpolation technique which predicts the value $Z^*(x_0)$ at the unsampled location x_0, as a linear combination of the observed values (Johnston et al., 2001). Therefore, based on OK, the predicted SR at an unsampled location $Z(x_o)$, using measured values $Z(x_i)$ $(i = 1, 2, \dots, n)$, is given by the following equation:

$$Z(x_o) = \sum_{i=1}^{n} \lambda_i * Z(x_i) \qquad [3.2]$$

Where λ_i is the weighting coefficient from the measured position to x_o. The fundamental aspect in the OK is the choice of a model and the corresponding geostatistical parameters used to fit an empirical semivariogram used in the interpolation (Goovaerts, 1997; Kitanidis, 1997) of specific points in a regular grid. In our study, the sample values were interpolated according to a regular grid of 10 m resolution. The semivariogram is defined as the expected value of the squared difference between pairs of the variables in space, and is given by the following equation:

$$\gamma(h) = \frac{1}{2}\{[Z(x_i) - Z(x_i + h)]^2\} \quad [3.3]$$

where $\gamma(h)$ is the semivariogram, $Z(x_i)$ is the observed value at point x, $Z(x_i + h)$ is the observed value of the variable at point $x_i + h$, and h is the distance between the pairs of observation. We used the function *autofitVariogram* from the package *automap* (Hiemstra & Skoien, 2023) in R, which automatically chooses a model based on the characteristics of the dataset. In our case, the models selected were the spherical models.

3.2.6.3 Inverse distance weighting for soil profile degree of saturation (dSR)

The IDW is a deterministic spatial interpolation model based on the assumption that the estimated values at a given point are more correlated with closer observed values compared to those at a greater distance. As the gap between estimated and measured points increased, the influence of the measured point diminishes (Hartkamp et al., 1999). The IDW equation is given as follows (Lu et al., 2006):

$$\hat{Z}(x_0) = \frac{\sum_{i=1}^{N} Z(x_i) w_i}{\sum_{i=1}^{N} w_i} \quad [3.4]$$

where the estimated value $\hat{Z}(x_0)$ in location x_0 is the linear combination of the weights (w_i) and the observed Z values at sampled locations $x_i, i = 1 \ldots N$. The weights (w_i)

are calculated as the inverse of distance between x_0 and x_i, raised to the power of α, which in this study was set at 2, indicating squared distance (Lloyd, 2005). The parameter α introduce a geometric factor that regulates the influence of distant location in the interpolation computations. The interpolation is performed on a regular grid with a resolution of 10 m. For the IDW interpolation we use the *idw* function from the package *gstat* (Pebesma & Graeler, 2023) in R.

3.2.6.4 Validation of spatial prediction for shallow and profile degree of saturation

The leave-out-cross validation (LOCV) was used to evaluate the model performance for predicting SR values at the unsampled locations. The indices used during LOCV were the root mean square error (RMSE) and the normalized root mean square error (NRMSE). The RMSE was calculated according to the following equation (Merdun et al., 2006):

$$RMSE = \sqrt{\frac{1}{v}\sum_{i=1}^{N}(Z(x_i) - Z(x_o))^2} \quad [3.5]$$

where $Z(x_i)$ are the observed values at v validation sample points, and $Z(x_0)$ are the predicted values. NRMSE was normalized using the range between the maximum and minimum of observed values as follows:

$$NRMSE = \frac{\sqrt{\frac{1}{v}\sum_{i=1}^{N}(Z(x_i) - Z(x_o))^2}}{\max\big(Z(x_i)\big) - \min\,(Z(x_i))} \quad [3.6]$$

Lower values of RMSE, and NRMSE indicate more accurate model predictions.

3.2.6.5 Kruskal Wallis test

The Kruskal-Wallis (K, Kruskal & Wallis, 1952) was used as a statistical test to assess the difference in tree species growth among the different zones and fertirrigation treatments. This non-parametric test is particularly useful when dealing with non-normally distributed continuous variable, such as ordinal or rank data. The null hypothesis (H_0) specifies that groups are subset from the same population, showing no significant difference among them. The test involves ranking the data variable of interest and calculating the H statistic according to the following equation:

$$K = (N-1)\frac{\sum_{i=1}^{g} n_i(\overline{r_i} - \overline{r_i})^2}{\sum_{i=1}^{g}\sum_{j=1}^{n_i}(r_{ij} - \overline{r_i})^2} \quad [3.7]$$

Where N is the number of total observations across groups, n_i is the number of observations within the group i, r_{ij} is the rank of the observed value j within the group i. If H exceeds the critical value (0.05), the null hypothesis is rejected, indicating that at least one group differs significantly from the others. A post-hoc test employing Bonferroni correction was applied to determine significant distinction among multiple groups. All statistical analysis were performed using R Statistical Software (version 2023.03.0; R Foundation for Statistical Computing, Vienna, Austria).

3.3 Results

3.3.1 Spatial interpolation for degree of saturation (SR)

Through modelling the spatial distribution of soil degree of saturation (SR), we enhance our understanding of site hydrological complexities and their potential impact on mixed-forest plantation growth. This is evidenced by the OK spatial prediction maps

for shallow degree of saturation (sSR) across seasons at both sites A and B, as illustrated in Figures 3 and 4. Table 3.2, presents the identified semivariogram parameters for the sSR data, alongside RMSE and NRMSE metrics, which highlight the good performance of the models in effectively capturing the spatial distribution of the variable.

Table 3.2: Semivariogram parameters of the ordinary kriging (OK) with root mean square error (RMSE) and normalized mean square error (NRMSE) for each model.

Site	Season	Sample Size	Model	Nugget effectC_0 (	C	r (m)	RMSE	NRMSE
A	Winter	60	Spherical	0.0069	0.012	60	0.08	0.11
A	Spring	60	Spherical	0.00065	0.02	91	0.09	0.15
A	Summer	60	Spherical	0	0.01	91	0.09	0.16
A	Autumn	60	Spherical	0	0.01	31	0.09	0.15
B	Winter	19	Spherical	0	0.01	16	0.10	0.19
B	Spring	19	Spherical	0.011	0.06	120	0.08	0.15
B	Summer	19	Spherical	9.65	5	120	0.06	0.11
B	Autumn	19	Spherical	0.00191	4.4	120	0.08	0.15

C0 nugget variance, C spatial dependency component, r the range.

In Figure 3.3 for site A, distinct spatial patterns emerge in each season, illustrating the dynamic nature of sSR. Appendix 3-S2 presents the semivariograms for each season, providing a detailed visualization of the models that fit the data. However, temporal, and cross-zonal analysis reveal some persistent sSR characteristics. In zones LFt1 and LFt2 at the foot slope, consistently elevated sSR values ranging from 0.6 and 1 are observed across all seasons, contrasting with the more variable state in zone LFt3. Similarly, zones SFt1, SFt2, and SFt3 at the shoulder and summit of the hill, exhibited a wider range of sSR values, from 0.3 to 0.9 depending on the seasons. For instance, during summer (Figure 3.3C), a southeast to northwest sSR gradient is visible, with only a few parcels between zones SFt2 and SFt3 showing high sSR. At site B (Figure 3.4), the spatial distribution of sSR display a consistent pattern across seasons, with LCt1 generally drier than LCt2, and the north edge often experiencing saturation.

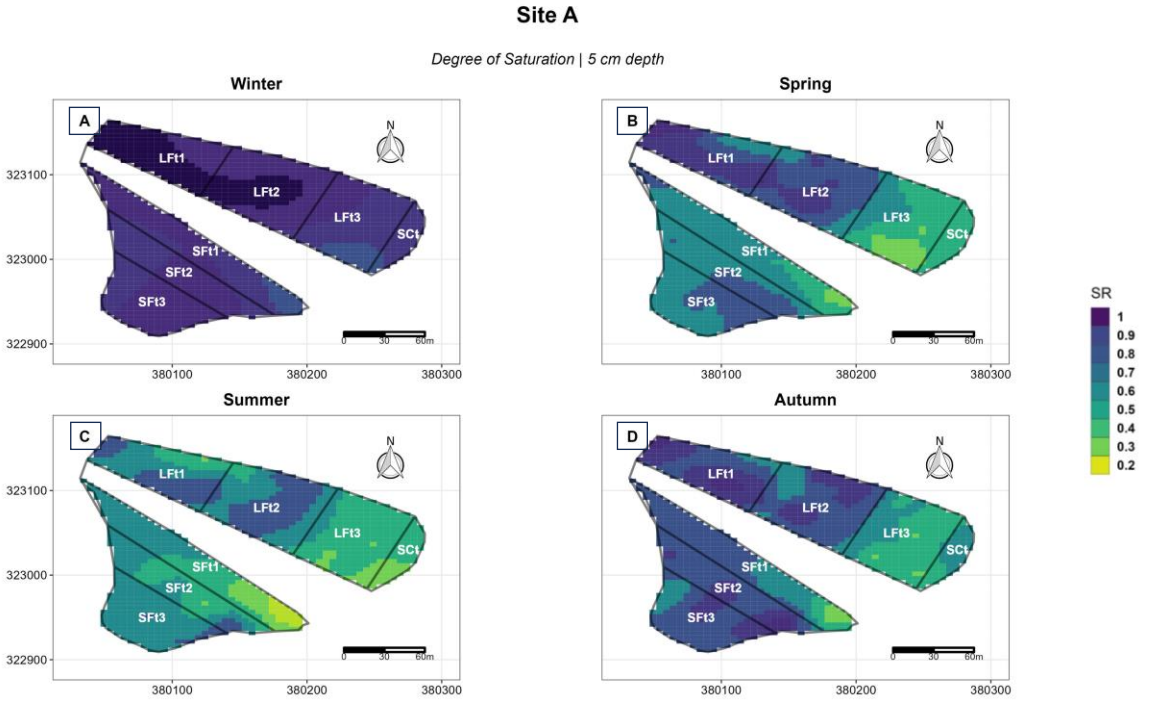

Figure 3.3: Map of the shallow degree of saturation (sSR) spatial distribution based on the measured data and fitted variograms at site A, which includes zones LFt1-LFt3, SFt1-SFt3, and SCt. Panels A-D indicate the variability of sSR across seasons.

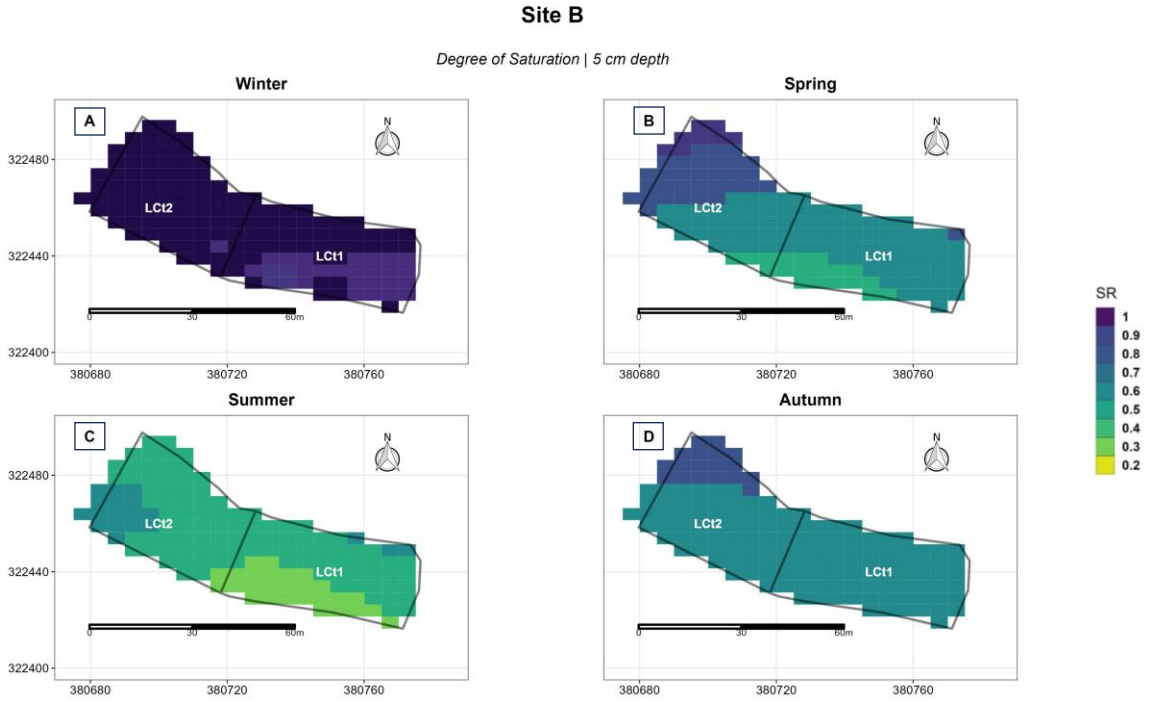

Figure 3.4: Map of the shallow degree of saturation (sSR) spatial distribution based on the measured data and fitted variograms at site B, which includes zones LCt1 and LCt2. Panels A-D indicate the variability of sSR across seasons.

The IDW interpolation maps for the 30 cm depth SR (dSR) at sites A and B (Figure 3.5, 3.6) offer additional insights into the spatial variability observed in the sSR (details for the interpolation maps at 10, 20, and 40 cm can be found in Appendix 3-S3:8). The robust performance of the IDW method is evident from the RMSE and NRMSE presented in Table 3.3. Zones LFt1 and LFt2 continue to show significant saturation levels, with the south-west area having persistent values of dSR above 0.6 across seasons. Zones SFt1-SFt3, LFt3, and SCt, on the other hand, exhibit more variable and drier conditions, echoing what was observed in the sSR dynamic (Figure 3.3). Similarly, the dSR patterns observed at site B (Figure 3.6) align with what was previously noted in the sSR spatial variability.

Table 3.3: RMSE and NRMSE for the IDW interpolation of 30 cm depth degree of saturation (dSR) at site A and site B.

Site	Season	RMSE	NRMSE
A	Winter	0.22	0.25
A	Spring	0.13	0.19
A	Summer	0.16	0.27
A	Autumn	0.21	0.39
B	Winter	0.00009	0.0023
B	Spring	0.0046	0.017
B	Summer	0.0008	0.004
B	Autumn	0.001	0.008

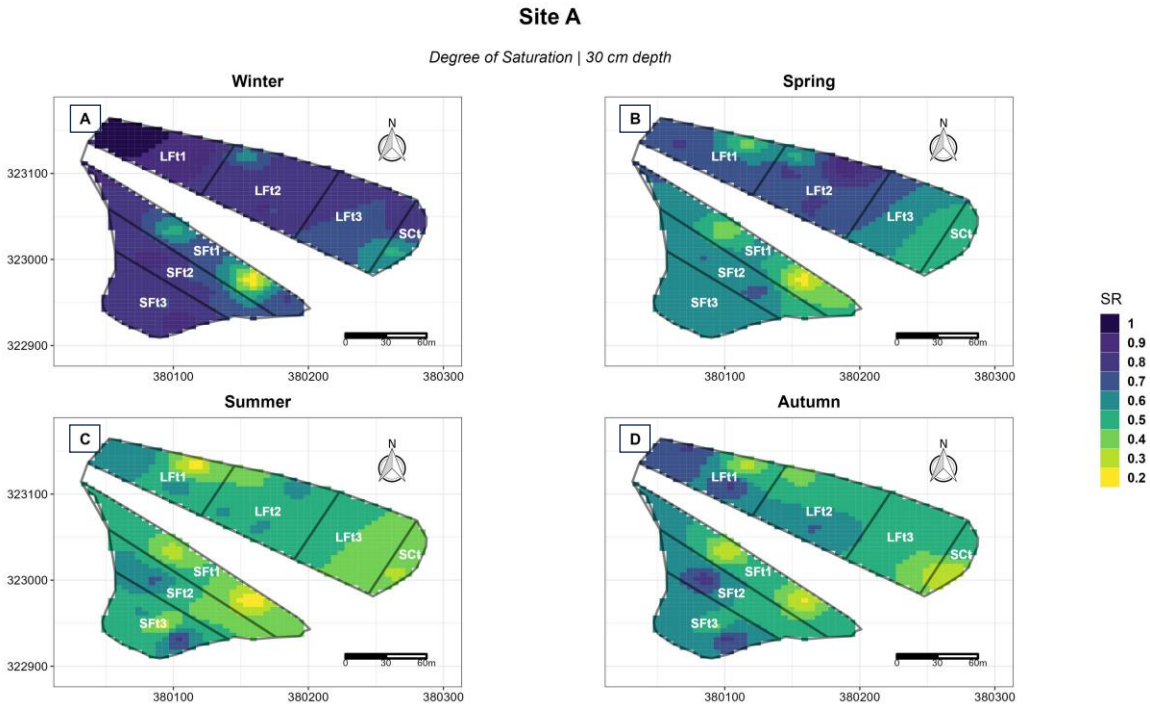

Figure 3.5: Map of 30 cm depth degree of saturation (dSR) spatial distribution based on measured data at site A, which includes zones LFt1-LFt3, SFt1-SFt3, and SCt. Panels A-D indicate the variability of dSR across seasons.

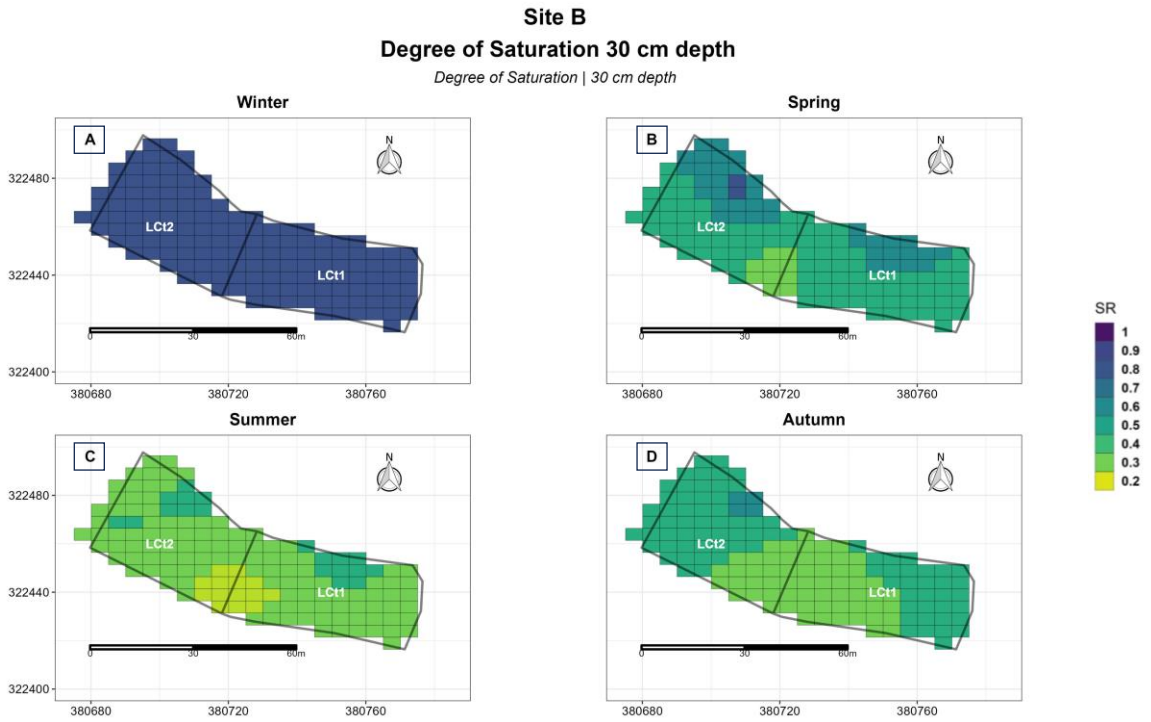

Figure 3.6: Map of 30 cm depth degree of saturation (dSR) spatial distribution based on measured data at site B, which includes zones LCt1and LCt2. Panels A-D indicate the variability of dSR across seasons.

3.3.2 Tree growth responses to fertirrigation management and site hydrological conditions

Variations in growth responses among conifer tree species were observed based on zones and soil types (Figure 3.7). Generally, conifer trees performed significantly better on sandy loam soil, exhibiting higher average heights compared to loamy soils. *Pinus sylvestris*, for instance, revealed a significant height difference ($p < 0.05$) between sandy loam zones SFt3, SFt2, SFt3, and SCt, and loamy zones LFt1 and LCt1. The lone exception was the loamy zone of LFt3, where conifer tree heights were comparable to those in sandy loam conditions. Fertirrigation, on the contrary, did not have a notable impact on the growth of conifer trees across soil types for most of the species. Specifically, under loamy conditions, *Pinus sylvestris*, *Picea abies*, *Abies fraseri*, and *Thuja plicata* did not demonstrated significant height differences when

comparing the fertirrigated LFt2 and LFt3 zones with their respective control LCt1. Similar results were obtained under sandy conditions, with only *Picea abies* showing a significant height difference (K test: p-value < 0.05) when fertirrigated SFt1, SFt2 and SFt3 zones were compared with SCt1 control. (Figure 3.7). Similarly, deciduous tree species showed higher growth performances in sandy soil than in loamy soil (Figure 3.8). *Betula pendula* and *Alnus incana* exhibited comparable growth, with an average 17% height increase in SFt1, SFt2, and Sft3 sandy zones compared to LFt3, and LFt2 loamy zones when fertirrigated. Under sandy control conditions the growth of *Betula pendula* and *Alnus incana* was even higher, with a 30% increase compared to what was observed in loamy soils. *Acer pseudoplatanus* showed similar growth patterns, with a 22% height increase when subjected to fertirrigation in sandy conditions compared to loamy soil. Under sandy control conditions in zone SCt, *Acer pseudoplatanus* showed a 64% increase in tree height compared to the LCt1 loamy control. *Carpinus betulus*, on the other hand, exhibited no significant height variations among the fertirrigated SFt1, SFt2, SFt3 sandy zones and LFt2, LFt3 loamy zones. Similar to other deciduous species, *Carpinus betulus* showed enhanced growth under control sandy conditions in zone SCt, with a 50% height increase compared to loamy control LCt1. In contrast to the observed effect on conifer trees, fertirrigation had a significant influence on the growth of deciduous trees across both loamy and sandy soil types (Figure 3.8). *Betula pendula, Alnus incana, Acer pseudoplatanus*, and *Carpinus betulus* showed significantly greater growth (K test: p-value < 0.05) under loamy fertirrigated zones LFt1 and LFt2 compared to their control LCt1 (Figure 3.8A, 3.8C, 3.8E, 3.8G). Similarly, in sandy fertirrigated zones SFt1, SFt2, and SFt3 *Betula pendula* and *Alnus incana* showed significantly higher growth (K test: p-value < 0.05) compared to the SCt control. However, *Acer pseudoplatanus* and *Carpinus betulus* did not show any significant differences in growth between fertirrigated sandy zones and the control.

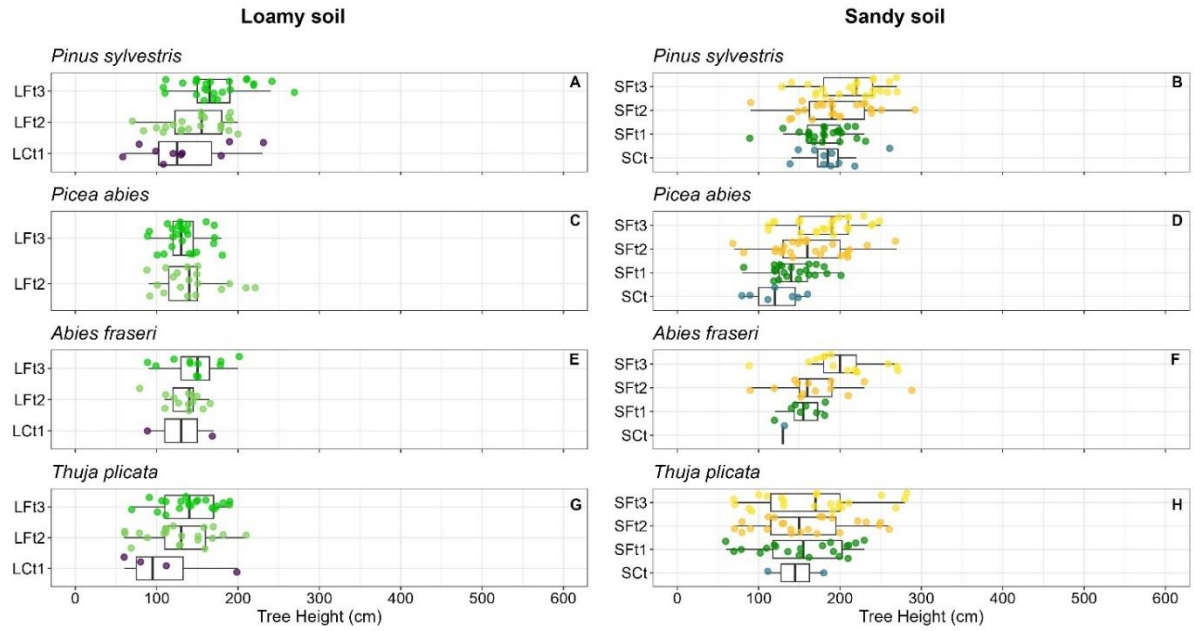

Figure 3.7: Boxplot with individual data points (with different colours for each zone) illustrating tree heights across different coniferous species and soil types. Panels A, C, E, G illustrates Pinus sylvestris, Picea abies, Abies fraseri, and Thuja plicata heights distribution under loamy fertirrigated (LFt2, LFt3) and control (LCt1) conditions. Panels B, D, F, H represent Pinus sylvestris, Picea abies, Abies fraseri, and Thuja plicata heights distribution under sandy fertirrigated (SFt1, SFt2, SFt3) and control (SCt) conditions.

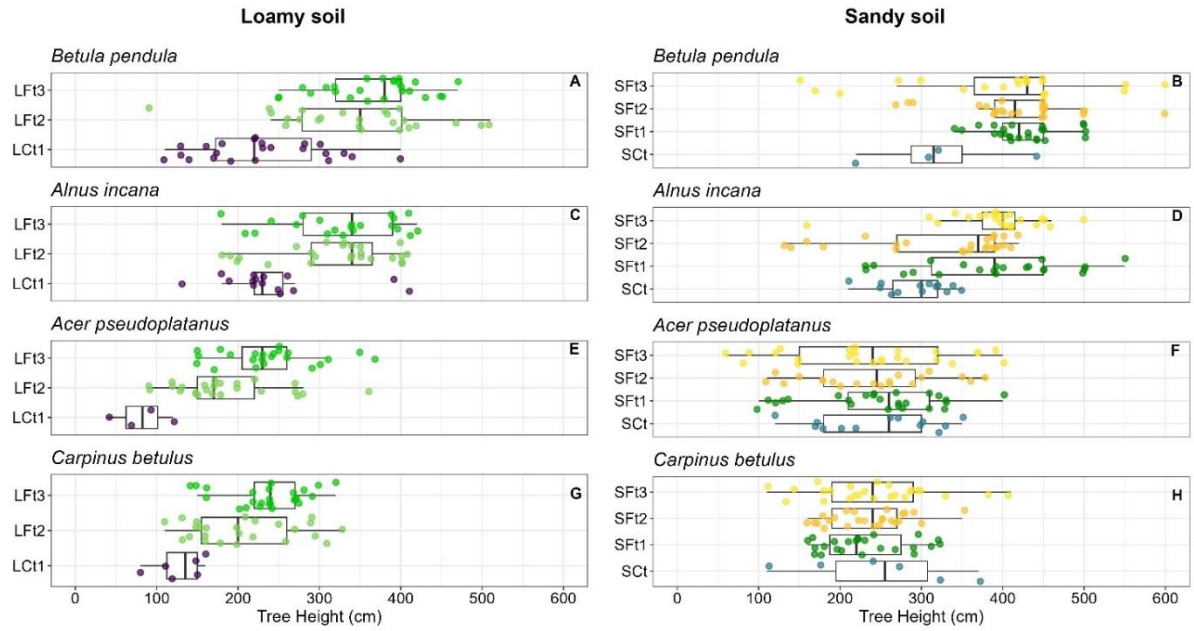

Figure 3.8: Boxplot with individual data points (with different colours for each zone) illustrating tree heights across different deciduous species, zones, and soil types. Panels A, C, E, G illustrates Betula pendula, Alnus incana, Acer pseudoplatanus, and Carpinus betulus heights distribution under loamy fertirrigated (LFt2, LFt3) and control (LCt1) conditions. Panels B, D, F, H represent Betula pendula, Alnus incana, Acer pseudoplatanus, and Carpinus betulus heights distribution under sandy fertirrigated (SFt1, SFt2, SFt3) and control (SCt) conditions.

Quercus robur, representing 60% of the forest population, was analysed separately from the other deciduous tree species (Figure 3.9). Different tree growth performances were observed across soil types, with *Quercus robur* in sandy fertirrigated zones SFt3-SFt1 significantly higher (K test: p-value < 0.01) than those in fertirrigated loamy zones LFt3-LFt1. Similarly, under control conditions, *Quercus robur* showed significantly (K test: p-value < 0.01) higher growth rates in sandy soil compared to those in loamy soil. Overall, fertirrigation influenced *Quercus robur* growth across all the fertirrigated zones, although there were few exceptions. For instance, in loamy fertirrigated zones LFt3 and LFt2, *Quercus robur* showed a significantly greater increment (K test; p-value < 0.05) compared to the control LCt1, but not when compared to the LCt2 control zone. Interestingly, the LCt2 zone demonstrated even higher *Quercus robur* growth (K test; p-value < 0.05) than the fertirrigated zone LFt1, suggesting how trees are responding to more complex interactions. On the other hand, sandy fertirrigated zones SFt3 and

SFt2 showed significantly higher growth of *Quercus robur* than the control SCt (K test; p-value < 0.05). Notably, SFt3 exhibited an even more pronounced growth response of *Quercus robur* compared to zone SFt1, which, in contrast, did not reveal substantial differences from the control SCt.

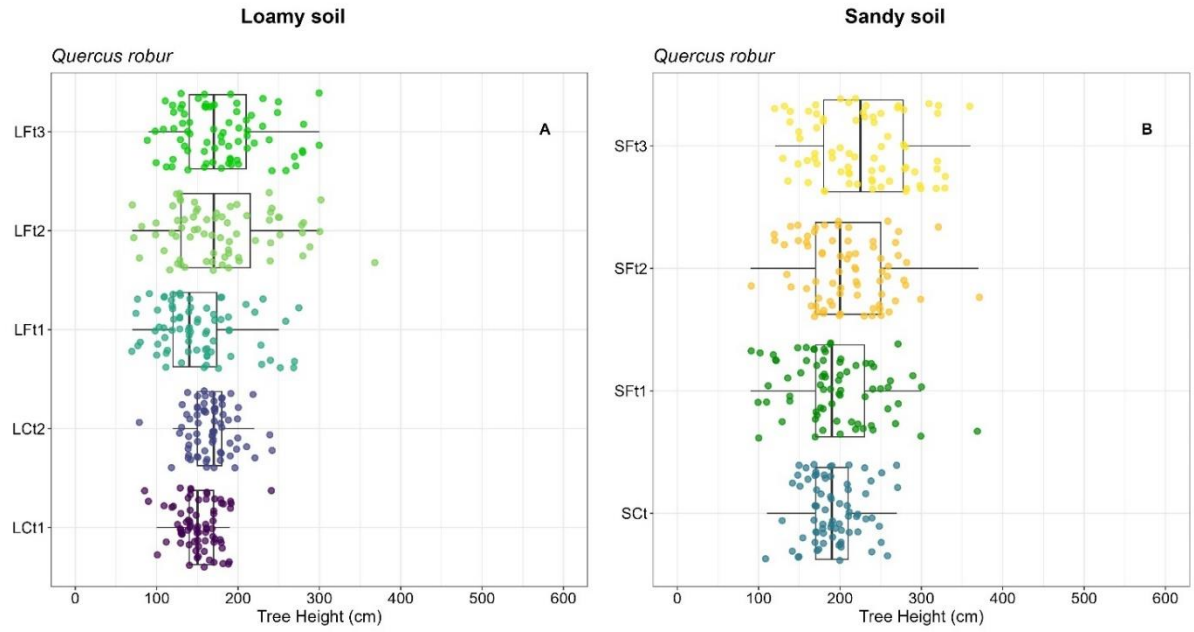

Figure 3.9: Boxplot with individual data points (with different colours for each zone) illustrating Quercus robur eights across various zones and soil types. *Panel A Quercus robur heights distribution under loamy fertirrigated LFt1, LFt2, LFt3 and the respective controls LCt1, LCt2. Panels B Quercus robur heights distribution under sandy fertirrigated SFt1, SFt2, SFt3 and control SCt.*

3.3.3 Gross CO_2 uptake

The Sandy fertirrigated zones SFt1, SFt2, and SFt3 showed the highest gross CO_2 uptake (GCU), with an average increase of 38% over the loamy fertirrigated zones LFt1, LFt2, and LFt3 (Figure 3.10). Fertirrigation significantly enhanced the carbon sequestration capacity of forest plantations on sandy soil, leading to an average increase of almost 70% compared to the control condition (Figure 3.10A). Conversely, the influence of fertirrigation on forest plantations located on loamy soils yielded inconsistent results. While LFt3 and LFt2 zones exhibited a positive response to

fertirrigation, with an average 38% increase in GCU compared to LCt2 and LCt1 controls, that was not the same for zone LFt1 (Figure 3.10B). In this instance, the GCU value did not significantly differ from that in control zone LCt2, indicating a limited effect of the fertirrigation treatment on trees growth. Finally, loamy control LCt2, did not show significant different GCU compared to sandy control SCt, unlike control LCt1, which showed a significantly lower GCU value.

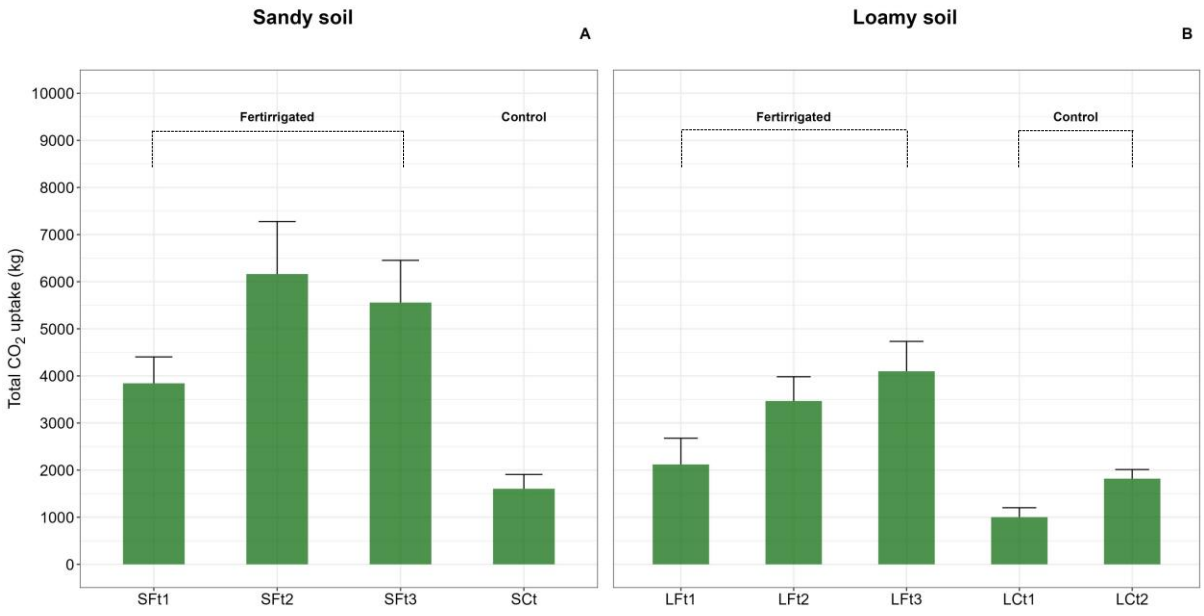

Figure 3.10: Forest plantation gross carbon uptake (GCU) across zones and soil types. In Panel A total CO_2 uptake is illustrated for sandy fertirrigated zones SFt1, SFt2, SFt3 and the respective control SCt, while Panel B displays the total CO_2 uptake in loamy fertirrigated zones LFt1, LFt2, LFt3, and the respective controls LCt1 and LCt2. Error bars represent the standard error of the mean (SEM).

3.4 Discussion

Overall, fertirrigation management improved the growth of the various tree species in the investigated forest plantations on both sandy and loamy soils, with only a few significant exceptions. In comparison to their controls, sandy and loamy fertirrigated zones showed a 70% and 56% increase in the gross carbon uptake, respectively

(Figure 3.10). These findings are consistent with previous research, demonstrating that active management through fertilizer application promotes reforestation initiatives (Campoe et al., 2014; Campoe et al., 2010; Cunningham et al., 2014). However, it is essential to note that distinct growth patterns emerged between sandy and loamy soil types. Forest plantations over fertirrigated SFt1, SFt2, and SFt3 sandy zones showed on average a GCU increase of 38% over fertirrigated LCt1, LCt2, and LCt3 loamy zones (Figure 3.10A, 3.10B). These findings challenge the traditional notion that loamy soils are better suited for afforestation efforts. Loamy soils, in fact, characterized by a balanced composition of sand, silt, and clay (Table 3.1), provide an optimal environment for tree root development due to their significant water retention capacity and nutrient availability. On the other hand, sandy soils, with their coarse texture and limited water holding capacity, are prone to rapid drainage and nutrient leaching, creating less favourable conditions that may hinder optimal tree growth and reduce potential carbon sequestration (Tew et al., 2021; Angers et al., 2011). Nevertheless, our study highlights how the influence of site soil water saturation on tree growth represents a critical factor, shaping the overall forest system response despite fertirrigation practices. The spatial analysis of degree of saturation (SR) at shallow and 30 cm depths revealed defined patterns that likely constrained tree growth responses. LTf1 and LFt2 zones, which showed lower GCU values among the fertirrigated loamy zones (Figure 10B), were characterized by consistently high levels of soil water saturation throughout all seasons (Figure 3.3, 3.5). This observation may be attributed to the interplay of shallow groundwater, site slope, and soil properties, which results in waterlogged conditions. This relationship is illustrated in Figure 3, where the spatial correlation range between winter and summer data varies significantly, suggesting a direction connection between surface conditions and groundwater levels. Higher groundwater levels can significantly prevent infiltration, creating more pronounced wet conditions on the surface. Consequently, the reduced oxygen availability in the rhizosphere, changes in soil chemical conditions (pH, Eh), and the accumulation of toxic by-products in anaerobic environments (Parent et al., 2008; Ashraf, 2012) led to detrimental effects on seedling establishment and development (Mu et al., 2022). This is clearly evident from the poor performances of *Quercus robur* in LFt1 zone. Despite

Quercus robur being recognized for its tolerance to waterlogging (Parelle et al., 2006), the consistently high levels of observed soil water saturation likely exceeded the resilience capacity of the trees. In fact, even with fertirrigation management the *Quercus robur* growth responses were significantly lower not only compared to the similar fertirrigated zones LFt2, and LFt3 but even to the control areas LCt1 and LCt2 (Figure 3.9). This also raises further considerations, extending beyond the scope of this research, such as the potential implications of NO_3^- surface runoff and leaching to groundwater, as well as enhanced N_2O emissions under anaerobic conditions. Similarly, for conifer tree species such as *Pinus sylvestris*, *Picea abies*, *Abies fraseri* and *Thuja plicata* the observed lack of significant growth response differences between fertirrigation loamy zones LFt2 and LFt3 and the control LCt1 suggests that high value of soil water saturation may have been detrimental to tree development. This is consistent with previous research that show how conifer species are not well-tolerant to waterlogging (Xin et al., 2023; Sanderson et al. 1980). On the contrary, deciduous tree species such as *Betula pendula*, *Alnus incana*, *Acer psuedoplatanus*, and *Carpinus betulus* in loamy zones LFt2 and LFt3 showed higher growth response under fertirrigation compared to their controls LCt1 and LCt2. However, their growth was lower compared to that observed in sandy fertirrigated zones (Figure 3.7, 3.8). Sandy soil, characterized by its coarse texture and improved macroporosity, mitigated the occurrence of waterlogged conditions, thereby facilitating oxygen diffusion. This more favourable environment likely contributed to superior tree growth responses compared to loamy zones, where limitations imposed by soil water saturation were evident. Interestingly, early successional species such as *Betula pendula* and *Alder incana* consistently showed a higher positive response to fertirrigation across both loamy and sandy soil types (Figure 3.8). Early successional trees are generally more tolerant to poor site conditions than slow-growing species (Jonczak et al., 2020; Uri et al., 2007), and more responsive to fertilization (Rowe et al., 2006; Sellstedt & Danell, 1986). This adaptability is a characteristic associated with pioneer species, as they are adapted to take advantage of resources when they become available. Additionally, *Alder incana* is recognized as a nitrogen-fixing species, highlighting specific nutrient requirement (Ekblad & Danell, 1995). This emphasizes the importance of considering

species-specific responses to fertilization in the context of afforestation or reforestation initiatives, representing a challenge for more precise forest restoration (PFR) methods as suggested by Castro et al. (2021). In fact, any intensive silvicultural management, and particularly fertirrigation, should follow previous knowledge of species behaviour according to soil physiochemical conditions. This assumes paramount importance in a scenario where resources such as water and fertilizer may represent the major limitations in implementing large-scale forest restoration, as well as higher investment that intensive silvicultural practices may initially require (Turchetto et al., 2018; Brancalion et al., 2019). Therefore, while fertirrigation may be considered a valuable silvicultural tool for managing forest plantations, our study suggests that its advantages and cost-effectiveness might vary based on site-specific conditions. This highlights, again, the importance of conducting detailed studies on site suitability and tree species selection to inform and optimize afforestation efforts (Castro et al., 2021). In this context, the integration of technological tools (e.g., remote sensing, drones), along with ecological knowledge for modelling species distribution at landscape or even microhabitat scale, emerges as a crucial approach. This synergistic strategy not only refine decision-making processes but also aligns with the principles of precision agriculture and forestry, aiming to increase efficiency and decrease environmental costs (Zellweger et al., 2019; Basso & Antle, 2020; St-Denis et al., 2018).

3.5 Conclusion

The finding of this research highlights the potential and the challenges associated with afforestation on former agricultural land with sandy and loamy soil types supported by actively managed fertirrigation. While fertirrigation increased overall tree growth and GCU on sandy and loamy soils by 70% and 56%, respectively, there were notable exceptions. The interplay of complex site hydrology and soil characteristics emerged as a crucial factor influencing the overall forest system response despite the application of fertirrigation. Consistent patterns of soil water saturation at 30 cm depth

caused reduced tree growth across sites. This was particularly evident for *Quercus robur*, whose exhibited distinct growth responses to fertirrigation depending on specific location of the afforested site. Similarly, conifer tree species such as *Pinus sylvestris*, *Picea abies*, *Abies fraseri* and *Thuja plicata* did not show significant response to fertirrigation, likely due to the limiting high moisture values observed across loamy zones. *Betula pendula* and *Alnus incana*, on the other hand, responded overall positively to fertirrigation, aligning with the general characteristics of early successional species in terms of taking advantage of nutrient availability. This underscores the importance of considering species-specific responses to fertilization, representing one of the main challenges in the context of afforestation initiatives under intensive management. As the shift from monoculture tree plantations to “climate-smart” mixed forests gains momentum for both ecological and economic benefits (Warner et al., 2023; Palacio-Agundez et al., 2015; Bolte et al., 2009) this research explores the advantages of fertigation-based management while addressing site-specific hydrological variability. Our findings underscore the need for a precise framework for forest restoration that prioritizes effective tree establishment and adapt to diverse conditions. The focus on an integrated approach, capable of combining new technology with ecological knowledge to model the tree species distribution, is essential to ensure the success of afforestation efforts.

3.6 References

Albaugh, T.J., Allen, H.L., Dougherty, P.M., Johnsen, K.H., (2004). Long term growth responses of loblolly pine to optimal nutrient and water resource availability. *Forest Ecology and Management*, 192, 1, 3-19, doi:10.1016/j.foreco.2004.01.002.

Ameray, A., Bergeron, Y., Valeria, O. *et al.*, (2021). Forest Carbon Management: A Review of Silvicultural Practices and Management Strategies Across Boreal,

Temperate and Tropical Forests. *Current Forestry Reports*, **7**, 245–266, doi:10.1007/s40725-021-00151-w.

Angers, D.A., Arrouays, D., Saby, N.P.A., Walter, C., (2011). Estimating and mapping the carbon saturation deficit of French agricultural topsoil. *Soil Use and Management*, 27, 448-452, doi:10.1111/j.1475-2743.2011.00366.x.

Bastin, J.F., Finegold, Y., Garcia, C., Mollicon, D., Rezende, M., Routh, D. *et al.*, (2019). The global tree restoration potential. *Science*, 365, 76-79, doi:10.1126/science.aax0848.

Basso, B., Antle, J., (2020). Digital agriculture to design sustainable agricultural systems. *Nature Sustainability*, 3, 254-256, doi:10.1038/s41893-020-0510-0.

Bateman, I.J., Anderson, K., Argles, A., Belcher, C., Betts, R.A., Binner, A., Brazier, R.E., Cho, F.H., Collins, R.M., Day, B.H., Duran-Rojas, C. Eisenbarth, S., Gannon, K., Gatis, N., Groom, B., Hails, R., Harper, A.B., Harwood, A., Hastings, A.,… Xenakis, G., (2023). A review of planting principles to identify the right place for the right tree for 'net zero plus' woodlands: Applying a place-based natural capital framework for sustainable, efficient and equitable (SEE) decisions. *People and Nature*, 5, 271-301, doi:10.1002/pan3.10331.

Blake, G.R. (1965). Particle Density. In Method of Soil Analysis, C.A., Black (Ed.). doi: 10.2134/agronmonogr9.1.c29

Bolte, A., Degen, B., (2010). Forest adaptation to climate change – Options and Limitations. *Landbauforschung Volkenrode*, 60, 111-118.

Bonan, G.B., (2008). Forests and climate change: forcings, feedback and the climate benefits of forests. *Science*, 320, 1444-1449, doi:10.1126/science.1155121.

Brancalion, P.H.S., Campoe, O., Mendes, J.C.T., Noel, C., Moreira, G.G., van Melis, J., Stape, J.L., Guillemot, J., (2019). Intensive silviculture enhances biomass accumulation and tree diversity recovery in tropical forest restoration. *Ecological Applications*, 29, e01847, doi:10.1002/eap.1847.

Campoe, O.C., Stape, J.L., Mendes, J.C.T., (2010). Can intensive management accelerate the restoration of Brazil's Atlantic forests? *Forest Ecology and Management*, 259, 1808-1814, doi:10.1016/j.foreco.2009.06.026.

Campoe, O.C., Stape, J.L., Albaugh, T.J., Allen, H.L., Fox, T.R., Rubilar, R., Binkley, D., (2013). Fertilization and irrigation effects on tree level aboveground net primary production, light interception and light use efficiency in a loblolly pine plantation. *Forest Ecology and Management*, 288, 43-48, doi:10.1016/j.foreco.2012.05.026.

Campoe, O.C., Iannelli, C., Stape, J.L., Cook, R.K., Mendes, J.C.T., Vivian, R., (2014). Atlantic forest tree species responses to silvicultural practices in a degraded pasture restoration plantation: From leaf physiology to survival and initial growth. *Forestry Ecology and Management*, 313, 233-242, doi:10.1016/j.foreco.2013.11.016.

Castro, J., Morales, F., Navarro, F.B., Löf, M., Vacchiano, G., Alcaraz-Segura, D., (2021). Precision restoration: a necessary approach to foster forest recovery in the 21st century. *Restoration Ecology*, 29: e13421, doi:10.1111/rec.13421.

Climate Change Committee. "Land use: Policies for a Net Zero UK", 23 Jan 2020. Available at: https://www.theccc.org.uk/publication/land-use-policies-for-a-net-zero-uk/.

Cobb, W.R., Will, R.E., Daniels, R.F., Jacobson, M.A., (2008). Aboveground biomass and nitrogen in four short-rotation woody crop species growing with different water and nutrients availabilities. *Forest Ecology and Management*, 255, 12, 4032-4039, doi:10.1016/j.foreco.2008.03.045.

Coyle, D., Aubrey, D.P., Coleman, M.D., (2016). Growth responses of narrow or broad site adapted tree species to a range of resource availability treatments after a full harvest rotation. *Forest Ecology and Management*, 362, 107-119, doi:10.1016/j.foreco.2015.11.047.

Cunningham, S.C., Mac Nally, R., Baker, P.J., Cavagnaro, T.R., Beringer, J., Thomson, J.R., Thompson, R.M., (2015). Balancing the environmental benefits of reforestation

in agricultural regions. *Perspectives in Plant Ecology*, *Evolution and Systematics*, 17, 4, doi:10.1016/j.ppees.2015.06.001.

DeSoto, L., Cailleret, M., Sterck, F., et al., (2020). Low growth resilience to drought is related to future mortality risk in trees. *Nature Communications*, 11, 545, doi:10.1038/s41467-020-14300-5.

Dubovyk, O., Menz, G., Khamzina, A., (2016). Land suitability Assessment for Afforestation with *Elaeagnus Angustifolia* L. in Degraded Agricultural Areas of the Lower Amudarya River Basin. *Land Degradation Development*, 27, 1831-1839, doi:10.1002/ldr.2329.

Ekblad, A., Danell, K., (1995). Nitrogen fixation by *Alnus incana* and nitrogen transfer from *A. incana* to *Pinus sylvestris* influenced by macronutrients and ectomycorrhiza. *New Phytologist*, 131, 453-459, doi:10.1111/j.1469-8137.1995.tb03082.x.

Forrester, D.I., Tachauer, I.H., Annighoefer, P., Barbeito, I., Pretzsch, H., Ruiz-Peinado, R., Stark, H., Vacchiano, G., Zlatanov, T., Chakraborty, T., Saha, S., Sileshi, G.W., (2017). Generalized biomass and leaf area allometric equations for European tree species incorporating stand structure, tree age, and climate. *Forest Ecology and Management*, 396, 160-175, doi:10.1016/j.foreco.2017.04.011.

Goovaerts, P., (1997). Geostatistics for natural resources evaluation. *Oxford University Press*, New York.

Grant, G.E., Tague, C.L., Allen, C.D., (2013). Watering the forest for the trees: an emerging priority for managing water in forest landscapes. *Frontiers in Ecology and the Environment*, 11, 314-321, doi:10.1890/120209.

Griscom, B.W., Adams, J., Ellis, P.W., Houghton, R.A., Lomax, G., Miteva, D.A., Schlesinger, W.H., Schoch, D., Siikamäki, Smith, P., Woodbury, P., Zganjar, C., Blackman, A., Campari, J., Conant, R.T., Delgado C., Elias P., Gopalakrishna, T., Hamsik, M.R., Herrero, M., Kiesecker, J., Landis, E., Laestadius, L., Leavitt, S.M., Minnemeyer, S., Polasky, S., Potapov, P., Putz, F.E., Sanderman, J., Silvius, M.,

Wollenberg, E., Fargione, J., (2017). Natural Climate Solutions. *PNAS*, 114, 44, 11645-11650, doi:10.1073/pnas.1710465114.

Jerzy Jonczak, Urszula Jankiewicz, Marek Kondras, Bogusława Kruczkowska, Lidia Oktaba, Jarosław Oktaba, Izabella Olejniczak, Edyta Pawłowicz, Nora Polláková, Thomas Raab, Edyta Regulska, Sandra Słowińska, Magdalena Sut-Lohmann, (2020). The influence of birch trees (Betula spp.) on soil environment – A review. *Forest Ecology and Management*, 477, 118486, doi:10.1016/j.foreco.2020.118486.

Johnston, K., Ver Hoef, J.M., Krivoruchko, K., Lucas N, (2001). Using ArcGis Geostatistical Analyst. ESRI, Redlands, CA.

Hart, K. M., Curioni, G., Blaen, P., Harper, N. J., Miles, P., Lewin, K. F., MacKenzie, A. R., (2019). Characteristics of free air carbon dioxide enrichment of a northern temperate mature forest. *Global Change Biology*, 26(2), 1023-1037, doi:10.1111/gcb.14786.

Hartkamp, A. D., De Beurs, K., Stein, A., and White, A.W., (1999). Interpolation Techniques for Climate Variables. Geographic Information Systems Series 99-01. International Maize and Wheat Improvement Centre (CIMMYT), Mexico. ISSN: 1405-7484.

Hiemstra, P., Skoien, J.O., (2023). Automatic Interpolation Package. *R package version 1.1-1* (available at: http://CRAN.R-project.org/package=automap)

Kitanidis, P.K., (1997). Introduction to Geostatistics. *Cambridge University Press*, 36 pp.

Lloyd, C. D., (2005). Assessing the Effect of Integrating Elevation Data into the Estimation of Monthly Precipitation in Great Britain. *Journal of Hydrology*, 308, 128–150, doi:10.1016/j.jhydrol.2004.10.026.

Lewis, S.L., Mitchard, E.T.A., Prentice, C., Maslin, M., and Poulter, B., (2019a). Comment on “The global tree restoration potential”. *Science*, 366, eaaz0388, doi:10.1126/science.aaz0388.

Lewis S.L., Wheeler C.E., Mitchard E., Koch A., (2019b). Restoring natural forests is the best way to remove atmospheric carbon storage in subtropical forests. *Nature*, 568(7750), 25-28, doi:10.1038/d41586-019-01026-84.

Lu, G.Y., Wong, D.W., (2007). An adaptive inverse-distance weighting spatial interpolation technique. *Computer & Geosciences*, 34, 1044-1055, doi:10.1016/j.cageo.2007.07.010.

Khamzina, A., Lamers, J.P.A., Vlek, P.L.G., (2008). Tree establishment under deficit irrigation on degraded agricultural land in the lower Amu Darya River region, Aral Sea Basin. *Forest Ecology Management*, 255, 168-178, doi:10.1016/j.foreco.2007.09.005.

Kruskal, W.H., Wallis, W.A., (1952). Use of Ranks in one-criterion variance analysis. *Journal of the American Statistical Association*, 47, 583-621, doi:10.1080/01621459.1952.10483441.

MacKenzie, A.R., Krause, S., Hart, K.M., Thomas, R.M., Blaen, P.J., Hamilton, R.L., Curioni, G., Quick, S.E., Kourmouli, A., Hannah, D.M., Comer-Warner, S.A., Brekenfeld, N., Ullah, S., Press, M.C, (2021). Water-soil-vegetation-atmosphere research in a temperate deciduous forest catchment, including under elevated CO_2. *Hydrological Processes*, 35, doi:10.1002/hyp.14096.

Merdun, H., Cinar, Ö. Meral, R., Apan, M., (2006). Comparison of artificial neural network and regression pedotransfer functions for prediction of soil water retention and saturated hydraulic conductivity. *Soil and Tillage Research*, 90, 108-116, doi:10.1016/j.still.2005.08.011.

Mu, Y. S., Liu, W. J., Zhang, G. X., (2022). Effects of flooding stress on photosynthetic and chlorophyll fluorescence parameters of chionanthus retusus seedlings from

different provenances. *J. Northwest A F Univ. (Natural Sci. Edition).* 50, 73–83, doi:10.13207/j.cnki.jnwafu.2022.07.009.

Mueller, T.G., Pierce, F.J., Schabenberger, O., Warncke, D.D., (2001). Map quality for site specific fertility management. *Soil Science Society of America Journal*, 1547-1558, doi:10.2136/sssaj2001.6551547x.

Mataruga, M., Cvjetković, De Cuyper, B., Aneva, I., Zhelev, P., Cudlin, P., Metslaid, M., Kankaanhuhta, V., Collet, C., Annighöfer, P., Mathes, T., Marianthi, T., Despoina, P., Jónsdóttir, Monteverdi, M.C., de Dato, G., Mariotti, B., Kolevska, D.D., Lazarević, J., Fløistad, Klisz, M., Wojciech, G., Paiva, V., Fonseca, T., Nicolescu, V.-N., Popović, V., Devetaković, Ivan Repáč, Božić, Kraigher, H., Böhlenius, H., Löf, M., Bilir, N., Villa-Salvador, P., (2023). *Forest Ecology and Management*, 546, 121308, doi:10.1016/j.foreco.2023.121308.

Mokany, K., Raison, R.J., Prokushkin, A.S., (2006). Critical analysis of root:shoot ratios in terrestrial biomes. *Global Change Biology* 12, 84-96, doi:10.1111/j.1365-2486.2005.001043.x.

Pawson, S.M., Brin, A., Brockerhoff, E, Lamb, D., Payn, T, Paquette, A., Parrotta, J., (2013). Plantation forests, climate change and biodiversity. *Biodiversity and Conservation*, 22, 1203-1227, doi:10.1007/s10531-013-0458-8.

Parelle, J., Brendel, O., Bodénès-Brezard, C., Berveiller, D., Dizengremel, P.P. *et al.*, (2006). Differences in morphological and physiological responses to water-logging between two sympatric oak species (Q.petraea [Matt.] Lieb., Q. robur L.). *Annals of Forest Science*, 63, 849-859, doi:10.1051/forest:2006068.hal-02656239.

Pebesma, E., Graeler, B., (2023). Spatial and Spatio-temporal Geostatical Modelling, Prediction and Simulation. *R package gstat version 2.1-1* available at (https://cran.r-project.org/web/packages/gstat/index.html).

Popkin, G., (2019). How much can forests fight climate change? *Nature*, 565, 280-282, doi:10.1038/d41586-019-00122-z.

Pugh, T.A.M., Lindeskog, M., Smith, B., Poulter, B., Arneth, A., Haverd, V., *et al*., (2019). Role of forest regrowth in global carbon sink dynamics. *Proc. Natl. Acad. Sci. U.S.A*., 116, 4382-4387, doi:10.1073/pnas.1810512116.

Ramsfield, T.D., Bentz, B.J., Faccoli, M., Jactel, H., Brockerhoff, (2016). Forest health in a changing world: effects of globalization and climate change on forest insect and pathogen impacts. *Forestry*, 89, 245-252, doi:10.1093/forestry/cpw018

Ryzak, M., Bieganoski, A., (2011). Methodological aspects for determining soil particle-size distribution using the lase diffraction method. *Journal of Plant Nutrition and Soil Science*, 174, 624-633, doi:10.1002/jpln.201000255.

Rockström, J., Gaffney, O., Rogelj, J., Meinshausen, M., Nakicenovic, N., Schellnhuber, H.J., (2017). A roadmap for rapid decarbonization. *Science*, 355, 1269-1271, doi:10.1126/science.aah3443.

Rowe, E.C., Healey, J.R., Edwards-Jones, G., Hills, J., Howells, M., Jones, D.L., (2006). Fertilizer application during primary succession changes the structure of plant and herbivore communities. *Biological Conservation*, 13, 510-522, doi:10.1016/j.biocon.2006.02.023.

Sanderson, P.L. & Armstrong, W., (1980). The response of conifers to some of the adverse factors associated with waterlogged soils. *The New Phytologist*, 85, 3, 351-362, *JSTOR*, http://www.jstor.org/stable/2431784, accessed 10 February 2024.

Sellstedt, A., Huss-Danell, K. (1986). Biomass production and nitrogen utilization by *Alnus incana* when grown on N_2^+ or NH_4^+ made available at the same rate. *Planta*, 167, 387-394, doi:10.1007/BF00391344.

Schulze, J., Gawel, E., Nolzen, H., Weise, H., Frank, K, (2017). The expansion of short rotation forestry: characterization of determinants with an agent-based land use model. *GCB Bioenergy*, 9, 1042-1056, doi:10.1111/gcbb.12400.

Smith, P., Davis, S., Creutzig, F. *et al.*, (2016). Biophysical and economic limits to negative CO_2 emissions. *Nature Climate Change*, 6, 42-50, doi:10.1038/nclimate2870.

St-Denis, A., Kneeshaw, D., Messier, C., (2018). Effect of predation, competition, and facilitation on tree survival and growth in abandoned fields: towards precision restoration. *Forest*, 9, 692, doi:10.3390/f9110692.

Tew, E.R., Vanguelova, E.I., Sutherland, W.J., (2021). Alternative afforestation options on sandy heathland result in minimal long-term changes in mineral soil layers. *Forest Ecology and Management*, 483, 118906, doi:10.1016/j.foreco.2020.118906.

Tromp-van Meerveld, H.J., McDonnell, J.J., (2006). On the interrelations between topography, soil depth, soil moisture, transpiration rates and species distribution at the hillslope scale. *Advance in Water Resources*, 29, 2, 293-310, doi:10.1016/j.advwatres.2005.02.016.

Turchetto, F., Machado, A., Tabaldi, L.A., Griebeler, A.M., Rorato, D.G., Berghetti, A.L., (2020). Intensive silvicultural practices drive the forest restoration in southern Brazil. *Forest Ecology and Management*, 473, doi:10.1016/j.foreco.2020.118325.

Uri, V., Lohmus, K., Ostonen, I., Tullus, H., Lastik, R., Vildo, M., (2007). Biomass production, foliar and root characteristics and nutrient accumulation in younger silver birch (*Betula pendula* Roth.) stand growing on abandoned agricultural land. *European Journal of Forest Research*, 126, 4, 495-506, doi:10.1007/s10342-007-0171-9.

UNFCCC (2013). Afforestation and Reforestation Projects Under the Clean Development Mechanism. Bonn, Germany, pp. 72, https://doi.org/ISBN 978-92-9219-120-7

Veldman, J.W., Aleman, J.C., Alvarado, S.T., Anderston, T.M., Archibald, S., Bond, W.J., *et al.*, (2019). Comment on “The global tree restoration potential”. *Science*, 366:7976, doi:10.1126/science.aay7976.

Weltzin, J.F., McPherson, G.R., (1997). Spatial and temporal soil moisture resource partitioning by trees and grasses in a temperate savanna, Arizona, USA. *Oecologia*, 112(2), 156-164: doi:10.1007/s004420050295.

Xin, R., Shenqi, Q., Yu, Z., Xiaokuan, G., Yuewei, D., Bingxiang, L., Changming, M., Hongxiang, M., (2023). Study of the causes of growth differences in three conifers after the rainy season in the Xiong'an New Area. *Frontiers in Plant Science*., 14, doi:10.3389/fpls.2023.1176142.

Yu, J., Berry, P., Guillod, B.P., Hickler, T., (2021). Climate change impacts on the future of forests in Great Britain. *Frontiers in Environmental Science*, 9, doi:10.3389/fenvs.2021.640530.

Zellweger, F., De Frenne, P., Lenoir, J. Rocchini, D., Coomes, D., (2019). Advances in microclimate ecology arising from remote sensing. *Trend in Ecology & Evolution*, 34, 324-341, doi:10.1016/j.tree.2018.12.012.

3.7 Appendix

3-S1: Irrigation diagram scheme

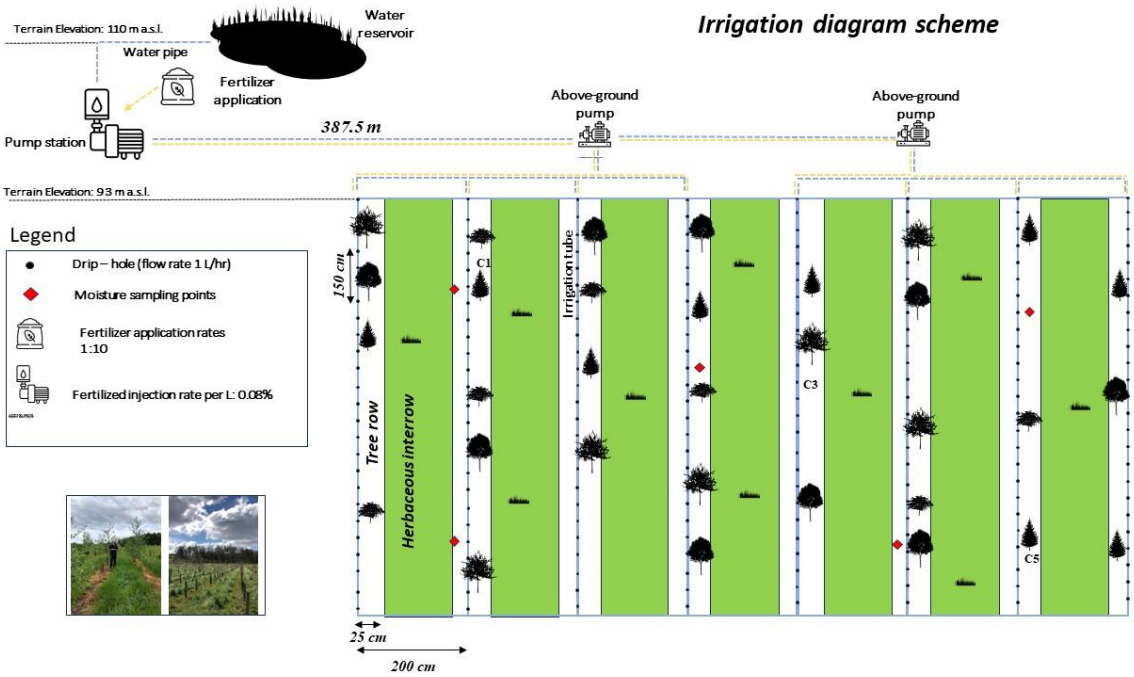

3-S2: Semivariograms

Semivariograms models fitting shallow soil moisture data (sSR) for the winter (A), spring (B), summer (C) and autumn (D) seasons, respectively.

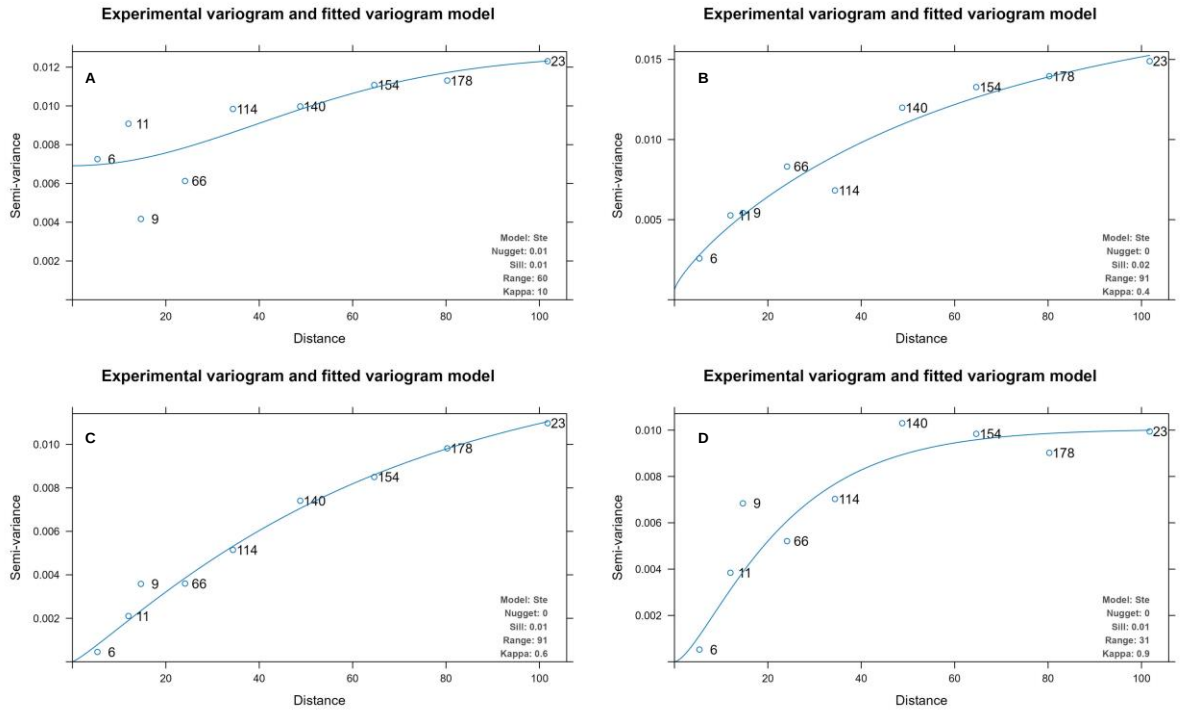

3-S3: Map of 10 cm depth degree of saturation (dSR) spatial distribution based on measured data at site A, which includes zones LFt1-LFt3, SFt1-SFt3, and SCt. Panels A-D indicate the variability of dSR across seasons.

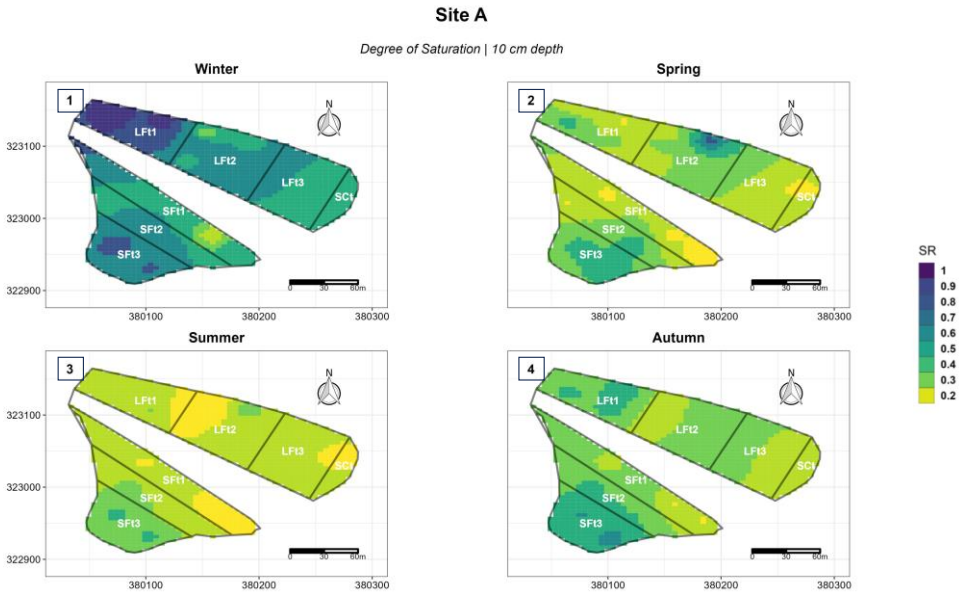

3-S4: Map of 10 cm depth degree of saturation (dSR) spatial distribution based on measured data at site B, which includes zones LCt1and LCt2. Panels A-D indicate the variability of dSR across seasons.

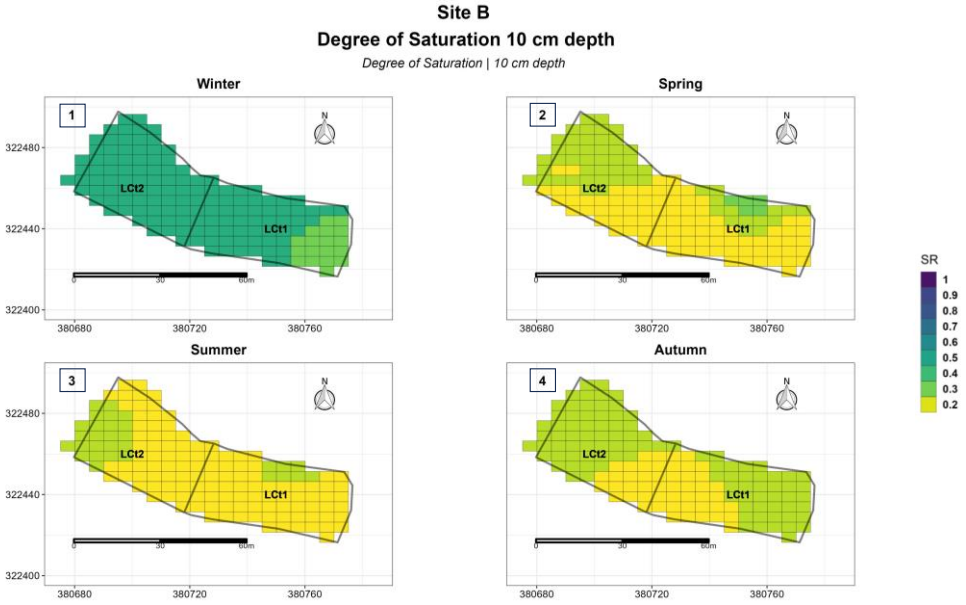

3-S5: Map of 20 cm depth degree of saturation (dSR) spatial distribution based on measured data at site A, which includes zones LFt1-LFt3, SFt1-SFt3, and SCt. Panels A-D indicate the variability of dSR across seasons.

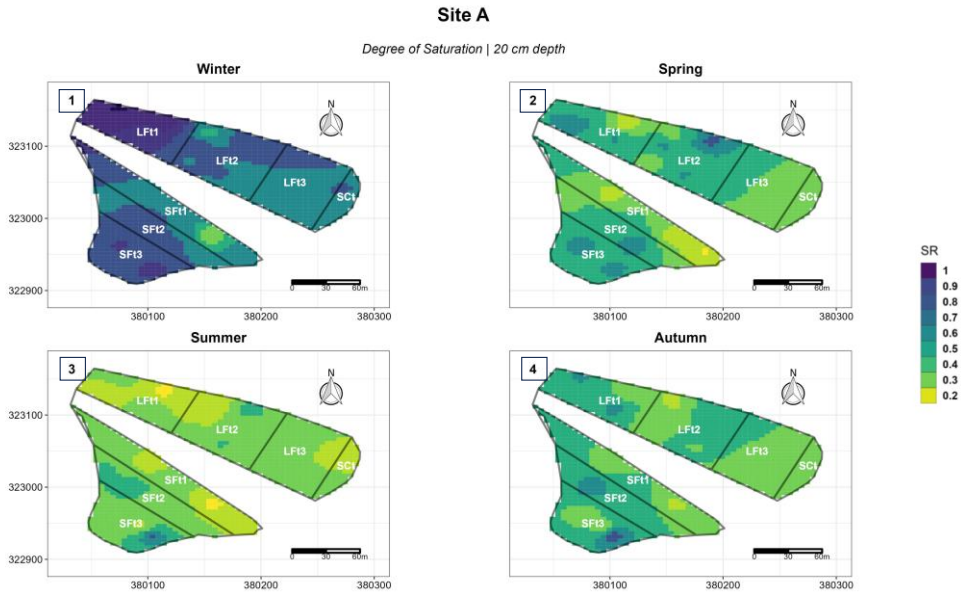

3-S6: Map of 20 cm depth degree of saturation (dSR) spatial distribution based on measured data at site B, which includes zones LCt1and LCt2. Panels A-D indicate the variability of dSR across seasons.

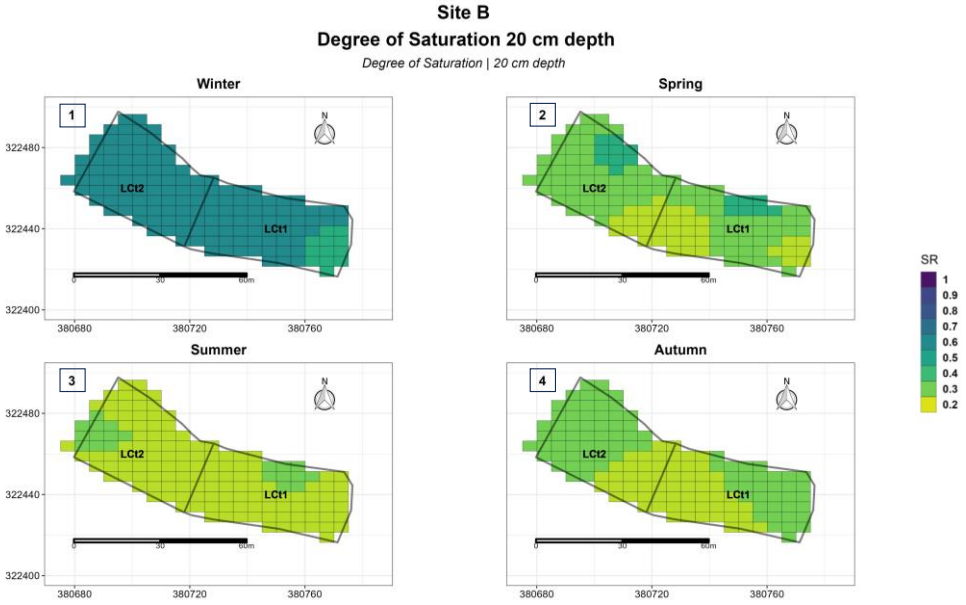

3-S7: Map of 40 cm depth degree of saturation (dSR) spatial distribution based on measured data at site A, which includes zones LFt1-LFt3, SFt1-SFt3, and SCt. Panels A-D indicate the variability of dSR across seasons.

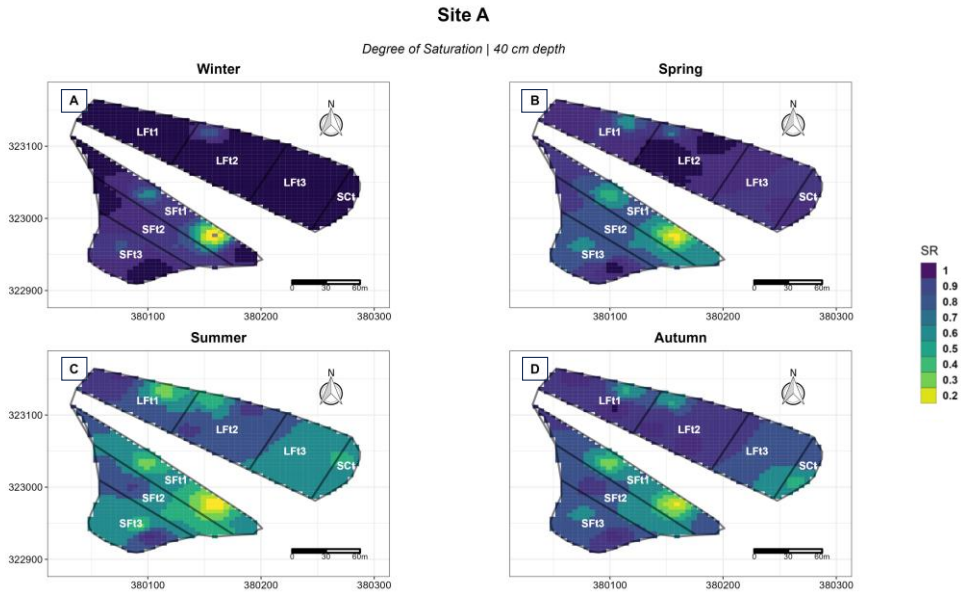

3-S8: Map of 20 cm depth degree of saturation (dSR) spatial distribution based on measured data at site B, which includes zones LCt1and LCt2. Panels A-D indicate the variability of dSR across seasons.

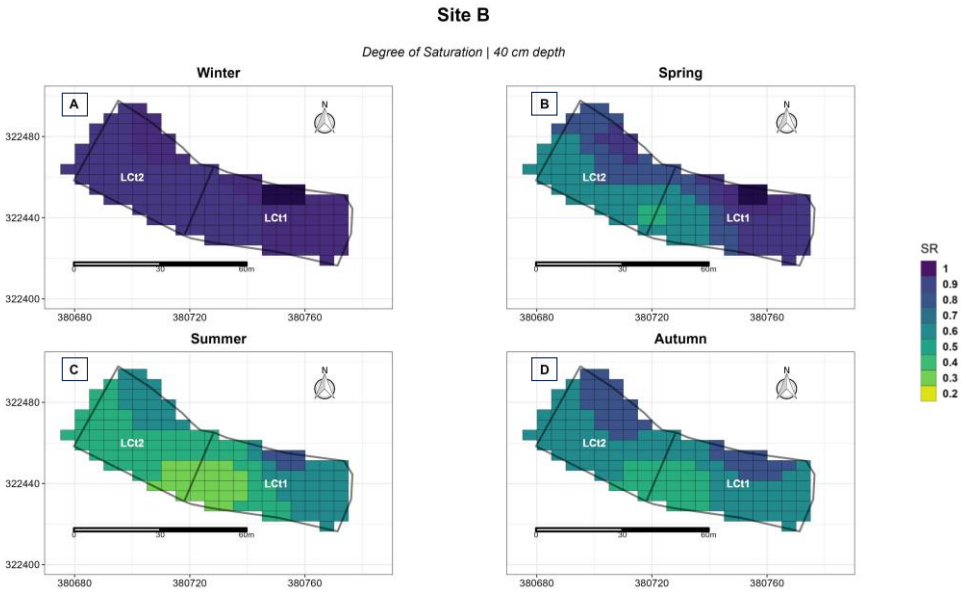

Chapter Three summary

This Chapter assesses the potential and challenges associated with afforestation efforts on former agricultural areas under fertirrigation management, which aimed to enhance tree growth, carbon capture, and mitigate potential detrimental effects caused by environmental stressors such as drought, as discussed in Chapter Two. In this study, despite the overall positive influence of fertirrigation on tree growth, hydrological site complexities emerged as a critical factor to consider when managing forest plantations. Geostatistical methods like Ordinary Kriging and Inverse Distance Weighting have been employed to analyse the soil moisture spatially, with a particular focus on saturation levels and their correlation with different soil properties. This approach has proved to be particularly effective in identifying areas characterized by a consistent pattern of water saturation conditions not suitable for supporting successful tree establishment. Moreover, the analysis of tree growth in response to fertirrigation revealed considerable differences among species. The growth of coniferous trees proved to be mostly driven by soil conditions, whereas fertilizer application has a significant impact on deciduous trees. In particular, early successional species such as *Betula pendula* and *Alder incana* showed the highest growth rates across the species studied. This aligns with their inherent capacity of nutrient uptake, characteristic of pioneer species. As forest management moves towards strategies focused on resource efficiency while meeting productivity and carbon sequestration goals, understanding how different species respond to fertilization becomes a critical challenge. Further recommendations and discussion based on these findings are provided in Chapter Five. Chapter four provides a more in-depth analysis of the potential effects of combining fertilizer application and irrigation on greenhouse gas emissions, with the aim of clarifying their influence on the carbon balance of the forest system.

Chapter Four

Fertilization-induced greenhouse gas emissions may partially offset carbon sequestration during afforestation.

Authors: Andrea Rabbai, Josep Barba, Marco Canducci, Kris M. Hart, A. Robert MacKenzie, Nicholas Kettridge, Giulio Curioni, Sami Ullah, Stefan Krause.

Running head: GHG emissions under intensive management of an afforest site.

Word count: 9.283

Corresponding author:

Andrea Rabbai

School of Geography, Earth and Environmental Sciences

University of Birmingham,

Edgbaston

West Midlands

United Kingdom

B15 2TT

Email: axr1049@student.bham.ac.uk

Abstract

Newly-planted forests require careful management to ensure the successful establishment of young trees; this can include herbicide application, irrigation, fertilization, or a combination of these treatments. The global rise in nitrogen (N) fertilizer application in managed forest plantations is driven by policies aiming at rapid tree growth and carbon sequestration as a strategy to tackle climate change. However, the impact of N-fertilizer on production and consumption of greenhouse gases (GHG), such as carbon dioxide (CO_2), nitrous oxide (N_2O), and methane (CH_4) is poorly understood, particularly when combined with irrigation. As a result, assessing forest GHG balance is key to defining effective climate mitigation strategies through afforestation projects.

This study assessed the response of GHG fluxes to irrigation and fertilization on recently afforested lowland arable land in central England, across loamy and sandy loam soils. The application of 180 kg ha^{-1} of N via an irrigation system, aimed at enhancing wood production and C sequestration, resulted in an increase of CO_2 and N_2O emissions for both soil types. Particularly, the N_2O emission factors (EF; kg N_2O/kg N applied) for loamy and sandy loamy soils were 3.9% and 2.1%, respectively, higher than the IPCC default estimate of 1% for agricultural and forest land. Furthermore, both sandy loam and loamy soils showed a distinct transition from being CH_4 sinks to sources. Thus, the combined application of irrigation and N-fertilizer had a significant impact on the total Global Warming Potential (GWP), which increased by 34% and 32% for sandy loam and loamy soil, respectively, when compared to their controls. Despite a significant increase in tree growth under fertilized conditions, the offset potential was only partial, highlighting the net contribution to GHG emissions. The outcomes of this study emphasise the potential for significant “carbon-equivalent-debt” from afforestation supported in its early years by irrigation and fertilization.

Keywords: climate change mitigation, Forest management, Nitrogen availability, GHG, BIFoR

4.1 Introduction

Climate change represents one of the most pressing environmental challenges of our time, driven by rising levels of atmospheric greenhouse gas concentrations (GHGs) such as carbon dioxide (CO_2), methane (CH_4), and nitrous oxide (N_2O) (IPCC, 2023). The increased frequencies and severity of hydrometeorological extremes are exerting growing pressure on ecosystems and societies (IPCC, 2023). International policy frameworks, including the UN Framework Convention for Climate Change, the Paris Agreement (2015), and the European Green Deal (2020), emphasise the importance of combining robust emission reduction strategies with effective CO_2 removal strategies (Griscom et al., 2017; IPCC, 2018). Within this context, forest ecosystems have been recognized as viable tools for mitigating climate change (He et al., 2024; Griscom et al., 2017; Bellassen & Luyssaert, 2014; McKinley et al., 2011), owing to their capacity to serve as a significant sink for CO_2 via photosynthesis and sequestering CH_4 via methanotrophy. While it has been recognised that forests may not represent a “silver bullet” for addressing this challenge (Palmer L., 2021), particular focus has been paid to actively increasing forest cover and growth rates to optimize their prospective contribution to climate change mitigation (Lundmark et al., 2014; BCMFR, 2007).

Increased forest growth rates, whether through natural processes (McMahon et al., 2010; Irland 2011) or through management interventions in support of growth optimizing conditions (Poudel et al., 2012; Le Nöel et al., 2021), can effectively impact the capacity of forests to act as a carbon (C) sink. Specifically, forest management techniques such as replanting, natural regeneration, species or genotype selection, and optimization of rotation durations can enhance forests’ growth and C sequestration (Liski et al. 2021; Ameray et al. 2021; Irland 2011). However, these

silvicultural techniques are primarily long-term strategies, often requiring over 50 years to fully achieve their potential benefits (Ameray et al., 2021; Ontl et al., 2020). Forest nitrogen (N) fertilization, on the other hand, has been shown to increase tree growth rapidly, particularly in N-limited forests (Tamm et al. 1991; Hedwall et al., 2014; Nohrstedt 2001). For instance, in Northen European coniferous forests the application of 150 kg N ha^{-1} resulted in a 30% increase of trees stem growth over a decade (Hedwall et al, 2014; Petterson et al., 2004). Similarly, in North America, the single application of 178 kg N ha^{-1} in mature Douglas fir (*Pseudotsuga menziesii*) stands led to 25% increase in stem volume over an 8-year period (Balster & Marshall, 2000). In North Wales, UK, birch (*Betula x aurata*) and willow (*Salix x reichardtii*) stem basal areas increased in their growth by 130% over two growing seasons after application of 175 kg N ha^{-1} (Rowe et al., 2006). To enhance wood production and CO_2 atmospheric removal, even more intensive fertilization regimes have been considered. Bergh et al. (2008), for example, demonstrated a yearly biomass increment of 7 m^3 ha^{-1} yr^{-1} after biannual fertilization with 125 – 150 kg N ha^{-1} in young Norway spruce plantations, whereas Groot et al. (1984) showed a 38% increment in stem growth over a 10-year period after a single application of 366 kg N ha^{-1}.

While high fertilization rates have been shown to significantly enhance tree growth in various studies, these practices often neglect forest N use efficiency (i.e. uptake rates vs supply in soil). This can result in increased N loss to the air (as NH_3, N_2O, NO, N_2 gases) and to water bodies, due to residual N not being absorbed by plants. In the context of afforestation, the release of climate active non-N2 N-gases may potentially outweigh the carbon sequestration achieved through fertilization-enhanced tree growth, thereby undermining the overall positive climate impact of these initiatives. Therefore, to assess the influence of fertilization on the climate change mitigation potential of new established forest, it is essential to understand how nutrients inputs may alter biogeochemical processes, resulting in changes to CO_2, CH_4, and N_2O fluxes (Shrestha et al., 2015; Liu and Greaver, 2009; Rütting et al. 2021; Gao et al., 2015).

In N-limited forest ecosystems, the supply of N can play a crucial role in stimulating plant growth, and thus, enhancing C sequestration (LeBauer & Treseder, 2008). The addition of N to forest ecosystems can have complex and diverse impacts on soil respiration. According to Johnson and Curtis (2001), N fertilization is one of the main forest practices that increases net primary production, resulting in a higher C stored in the soil (Bowden et al., 2019). However, in some settings, plant N content can also increase autotrophic respiration (Ra) and produce leaf litter with higher N content which decomposes faster, increasing soil respiration (Cornwell & Weedon, 2014). Additionally, increased N may stimulate microbial mineralization, and thus soil respiration (Wang et al., 2016: Johnson and Curtis, 2001).

Forest mineral soils generally act as a biological sink for CH_4 (Ullah et al., 2009; Ullah et al., 2008; Dalal and Allen, 2008), although the response to N fertilizer application is not always consistent. Application of NH_4^+-based fertilizer (100 kg ha^{-1} yr^{-1}) can promote CH_4 uptake through the stimulation of growth and activity of methane oxidisers (Aronson and Helliker, 2010; Papen et al., 2001; Börjesson & Nohrstedt, 2000). Also, enhanced NO_3^- concentration can raise the soil redox potential in anoxic circumstances, reducing the operating conditions for methanogenic archaea and, decreasing CH_4 production (Le Mer & Roger, 2001; Conrad, 2020). On the other hand, higher application of NH_4^+-based fertilizer tends to reduce CH_4 uptake (Hakansson et al., 2021; Jassal et al., 2011; Bodelier & Laanbroek, 2004; Steudler et al., 1989) due to the competitive inhibition for the active site of the methane monooxygenase (MMO). Nevertheless, while CH_4 and NH_4^+ oxidation occur at different levels of the redox ladder, their coexistence and the likelihood of their oxidation are influenced by soil environmental conditions, redox status, and nutrient availability (Bodelier & Laanbroek, 2004).

Globally, forest ecosystems are net sources of N_2O (Chapuis-Lardy et al., 2007; Yu et al., 2022), accounting for more than 30% of total biogenic emissions (Tian et al., 2020). However, under specific environmental conditions, forests can act as a N_2O sink (Chapuis-Lardy et al. 2007; Schlesinger & Bernhardt, 2020; Ryden 1981). For instance, soils characterized by limited NO_3^- availability and high moisture and C

content appear to have major net N_2O consumption capacity (Siljanen et al., 2020; Chapuis-Lardy et al., 2007; Frasier et al. 2010; Castro et al., 1992). The primary drivers of N_2O production in forest soil are microbial denitrification and nitrification (Dalal et al., 2003). According to Houlton et al. (2006), denitrification is responsible for substantial (24% to 53%) nitrogen losses from forest ecosystems, particularly under high soil moisture and sufficient NO_3^- availability (Dobbie et al., 1999). Denitrifying bacteria, produce N_2O during the reduction of NO_3^- or NO_2^- under anoxic conditions. Under well-drained conditions, however, N_2O is released as an intermediate product when nitrifying bacteria oxidize NH_4^+ to NO_3^- (Sahrawat, 2008). The widespread use of synthetic fertilizer as a common silvicultural practice has led to an increase in N_2O emissions from forest ecosystems (Fowler et al., 2011), with even old forests emerging as significant hotspots (Zhang et al., 2008). Sgouridis and Ullah (2015) have demonstrated how forests can revolatilise nearly 50% of deposited N through denitrification. However, the N additions due to fertilizer application are usually higher than those due to deposition, leading to N soil saturation and an increased risk of environmental harm through leaching (Wang et al., 2021).

This wide range of responses in N_2O and CH_4 production and consumption is mainly due to the complexity of the synergistically or antagonistically interacting processes (Butterbach-Bahl et al., 2013). Additionally, the high seasonal and spatial variability of GHGs fluxes makes generalising the understanding of underlying mechanisms and resulting emissions challenging (Gundersen et al., 2012). Unfortunately, there has been limited focus on understanding the complex relationship between fertilizer application and GHGs emission in forest soil. Addressing these knowledge gaps is crucial, especially in light of the steady increase in European forest area over the last 50 years (Fuchs et al., 2013), and subsidising activities, such as the proposed increase in afforestation activities by the UK Common Agriculture Policy (CAP) that have encouraged the reconversion of former agricultural land back to woodland for supporting increased C storage (Frei et al., 2024). In addition, most previous research has concentrated on investigating fertilization impacts on existing forest stands, almost neglecting the crucial initial phase of transitioning from an agricultural ecosystem to

forest. Therefore, the hypothesis of this study is that applying 180 kg N ha^{-1} y^{-1} of synthetic NPK fertilizer combined with soil irrigation would significantly alter soil CO_2, N_2O, and CH_4 fluxes, potentially undermining the beneficial trade-off associated with the afforestation initiative. Furthermore, we hypothesize that soils with varying textures, which interact differently with environmental conditions (e.g. controlling soil moisture), will show distinct patterns of GHG emissions.

4.2 Material and methods

4.2.1 Field site

This study focuses on a newly afforested site in rural Staffordshire, central England, UK, on the Norbury Park Estate. The forest plantation was established in 2019 on a former arable farmland grown with sunflowers for the preceding two years. The research site (52º 80' 43" N, 2º 29' 62" W) is adjacent to the Birmingham Institute of Forest Research Free-Air Carbon Dioxide Enrichment (BIFoR FACE) facility (MacKenzie et al., 2021; Hart et al., 2019) and is situated 95 m above mean sea level (AMSL). The climate is temperate maritime, with a total rainfall of 1250 mm over the 14-month study period. The annual average above-canopy temperature was 10.83 (± 0.3 SE) °C, based on a daily average from May 2022 to May 2023, with a maximum of 28.7 °C and a minimum of - 4.3 °C (Figure 4.1).

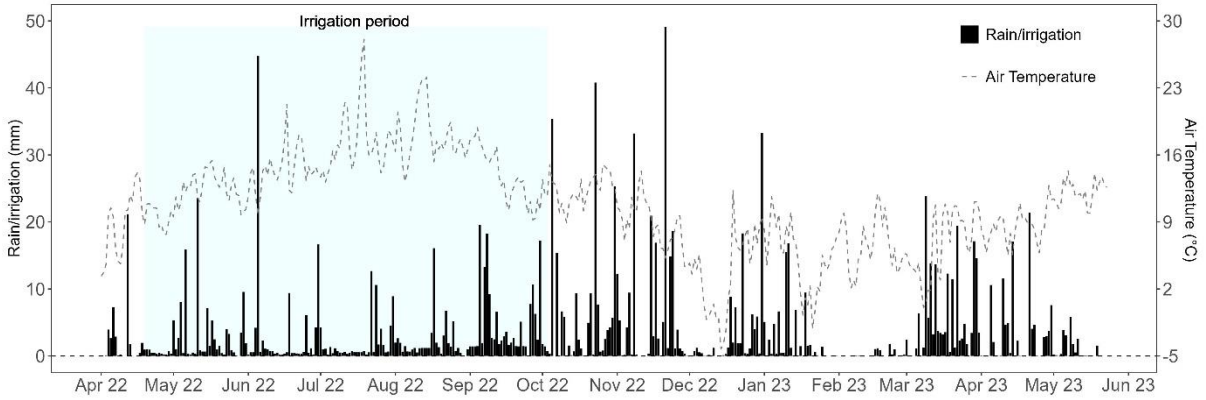

Figure 4.1: Daily mean air temperature (grey line), and precipitation/irrigation (black bars). The azure box highlights the period of irrigation and fertilizer application from April to October 2022.

The forest plantation (herein referred to as "juvenile forest") is a 4.3 ha aggrading complex mixture of broadleaves and conifers (intimate mixture rather than compartments or lines of distinct species) with a few parcels of monoculture (Figure 4.2). Saplings, typically ranging from 40-60 cm in height, were planted in 2019 at a density of 2600 trees per hectare. These saplings were arranged in rows with average distances of 2.4 m between rows and 1.6 m between each tree within the same row. *Quercus robur* (English oak) from various geographical origins (England, Netherlands, and France) accounts for the 60% of the entire juvenile forest population. Additionally, other native or long-established UK tree species, including *Betula pendula* (silver birch), *Picea abies* (Norway spruce), *Pinus sylvestris* (Scots pine), *Alnus incana* (grey alder), *Acer pseudoplatanus* (European sycamore), *Carpinus betulus* (hornbeam), and a few US native species, such as *Abies fraseri* (fraser fir), and *Thuja plicata* (western red cedar) were planted in a 1:4 ratio with oaks, the non-oak species serving as "nurse trees" and/or N fixers for enhancing soil fertility. The forest site was prepared by ploughing to a depth of 0.4 m, and the soil depth at the site is nearly 2 m, with varying properties ranging from loamy to sandy loamy conditions. The underlying geology consists of superficial till deposits, with limited presence of glaciofluvial deposits overlying the Permotriassic Sandstone of the Helsby formation (BGS, 2020).

4.2.2 Experimental design

The study encompasses two afforested locations: the principal site A, spanning 3.5 ha, situated on very gentle slope, with elevations ranging from 95 to 92 m, and site B, located at 650 m distance from the south-east, covering an area of 0.8 ha with elevations ranging between 94 and 93 m (Figure 4.2). Site A covers the zones under fertilization LFt1-LFt3, SFt1-SFt3, and the control SCt, while site B was selected for the other control LCt. The eight zones within the two sites were categorized based on soil type, allowing the distinction of two groups according to the USDA soil texture classification (Table 1). Zones LFt1-LFt3 and LCt are representative of loamy conditions, while zones SFt1-SFt3 and SCt exhibit sandy loamy characteristics. Despite the difference in size between controls and fertilized areas, visual inspections and soil characteristics assessment confirmed that the control areas matched the necessary criteria, ensuring their suitability for comparison in the study. According to the national Agricultural Land Classification (ALC; MAGIC, 2008) these arable sites are Grade 3, indicating good to moderate quality. The fertilization regime involved the application of 180 kg ha^{-1} of N over a period of 4.5 months, from 17/05/22 to 03/10/22. Hortimix Extra (Hortifeeds©, Park Farm, Lincoln, UK) fertilizer was used, which has an NPK nutrition ratio of 18:18:18 plus other micronutrients. While the treatment regime ensured balanced nutrient supply, in this study particularly emphasis was placed on N due to its pivotal role in numerous biological processes (Zhang et al., 2020). Fertilizer management involved two weekly applications (Tuesday and Friday) via a pumped drip-irrigation system with drip holes 50 cm apart across the entire fertilized sites (details in Supplementary Material 4-S1). Daily irrigation, scheduled for early morning and late afternoon, was established to maintain volumetric soil moisture at approximately 35%. Soil moisture levels were controlled by the estate managers at a depth of 10 and 30 cm using a SM150T probe (Delta-T Devices LTD, UK) at fixed points within the designated zones. The annual estimated irrigation water for each

zone was 145 ± (3.9 SE) mm supplementing the mean annual (2016-2019) precipitation at the site of 676 ± 66 mm (MacKenzie et al., 2021). In June 2022, there were reported malfunctions in the irrigation system with no water delivered to zones LFt2 and LFt3. Intensive weed control was conducted through quarterly application of glyphosate over spring and summer.

Table 4.1: soil texture characteristics of each individual zone, grouped according to the USDA soil texture classification (USDA). Also reported are the average value of bulk density (BD) for each zone and the number of samples (n) used for soil characterization.

Zone	Management	n (samples)	Sand (%)	Silt (%)	Clay (%)	Soil texture	BD
			Group 1				
LFt1	Fertilized	5	36.2	38.3	25.5	Loam	1.06
LFt2	Fertilized	5	38.6	37.4	24.6	Loam	1.04
LFt3	Fertilized	5	39.9	36.1	24.0	Loam	0.95
LCt	Control	5	39.4	38.3	22.3	Loam	1.05
			Group 2				
SFt1	Fertilized	5	52.7	28.3	19.0	Sandy Loam	1.22
SFt2	Fertilized	5	51.3	29.5	19.2	Sandy Loam	1.40
SFt3	Fertilized	4	52.4	18.9	28.6	Sandy Loam	1.42
SCt	Control	4	52.20	28.9	18.8	Sandy Loam	1.12

4.2.3 Greenhouse gas flux measurements

Greenhouse gas (GHG) emissions were measured monthly using static chambers over a 12-month period spanning from May 2022 to May 2023 (except for December 2022 and April 2023). To investigate the long-lasting effect of the N-fertilizer, GHG

emissions were measured consistently the day after direct application beginning in June 2022.

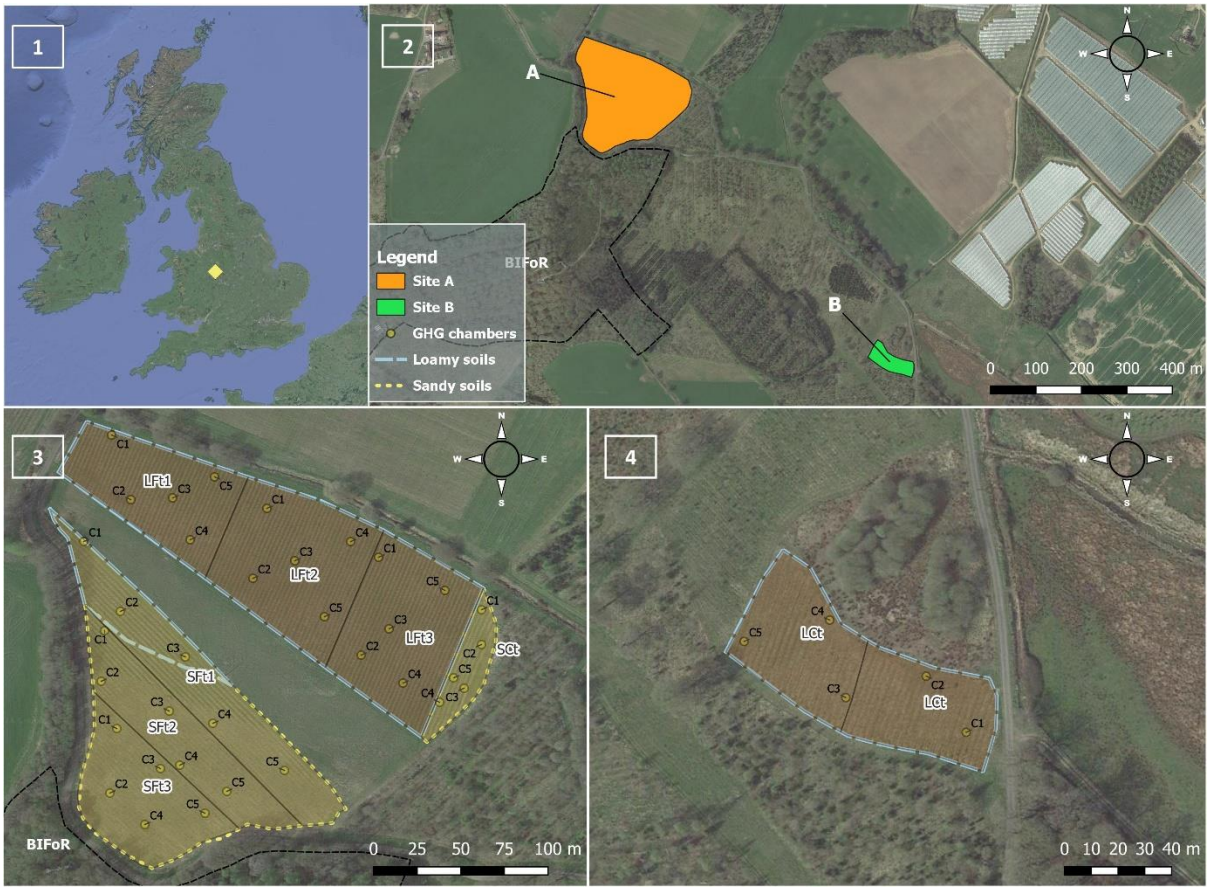

Figure 4.2: Field site map. Panel 1 shows the research site location in the UK. Panel 2 displays the research areas across Norbury Park Estate with the main site A in orange and the control B in green. Panel 3 outlines the main site A which covers the fertilized zones LFt1-LFt3, SFt1-SFt3, and the control SCt, while panel 4 shows site B with the control LCt. The different soil texture zone groupings are represented by blue dashed lines for loamy conditions and yellow dashed lines for sandy loam conditions. The Zigzag transect for GHGs is also illustrated, with C1 and C2 soil collars in zone SFt1 assigned to loamy conditions.

Forty round PVC collars (basal area of 0.3 m^2, 10 cm height) were installed at 5 cm depth across all zones to measure CO_2, N_2O, and CH_4 soil emissions. Five collars were placed in each plot following a zigzag pattern (Figure 4.2) four weeks ahead of the start of the experiment and remained *in situ* throughout. The collars within fertilized plots were positioned beneath the irrigation tube to receive input directly from the

dripping hole allowing for accurate measurement of GHG emissions. In the control area SCt, the soil collars were placed at least two rows of trees (4 m) away from the boundary, to minimize potential edge effects. For each CO_2, N_2O, and CH_4 flux measurement, a non-steady chamber was attached on top of the soil collar, ensuring an airtight seal (details in supplementary materials 4-S2). To obtain a sequence of measurements from each collar, air samples were collected at 0, 30, and 60 minutes using a 20-mL plastic syringe. Detailed information on GHG gas samples collection, storage, and analysis are addressed in the supplementary section 4-S3. The rates of change in CO_2, CH_4, and N_2O concentrations (ppm min^{-1}) were determined by fitting a linear model to the raw gas measurements obtained from the GC. Data quality assessment (QA/QC) was performed using the R^2 derived from the fitted models. With R^2 values for calculated CO_2 fluxes lower than 0.8 (12 of 440 measurements; 2.72% of the data), the physical conditions within chambers were considered unsuitable for precise flux calculations, probably due to improper chamber closure (Barba et al., 2019). For these low-R^2 measurements, we removed CO_2, CH_4, and N_2O fluxes, replacing them with not-a-number (i.e., NaN). However, with proper physical conditions within the chambers (R^2 for CO_2 > 0.8), we retained all gas flux measurements regardless of the R^2 of CH_4, and N_2O. GHG flux rates were determined using the equation by Collier et al. (2014):

$$F = \frac{dC}{dt} * \frac{mPV}{ART} = H * \frac{dC}{dt} * \frac{mP}{RT} \quad [4.1]$$

where F is the areal flux rate (mg m^{-2} h^{-1} for CO_2 and N_2O or µg m^{-2} h^{-1} for CH_4) and $\frac{dC}{dt}$ is the rate of change of concentration of GHGs at the sampling time (ppm min^{-1}). Parameters H, m, P, R, and T represent chamber height (m), molecular weight (g mol^{-1}), atmospheric pressure (Pa), the universal gas constant (8.314 m^{-3} Pa K^{-1} mol^{-1}), and temperature (K), respectively. The GHG data cleaning and preparation procedure, including the removal of outliers is discussed in detail in the supplementary materials

4-S4. For calculating GHG emissions trends based on monthly average values, we used a sample size of 18 chambers for loamy soil, 12 chambers for sandy loam soils, and 5 chambers for the two control zones (Figure 4.2). Cumulative emissions for CO_2 (t ha^{-1} $year^{-1}$), N_2O, and CH_4 (kg ha^{-1} $year^{-1}$) were calculated using a combination of linear interpolation and integration via the trapezoid rule for treatment and control plots. To account for potential overestimation from soil flux measurements under the irrigation tubing in the fertilized plots, we calculated cumulative emissions for a conservative treatment, named “Intermediate”. This approach applies only to the computation of the cumulative curve of GHG emissions and not for the subsequent analyses. The Intermediate treatment assumes that only 25% of the entire theoretical surface emits at fertilized rates, and the other 75% of the surface emits at the same rate as the control plots. This assumption is based on average wetted areas under irrigation lines derived from soil moisture measurements transects. Global Warming Potential (GWP), defined as the cumulative radiative forcing capacity of a GHG (i.e., CH_4 and N_2O) relative to CO_2 (IPCC, 2021), was calculated using the equation:

$$GWP = CO_2 + CH_4 * 25 + N_2O * 298 \quad [4.2]$$

where CO_2, N_2O, and CH_4 cumulative emissions were multiplied by 100-year scenario GWP values to obtain CO_2-eq (Myhre et al., 2013; Forster et al., 2007). To disentangle the relative contribution of microbial respiration to total respiration, we applied a partitioning coefficient of 0.7 (Wei, et al. 2022). The supplementary materials 4-S5 reports the overall GWP which includes in the calculation the roots respiration.

4.2.4 Soil physical and chemical properties

One undisturbed soil core (4.2 cm in diameter; 15 cm in length) was collected adjacent to individual soil collars, resulting in a total of 40 samples, 8 weeks prior to start of the GHG campaign. Soil cores were air dried for 72 hours for bulk density (BD) and total

porosity (TP) determination. In addition, volumetric water content (θ_v) was derived from the gravimetric water content (θ_g) of 5 gr of soil subsamples dried in the oven at 105 ºC. Water-filled pore spaces (WFPS) were determined based on soil porosity according to the following equation:

$$WFPS = \frac{(\theta_v) * 100}{TP} \quad [4.3]$$

Soil texture was determined employing laser diffraction particles size analysis via Mastersizer 2000, coupled with the Hydro Mu attachment (Malvern Ltd., UK). Soil temperature was measured near each collar during gas flux sampling, employing a 10 cm long portable calibrated thermometer (VWR® Traceable® Lollipop™, ± 0.4 ºC) to a depth of 5 cm. For soil chemical properties, one soil sample (0-15 cm depth) was collected monthly during GHG campaign near each collar (within 30 cm radius) along the irrigation line. Detailed procedures for soil texture analysis, as well as soil processing, including extraction and analysis of extractable NO_3^- and NH_4^+, as well as DOC, DN, pH, and soil cation exchange capacity (CEC) measurements, along with soil initial properties, are provided in the supplementary materials 4-S6.

4.2.5 Quantification of forest plantation Gross CO_2 uptake calculation

Assessing the gross CO_2 uptake (GCU) of the juvenile forest plantation is essential for understanding its climate change mitigation potential, especially with the external N fertilizer application aiming to enhance growth rates. A total of 1764 trees across nine species were surveyed in 2021 and 2022. Within each zone, 25 trees per species were randomly sampled and measured for diameter at breast height (DBH) at 1.3 m aboveground and at the root collar, according to the tree heights. To ensure consistency over the 2-year campaign, the DBH measurement points were marked with biodegradable paint. Tree heights for all trees were measured using a height stick

and clinometer. Tree biomass was computed using species-specific generalized allometric equations adapted for young trees (Forrester et al., 2017). The carbon content (CC) fraction of 0.47, in accordance with the 2006 IPCC guidelines, was then applied to estimate tree carbon content. The total biomass, including above- and below-ground biomass, was estimated using a root-shoot ratio of 0.3 (Mokany et al., 2006). The total CC has been used to calculate the net CO_2 uptake. It is important to note that while carbon uptake by ground vegetation may contribute to offsetting GHG emissions, it was not included in the overall calculation as it was beyond the aim of this study.

4.2.6 Statistical analysis

4.2.7.1 Data preparation

Prior to the data analysis, missing CH_4 values due to outlier removal were filled using linear interpolation. Subsequently, we normalized CO_2 fluxes using the Box-Cox transformation, and the normal quantile approach to N_2O and CH_4 fluxes, as suggested by Moulin et al. (2014). All environmental variables were centred and standardized (i.e., rescaled with a variance of one) using the function *scale* from the base package in R. For the subsequent analyses, we only distinguish between fertilized and control conditions, as previously mentioned.

4.2.7.2 Principal component analysis

The inherent spatial heterogeneity of soil properties poses challenges in highlighting the key factors influencing GHG fluxes. Principal component analysis (PCA) aids in the identification of these mechanisms, particularly during initial data exploration (Joliffe et al., 2016. Therefore, PCA was conducted to explore the relationship between soil edaphic factors (nitrate (NO_3^-), ammonium (NH_4^+), dissolved organic carbon (DOC), dissolved nitrogen (DN), water-filled pore space (WFPS), carbon to nitrogen

ratio (CN ratio), and soil temperature (Tsoil)), climatic factors (cumulative precipitation over 4 days (Pr4)), and site management (cumulative irrigation over 4 days, (Irr4)) with GHG emissions. Detailed definitions of these variables can be found in supplementary material 4-S7. PCA was performed using *prcomp* from the *stats* package, retaining principal components that explained over 40% of the variance. PCA results visualization was done using the R-package *FactoMineR* (Lê et al., 2008) and *factorextra* (Kassambara and Mundt, 2020).

4.2.7.2 Mixed effect models for GHGs environmental drivers

For studying the relationship between GHG emissions and various environmental factors, linear mixed-effects models (LMMs) have been used (Zuur et al., 2009). LMMs are designed to address the hierarchical nature of the data by incorporating both fixed effects (systematic factors) and random effects (unsystematic factors). This approach helps to prevent pseudo-replication and reduce the possibility of type I and II error rates (Harrison et al., 2018; Crawley, 2013). We examined soil fluxes of CO_2, N_2O, and CH_4 as a distinct response variable with random effects that were commonly defined based on the experimental design, which included chambers, nested zones, and seasons. The 13 different fixed effects considered for modelling with the relative selection process are indicated in detail in supplementary material 4-S7. For model selection, we initially created a saturated model including all the selected predictor variables, their first interaction, and random effects. Akaike Information Criterion (AIC) was used for model selection (Zuur, 2010) employing the *dredge* function from the *MuMIn* package (Barton, 2019). When the difference in AIC values between models was less than 2 units and not statistically significant, we kept the simplest model. Finally, a partially Bayesian approach with the *blmer* function of the package *blme* (Chung et al., 2013) was used to fit models and address the singularity issues using maximum a posteriori (MAP) estimates. Computational methods for marginal and conditional R^2 for the selected models, and model results visualization methods are discussed within the supplementary material 4-S8.

4.3 Results

4.3.1 Temporal trend and cumulative emissions

CO_2 emission rates in fertilized loamy soils (Figure 4.3A) were over 20% higher than under control conditions from June 2022 to May 2023. In June 2022, both fertilized and control plots showed similar CO_2 emission rates. However, CO_2 emissions sharply increased in fertilized plots from August 2022, peaking and remaining significantly higher than the control until January 2023. Correspondingly, from June to August 2022 cumulative CO_2 emissions in fertilized and control plots remained comparable, with the difference gradually increasing over time, reaching 25.5% by January 2023 (Figure 4.3B). Thus, the higher annual CO_2 emissions were recorded in fertilized plot with 8.91 t ha^{-1}, closely followed by the intermediate treatment at 8.20 t ha^{-1}, where only 25% of the theoretical surface emits at fertilized rates. Control plots showed the lowest annual CO_2 emissions at 7.96 t ha^{-1}.

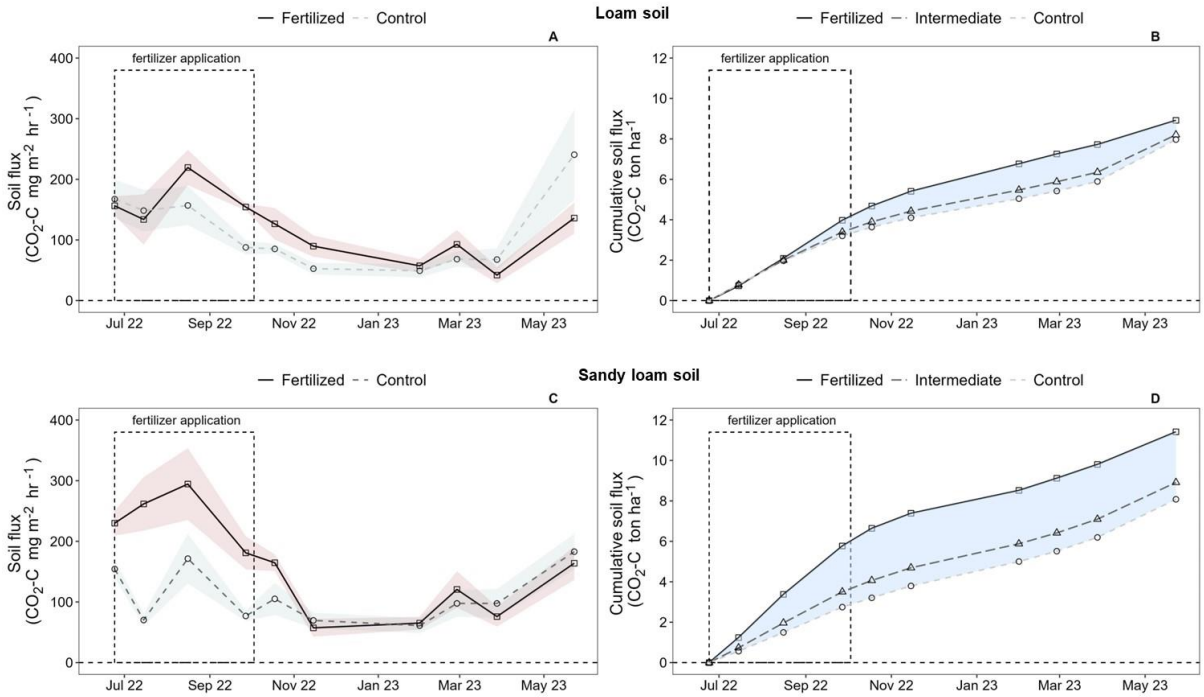

Figure 4.3: Temporal dynamics of actual and cumulative emissions of CO_2 in loamy (A, B), and sandy loam soil (C, D) over the period June 2022 – May 2023. Averaged CO_2 emissions for both soil type (A, C) for fertilized (black solid line) and Intermediate (grey dashed line) plots were calculated along with the standard error of the mean (SE). Panels B and D show cumulative CO_2 emissions for both soil conditions for three different treatments: Fertilized (black solid line), Intermediate (black long-dashed line), and Control (grey dashed line). Dashed box indicates the period of fertilizer application.

In contrast to fertilized loamy conditions, CO_2 emission in fertilized sandy loam soils exhibited significantly higher rates and a distinct temporal dynamic with the absence of an initial similarity to the control and a sharp decline after fertilization ceased in October 2022 (Figure 4.3C *cf.* Figure 4.3A). This on-off pattern is echoed in the annual cumulative CO_2 emissions (Figure 4.3D *cf.* Figure 4.3B), which highlights the net distinction between Fertilized, Intermediate, and Control conditions (Figure 4.3D), with values of 11.41, 8.9, and 8.1 t ha^{-1}, respectively.

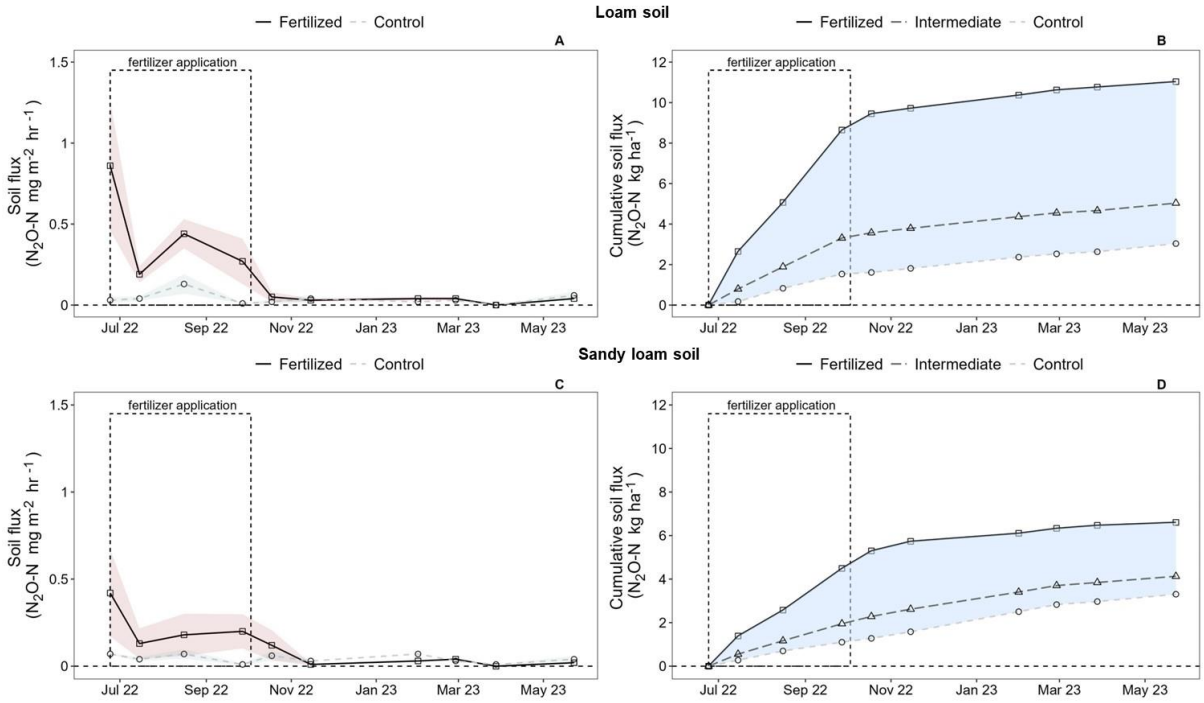

Figure 4.4: Temporal dynamics of actual and cumulative emissions of N_2O in loamy (A, B), and sandy loam soil (C, D) over the period June 2022 – May 2023. Averaged N_2O emissions for both soil type (A, C) for Fertilized (black solid line) and Control (grey dashed line) plots were calculated along with the standard error of the mean (SE). Panels B and D show cumulative N_2O emissions in both soil conditions for three different treatments: Fertilized (black solid line), Control (grey dashed line), and Intermediate (black long-dashed line). Dashed box indicates the period of fertilizer application.

In loamy soils under fertilized and irrigated conditions, with an average WFPS of 63.3% from June to October, N_2O emissions were 80% higher than the control (Figure 4.4A). Peak N_2O fluxes occurred in June and August, followed by a decline and stabilization at emission rates equivalent to control plot after fertilization ceased in October 2022. Despite a moderate emission peak in August, control plots maintained background emission level averaging 0.02 ± 0.017 mg m^{-2} hr^{-1} throughout the study. Again, the on-off dynamic was mirrored within the cumulative N_2O emissions pattern with Fertilized treatment showing a steep increase until October 2022, followed by a levelling off as emissions decreased until May 2023 (Figure 4.4B). As a result, the cumulative N_2O emission for Fertilized plot were 2.2 and 3.6 times larger than the Intermediate and Control emission treatments with 11.03 kg ha^{-1}, 5.03 kg ha^{-1}, and

3.03 kg ha^{-1}, respectively. Sandy loam soils had N_2O emission patterns comparable to loamy soils, with a 70% increase under fertilized conditions compared to the control (Figure 4.4C). Even in this situation, fertilization had a short-lived effect on N_2O fluxes after being stopped in October. The cumulative N_2O emissions for the fertilized condition was nearly double those of the control. The calculated annual total emission in sandy loam soil were 6.06 kg ha^{-1} for the Fertilized plot, 4.12 kg ha^{-1} for the Intermediate treatments, and 3.30 kg ha^{-1} for the Control.

Analysis of the temporal patterns and the cumulative CH_4 emissions reveals a substantial contrast between areas subjected to fertilization and those in the control group (Figure 4.5). When fertilizer was applied, loamy soils initially exhibited CH_4 uptake, transitioning to net CH_4 emissions once fertilization ceased in October (Figure 4.5A). From October to April 2023, CH_4 emissions peaked before gradually declining. In contrast, control plot showed CH_4 general consumption capacity. The cumulative CH_4 emissions highlight the shift from consumption to net emission in plots subjected to fertilization, while both the Control and Intermediate treatments exhibited clear consumption of atmospheric CH_4. The estimated annual CH_4 emissions in loamy soil amounted to 0.69 kg ha^{-1} within the Fertilized plot, -0.58 kg ha^{-1} in the Intermediate treatments, and -1.01 kg ha^{-1} for the Control.

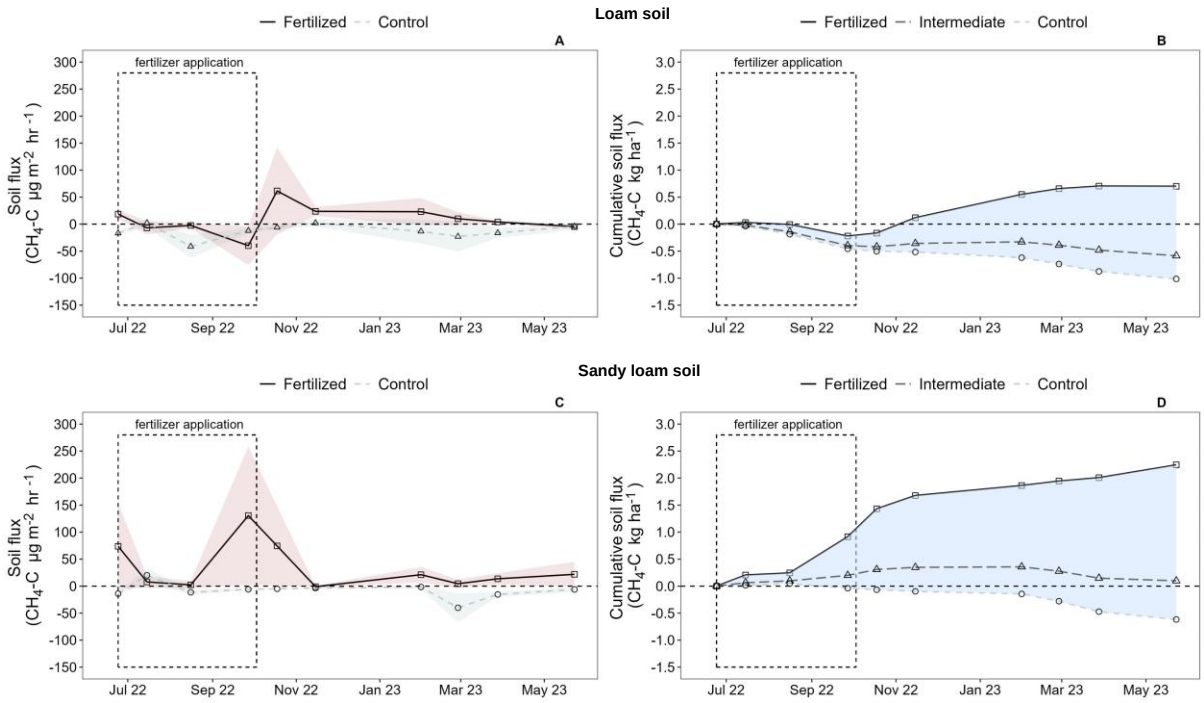

Figure 4.5: Temporal dynamic of actual and cumulative emissions of CH_4 in loamy soil (A, B), and sandy loam soil (C, D) over the period June 2022 – May 2023. Averaged CH_4 emissions for both soil types (A, C) for Fertilized (black solid line) and Control (grey dashed line) plots were calculated along with the standard error of the mean (SE). Panels B and D show cumulative CH_4 emissions in both soil conditions for three different treatments: Fertilized (black solid line), Control (grey dashed line), and Intermediate (black long-dashed line). Dashed box indicates the period of fertilizer application.

In contrast, fertilized sandy loam soil exhibited net CH_4 emissions throughout the study period (Figure 4.5B). The highest CH_4 emissions were observed in September-October 2022, followed by a persisting emission after fertilization ceased in October. In contrast, the control plot showed a clear CH_4 consumption capacity, albeit 35% lower than that of loamy soil. Again, cumulative CH_4 fluxes reflected these trends, with fertilized sandy loam soil serving as a net source of CH_4, while the control plot acting as a sink (Figure 4.5D).

4.3.2 Interrelationship between GHG, soil physicochemical, and climate factors.

PCA for fertilized conditions data revealed that more than 40% of the total variance of GHG emissions, soil physicochemical, and climate factors relationship is retained by the first two PCs. PC1 and PC2 account for 24.8% and 20.5% of the variance, respectively, defining a hyperplane that distinctly separates sandy loam and loamy soil samples under fertilized conditions (Figure 4.6A). PC1 correlates positively with CO_2, N_2O, WFPS, Tsoil, DN, and Irr4 whereas PC2 shows positive correlation with NO_3^-, DOC, DN, and Pr4, but negatively with CO_2 fluxes and Tsoil (Table 4.2). Panel 6B, which represents the two soil types under control conditions, shows that PC1 and PC2, accounting for 23.8% and 19.2% of the variance, respectively, do not clearly separate loamy and sandy loam soil samples.

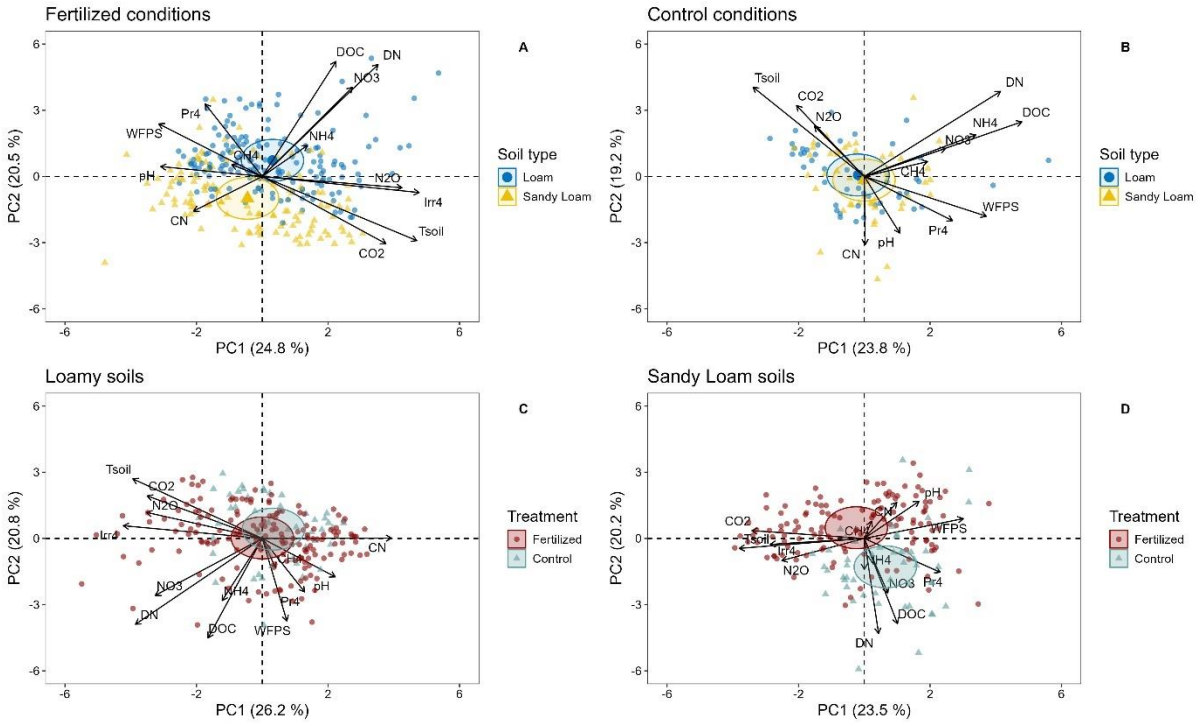

Figure 4.6: Principal component analysis (PCA) including GHG fluxes (CO_2, CH_4, and N_2O), soil physiochemical properties (Tsoil, pH, DN, DOC, NH_4^+, NO_3^-, WFPS, C:N ratio), cumulative precipitation at 4 days (Pr4), and irrigation management (Irr4) for both sandy loam and loamy conditions. Panels A and B illustrate the relationship between loamy (blue) and sandy loam (yellow) soils under fertilization

treatment, while panels C and D show how responses differ within the same soil type under fertilized (brown) and unfertilized (blue) conditions.

To highlight the significance of PC1 and PC2 for fertilized conditions, the control data for both soil types were re-projected onto the corresponding hyperplane. The absence of a distinct separation indicates that PC1 and PC2 for fertilized conditions are informative directions for separating sandy loam and loamy samples (Table 4.2). We conducted PCA both on loamy and sandy loam soil types separately to investigate the direct Impact of fertilization.

Table 4.2| Matrix of the PCA obtained with GHG, soil properties, and climatic factors in fertilized sandy loam and loamy soils over the entire experimental period (4.6A). Percentage variance explained by each principal component is reported in the head of each column.

Variance explained	PC1 (24.8%)	PC2 (20.5%)
CO_2	**0.328**	**-0.296**
N_2O	**0.372**	-0.049
CH_4	-0.027	0.080
WFPS	**-0.272**	0.229
Stemp	**0.409**	**-0.281**
NO_3^-	0.242	**0.384**
NH_4^+	0.120	0.130
Pr4	-0.149	**0.313**
DOC	0.198	**0.496**
DN	**0.310**	**0.482**
Irr4	**0.417**	-0.073
pH	-0.265	0.043
CN ratio	-0.184	-0.148

Bold values represent the variables most related to each PCs.

In loamy soil (Figure 4.6C), PC1 and PC2 represent 26.2% and 20.8% of the variance, respectively, showing no substantial difference between fertilized and control conditions. Conversely, in sandy loam soil, distinct clusters for fertilized and control conditions were observed (Figure 4.6D). PC1, which contributed the most to the cluster separation with 23.5% of the variance explained, was positively correlated with WFPS and PR4, and negatively correlated with CO_2, N_2O, Tsoil, and Irr4 (Table 4.3).

4.3.3 Drivers of GHG emissions

In examining soil CO_2 fluxes, the minimum adequate model included fertilization, pH, soil type, soil temperature, and the interaction between fertilization and pH as fixed effects. This model explained 73% of the variance, with fixed effects accounting for

43.5%. Soil temperature showed a significant positive effect on CO_2 emissions (Figure 4.7A and Table 4.4).

Table 4.3| Matrix of the PCA obtained with GHG, soil properties, and climatic factors in fertilized sandy loam and loamy soils over the entire experimental period (4.6D). Percentage variance explained by each principal component is reported in the head of each column.

Variance explained	PC1 (23.5%)	PC2 (20.2%)
CO_2	**-0.438**	0.130
N_2O	**-0.322**	-0.147
CH_4	-0.013	0.027
WFPS	**0.385**	0.130
Stemp	**-0.487**	-0.070
NO_3^-	0.097	**-0.337**
NH_4^+	0.004	-0.193
Pr4	0.297	**-0.217**
DOC	0.136	**-0.535**
DN	0.063	**-0.598**
Irr4	**-0.369**	-0.050
pH	0.209	0.230
CN ratio	0.126	0.237

Bold values represent the variables most related to each PCs.

The interaction between fertilization and pH exhibited a positive effect on CO_2 emissions (Table 4.4; Figures 4.7A, 4.7B). In contrast, soil type did not significantly influence soil CO_2 fluxes (Table 4.4).

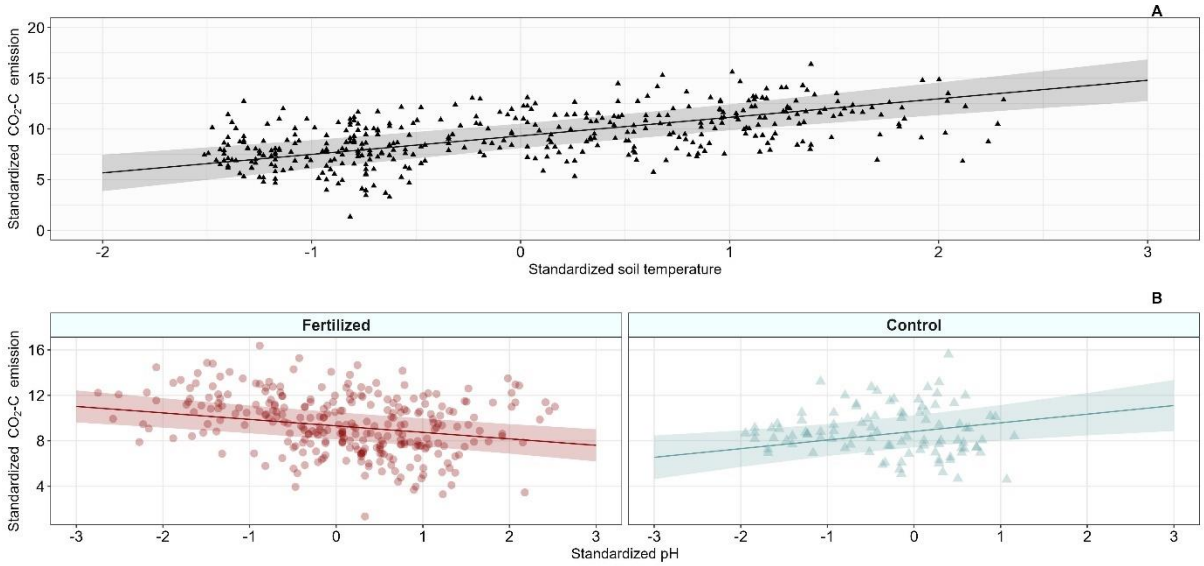

Figure 4.7: Predictions from the minimum adequate model explaining CO_2 fluxes with 95% confidence intervals. Panel A shows the soil temperature effect on CO_2 fluxes, while panel B exhibits the interactions between fertilization and pH.

The selected model for N_2O emissions involved four-day cumulative irrigation and soil temperature as fixed effects, both showing significant positive effects on soil fluxes (Figure 4.8 and Table 4.4). The model described 52% of the variability in N_2O fluxes, with fixed effects accounting for 16.7%.

The minimum adequate model for environmental drivers and soil CH_4 fluxes explained 21.2% of the total variance, with fertilization as the only fixed effect accounting for 5%.

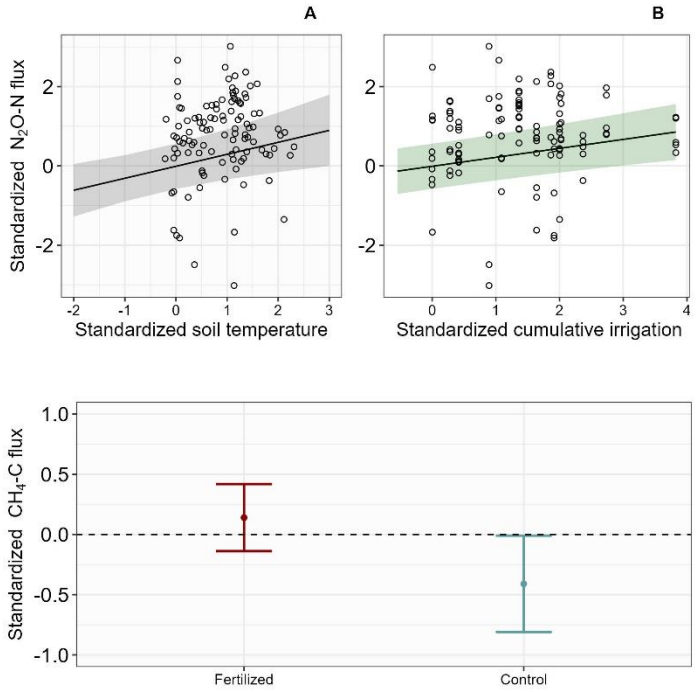

Figure 4.8: predictions from the selected models explaining N_2O and CH_4 fluxes with 95% confidence intervals. Panel A indicate the relationship between N_2O fluxes and soil temperature, whereas panel B the interaction between cumulative irrigation (4 days) and N_2O fluxes response. Panel C highlights the different model outcome for CH_4 fluxes according to fertilized (red) and unfertilized (blue) conditions.

The significant negative coefficient (-0.56) of control conditions is associated with CH_4 soil consumption (Figure 4.8C, Table 4.4).

Table 4.4: Summary of the linear mixed-effects models for CO_2, N_2O, and CH_4 emissions. R^2_m is the variance explained by the fixed effects (marginal) and R^2_c is the variance explained by the entire model, including both fixed and random effects.

CO_2	**Variables**	**Estimate (SE)**	**p-value**
R^2_m: 0.435	(intercept)	9.31 (0.61)	**<0.001**
R^2_c: 0.730	Fertilization [untreated]	-0.49 (0.50)	0.328
	pH	-0.57 (0.12)	**<0.001**
	Soil type [Sandy Loam]	0.59 (0.42)	0.165
	Stemp	1.82 (0.30)	**< 0.001**
	Fertilization*pH[untreated]	1.33 (0.28)	**<0.001**
N_2O	**Variables**	**Estimate (SE)**	**p-value**
R^2_m: 0.167	(intercept)	-0.01 (0.29)	0.976
R^2_c: 0.518	Irr4	0.23 (0.05)	**<0.001**
	Tsoil	0.30 (0.10)	**0.005**
CH_4	**Variables**	**Estimate (SE)**	**p-value**
R^2_m: 0.053	(intercept)	0.14 (0.14)	0.324
R^2_c: 0.212	Fertilization [untreated]	-0.56 (0.21)	**0.008**

4.3.4 Global warming potential and Net CO_2 uptake

Fertilized conditions resulted in the highest Total GWP among all treatments, with values of 10 and 9.5 t ha^{-1} CO_2-eqv in sandy loam and loamy soil, respectively (Figure 9A). Control exhibited lower yet significant GWP, with CO_2-eqv values of 6.6 and 6.4 t ha^{-1} for sandy loam and loamy soils, respectively. Fertilized application, thus, increased GWP by 34% in sandy loam soil and 32% in loamy soils compared to controls. GWP observed for Intermediate treatment was 11% and 10% greater on sandy loam and loamy soils, respectively, than the controls. Figure 9A also depicts tree growth responses across soil types and treatments, through Gross CO_2 Uptake (GCU). Under fertilizer conditions, GCU values resulted in 3 and 2.1 t ha^{-1} of CO_2 in sandy loam and loamy soils, respectively. Conversely, in the Control treatment, NCU values were 813 and 516 kg ha^{-1} of CO_2 for loamy and sandy loam soil respectively. This represents an 82% and 62% reduction in tree growth for sandy loam and loamy soils, respectively, compared to the Fertilized treatment. Figure 9B shows net GWP (defined as Gross GWP minus the tree C offset potential given by the GCU), for

different soil types and treatments. Under fertilized conditions, net GWP values were 7 and 7.3 t ha^{-1} CO_2-eqv, with tree C offset potentials of 30% and 22.7% for sandy loam and loamy soils, respectively. In the Control treatment, net GWP values were, 6 and 5.6 t ha^{-1} CO_2-eqv, with tree C offset potential of 8.9% and 12.6% for sandy loam and loamy soils, respectively. The Intermediate treatment exhibited the lowest net GWP values, at 4.5 and 5 t ha^{-1} CO_2-eqv, along with the highest tree C offset potential at 40% and 30%, respectively, for sandy loam and loamy soils.

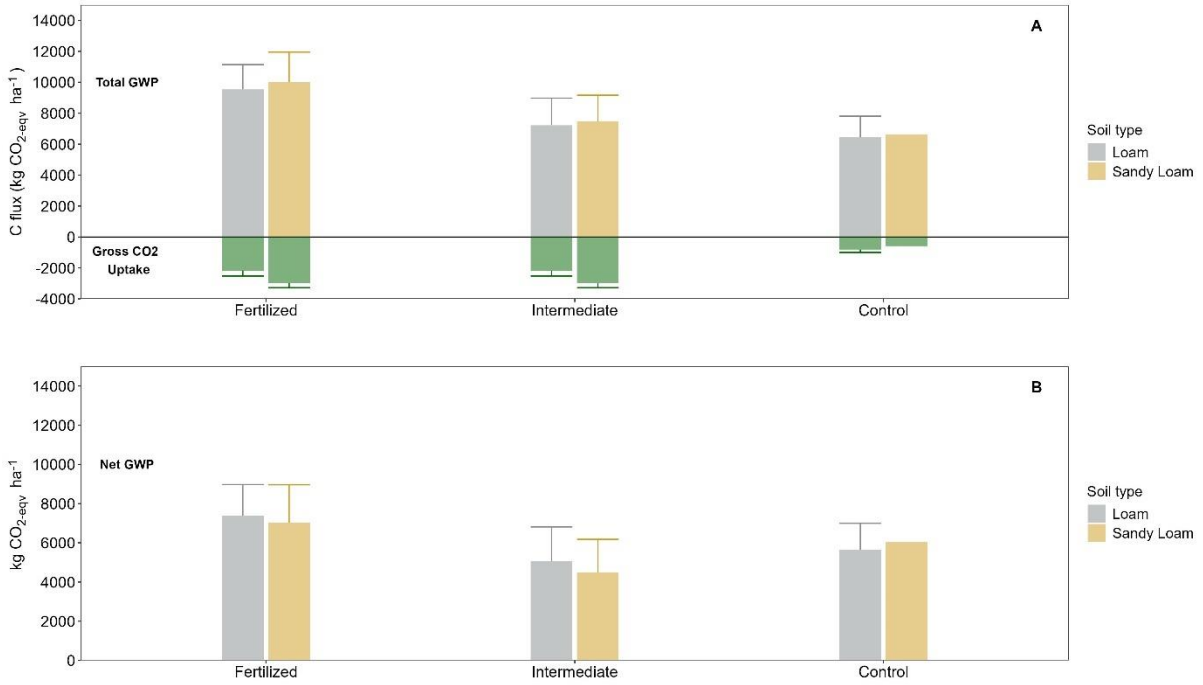

Figure 4.9: Global warming potential (GWP) and Gross CO_2 uptake (GCU) in Loam (grey) and Sandy Loam (brown) soils for three different treatments: Fertilized, Intermediate, and Control. Panel A illustrates the Total GWP calculated in kg CO_2-eqv ha^{-1} for both soil types compared to the respective GCU (green) in kg ha^{-1} for the three treatments, with error bars indicating the standard errors of the mean (SEM). Panel B depicts the net GWP in kg CO_2-eqv ha^{-1} with errors bars representing the standard error of the mean (SEM).

4.4 Discussion

4.4.1 Effect of N fertilization on soil respiration.

Continuous N fertilizer application increased CO_2 fluxes in both loamy and sandy loam soils (Figure 4.3). The results from LMMs highlight a positive interaction between the application of fertilizer and soil acidification (Table 4.4). An effect of N-fertilizer is to decrease soil C:N ratio which fosters microbial growth and organic matter degradation, which in turn, enhances soil heterotrophic respiration (Rh). Additionally, N fertilization enhanced gross system productivity, likely stimulating autotrophic respiration (Ra). Higher vegetation growth under fertilized conditions leads to more fine root production, and thus, an increase in resource acquisition efficiency (Grime et al, 1994; Cleveland et al., 2006), and high respiration rates. The accelerated turnover of fine roots biomass due to fertilizer application may stimulate C allocation belowground (Chapin et al., 1990; Field et al., 1992), thereby increasing soil respiration by sustaining microbial, mycorrhizal, and faunal communities. Moreover, enhanced aboveground litter contributes to increasing soil carbon content through its decomposition, further stimulating Rh.

The combined application of N fertilizer and irrigation also provided the conditions for sustaining higher soil respiration. Soil moisture and soil microbial activity influences carbon dynamics and CO_2 emissions rates (Fairbairn et al., 2023; Davidson et al., 1998). This was particularly evident when a malfunction in the irrigation system in loamy soil in June 2022 resulted in a significant decline in soil respiration, reaching levels even lower than those observed in the control (Figure 4.3A). In contrast, in sandy loam soil (Figure 4.3C), where irrigation was never interrupted, CO_2 fluxes in fertilized treatments consistently exceeded those of the control throughout the entire fertilizer application period.

Soil texture plays a crucial role in the carbon dynamics by influencing the interplay between microbial activity, nutrient availability, water retention, and plant growth (Li et

al., 2020; Dilustro et al., 2005). Sandy loam plots, characterized by their coarse texture (Table 1), ensure macroporosity and foster oxidizing environment. In addition, the low clay and organic matter content may reduce soil organic carbon (SOC) stabilization against microbial degradation (Reichenbach et al., 2021). This aligns with PCA patterns (Figure 4.6D), where fertilized sandy loam soil separation was driven by higher DOC, DN, NO_3^-, and NH_4^+ concentrations compared to the control. This highlights the direct effect of N application on increasing microbial activity, accelerating substrate degradation and CO_2 release. Prior land use practices, such as regular tilling (Abdalla et al., 2013), may exacerbate this process through soil aggregates breakdown, leading to rapid loss of C (Six et al., 2004). The rapid transition to similar-control fluxes in the sandy loam plots following irrigation cessation (Figure 4.3C) suggests limited legacy effects of fertilization on CO_2 fluxes, likely due to the inherent low capacity of sandy loam soil to retain nutrients (Zheng et al., 2021).

This highlights the importance of accounting for soil type when establishing management strategies aimed to increase carbon uptake (Amelung et al., 2020; Rodrigues et al., 2023). Loamy soil fosters biological activity due to its high nutrient retention capacity, as evidenced in Figure 4.6A, while also slowing organic matter decomposition, which results in increased carbon storage (Bear et al., 1994; Krull et al., 2003). In this context, it is noteworthy that Control and Fertilized treatments in loamy soils show significant overlap despite nitrogen fertilization (Figure 4.6C). This suggests that nutrient levels may have reached a soil saturation point, thus limiting the effects of further fertilization. Sandy loam soils, on the contrary have higher N mineralization and N supply capacity than loamy soils (Figure 4.6A). N fertilizer application may accelerate the decomposition, altering SOC dynamics and potentially influencing the equilibrium of soil carbon storage (Borges et al., 2019; Duan et al., 2023) evidencing the need of additional research in this area.

Finally, the influence of soil temperature on both soil types is evident in the CO_2 fluxes temporal pattern and cumulative emissions (Figure 4.3, Table 4.4). Between May and September 2022, the average soil temperature was 17.02 ± 3.1 ºC, which, coupled with fertilizer and irrigation, led to increased soil respiration rates as a positive

feedback of increased microbial and fine roots metabolism. During the subsequent colder period, with soil temperature averaging around 7.6 ± 1.9 ºC, CO_2 fluxes decreased by 30% in loamy soil and 50% in sandy loam soil, respectively.

4.4.2 Effect of N fertilization on soil N_2O emissions.

Irrigation increases soil moisture, influencing soil N dynamic and N_2O emissions (Table 4.4; Figure 4.8B). The high volumetric water content threshold (~35%) set for the irrigated areas may have lowered oxygen levels, facilitating denitrification (Khalil et al., 2024; Butterbach-Bahl, 2013). In fact, depending on soil properties, high moisture content can result in WFPS values greater than 60%, supporting anaerobic conditions and N_2O production by denitrifying bacteria (Khalil et al., 2024; Butterbach-Bahl, 2013).

In this context, our study found that fertilized loamy and sandy loam soils had yearly cumulative N_2O emissions of 11.03 kg ha^{-1}, and 6.06 kg ha^{-1}, respectively (Figures 4.4B, 4.4D). These emissions far exceed the estimated 1.57 kg N_2O ha^{-1} yr^{-1} for UK forest (Dalal & Allen, 2008), underlining the significant impact of irrigation and fertilization regime on our N_2O site emissions. Soil texture, organic content, soil temperature, and land use history, may also have contributed to high N_2O fluxes (Wang et al., 2021; Compton et al., 2000). The higher N_2O emissions in loamy soil are consistent with previous studies, which showed how fine-textured soils promote positive N_2O fluxes due to the occurrence of anaerobic conditions (Harrison-Kirk et al., 2013; Gu et al., 2012). The average 63.6% WFPS measured under loamy conditions during irrigation likely increased anaerobic microsites, promoting N_2O generation (Wolf et al., 2000; Schlesinger & Bernhardt, 2020). Higher soil temperatures increase microbial metabolism and soil respiration, which lowers soil O_2 enhancing N_2O emissions (Butterbach-Bahl et al., 2013; Cardoso et al., 2020), as suggested by the concurrent peaks in soil CO_2 and N_2O emissions in fertilized loamy soil (Figures 4.3A, and 4.4A). The loamy Control plot, on the other hand, had lower N_2O cumulative

emissions than the Fertilized one (Figure 4.4A). Past land use likely contributed to these emissions by causing N soil accumulation and altering the labile soil C pool fraction (Compton and Boone, 2000), resulting in an anthropogenic “legacy effect” on soil emissions (Wang et al., 2020; Abraha et al., 2018).

In sandy loam soil, annual N_2O cumulative emissions were 45% lower than in loamy soil (Figure 4.4D). The difference in cumulative N_2O emissions, despite same land management practices, is probably due to the coarser texture of the soil facilitating oxygen diffusion, thereby reducing denitrification, and limited C availability due to elevated mineralization rates (Ding et al., 2006; Mitchell et al., 2013). Additionally, higher tree growth rates (net CO_2 uptake, Figure 4.9A) were likely to lead to greater root biomass, which in turn, enhances soil aeration reducing denitrification processes (De Bernardi et al., 2021).

N_2O emissions from mineral fertilizer in agricultural soil are generally estimated for national reporting using a default emission factor (EF) of 1% based on IPCC 2006 guidelines (IPCC, 2006; De Klein et al., 2006). This EF is also used to estimate direct N_2O emissions from fertilizer in forest ecosystems (Skiba et al., 2012). In our investigation, where 180 kg ha^{-1} of N was added over 5 months, the N_2O emissions would be equivalent to 842.91 kg ha^{-1} CO_2-eqv using the default EF. However, measured CO_2-eqv emissions in loamy and sandy loam soil were higher, with 3286.9 kg ha^{-1} and 1805.9 kg ha^{-1} respectively. Thus, EF in our forest plantation ranged from 2.1% to 3.9%, depending on soil type. These EF values, similar to those found by Tian et al. (2020) for agricultural soil, are 2 – 4 times fold than those predicted by the IPCC (2006). This highlights the importance of directly measuring net N_2O emissions to accurately assess the impact of N-fertilization across different soil types, management, and environmental conditions (Oertel et al., 2016; Snyder et al., 2009).

4.4.3 Effect of N Fertilization on soil CH_4 emissions.

CH_4 fluxes can be partially explained by fertilizer application, despite most of the CH_4 flux variability remained unsolved (Table 4.4; Figure 4.8C). The general poor performance of the LMMs is also corroborated by the low CH_4 scores in the PCA analysis (Figure 4.6). This may be due to the complex influence of multiple variables on CH_4 fluxes, which is not fully captured by the LMMs. Despite the limitation of the models in accounting for CH_4 fluxes variability, evident differences in temporal trends between soil types are observable. The loamy soil exhibited CH_4 uptake capacity during the fertilization period, after which it turned into a net source of CH_4 (Figure 4.5A). Conversely, sandy loam soil consistently acted as a net emitter throughout the investigated period (Figure 4.5C).

To our knowledge, no other research studying the fertilization effect on CH_4 fluxes has illustrated such a clear transition from sink to source. Generally, N application is recognized either to diminish CH_4 uptake due to substrate competition (Fender et al., 2012; Liu et al., 2009) or to enhance CH_4 uptake due to altered activities of methanogenic and methanotrophic microbes (Venterea et al., 2005). In fertilized loamy soil, the significant rainfall beginning in October 2022 that caused WFPS to exceed 75%, contributed to net positive CH_4 emissions. The resulting anoxic conditions slowed nitrification, causing further rise in NH_4 levels (4.6C; supplementary materials 4-S9), which in turn competitively inhibited the methane monooxygenase (MMO) activity of methanotrophic bacteria (Bodelier & Laanbroek, 2004; Hütsch et al., 2001).

Conversely, fertilized sandy loam soil consistently showed positive net CH_4 emission (Figure 4.5C). This aligns with the well-established findings of prolonged application of N-based fertilizer (Mosier et al., 1996; Hütsch et al., 1998). This could be associated with changes in community composition, which may lead to a transition between NH_4^+-tolerant and ammonium-intolerant CH_4-oxidising species, as well as a relative increase in NH_4^+ oxidisers consuming CH_4 (Smith et al, 2000; Bodelier & Laanbroek, 2004). Jensen et al. (1999), demonstrated how in aerobic soil under competitive inhibition of MMOs by NH_4^+, CH_4-oxidizing bacteria can starve. This process echoes other studies indicating that the recovery of soil CH_4 oxidation capacity may require decades (Bayer et al., 2012; Jacinthe and Lal, 2006; Suwanwaree and Robertson, 2005). Furthermore,

rainfall events after October 2022 may have further increased high values of WFPS (>75%), reducing oxygen diffusion and sustaining CH_4 emissions (Figure 4.5C).

Beyond the combined effect of NH_4^+-based fertiliser application and increased methanogenic conditions, soil properties may play a crucial role in regulating CH_4 flows at the soil-atmosphere interface. Low CH_4 solubility in water limits its diffusive transport, potentially constraining emissions under high soil moisture conditions (Topp & Pattey, 1997). We suggest that this mechanism could account for the difference in magnitude in CH_4 emissions between loamy and sandy loam soil (Figure 4.5B, 4.5D), with the former able to retain more moisture, 62% on average, compared to an average of 55% in sandy loamy during the irrigation period.

4.4.4 Comparing GWP potential of soil fluxes with net vegetation CO_2 uptake.

The assessment of an afforestation project success in terms of climate mitigation action requires a thorough evaluation of the C balance, particularly in cases of intensive fertilizer management. Our study revealed that fertilization via irrigation system increased the Total Global Warming Potential (GWP) of sandy loam and loamy soils by 34% and 32%, respectively, as compared to the Control conditions (Figure 4.9A). At the same time, fertilizer application enhanced tree growth, resulting in a GCU of 3 and 2.1 t ha^{-1} of CO_2 for sandy loam and loamy soils, reflecting an 82% and 62% increase over Control conditions (Figure 4.9A). However, while fertilizer application increased GCU, the offset potential was 30% and 22.7% of the Total GWP for sandy loam and loamy soil, respectively, resulting in a positive net contribution to GHG emissions (Figure 4.9B). Considering the N_2O lifetime of about 114 years (IPCC, 2021), we should consider the long-lasting implications for climate change impacts. Although our GWP estimate was conservative by accounting only for microbial activity, adding root respiration to the overall GWP calculation (supplementary material 4-S5) further strengthens our findings. These results demonstrate how, despite the potential of fertilizer application as a silvicultural practice to enhance wood production and

carbon sequestration (Hakansson et al., 2021; Bergh et al., 2020), its application during early stages of afforestation on former agricultural land may undermine those intended objectives.

4.5 Conclusion

This work highlights the potential challenges associated with the coupled management of N-fertilization and irrigation during an afforestation project in two different soil types: sandy loam and loamy. The application of 180 kg ha^{-1} of N via an irrigation system to enhance wood production and C sequestration resulted in an overall significant increase in CO_2 and N_2O emissions for both soil types. CO_2 emissions were significantly influenced by fertilizer application, while N_2O were positively associated with the irrigation regime. The estimated N_2O emission factors (EF) (3.9% and 2.1% for loamy and sandy loamy soils, respectively) were much higher than those estimated by the IPCC (2006) for agricultural soil. Furthermore, both soil types exhibited net CH_4 fluxes, albeit with distinct temporal patterns and magnitudes. While soils from afforested sites are usually considered CH_4 sinks, the coupled application of fertilizer and irrigation determined a clear shift from sink to source. In conclusion, the total GWP was significantly increased by the fertilizer application via irrigation for both sandy loam and loamy soil types, with 34% and 32% increase compared to the controls. Despite tree growth was higher under the fertilized conditions, the offset was only partial, highlighting the net positive contribution to GHG emissions. These findings underscore the potential adverse effects of coupled irrigation and fertilization, which may have higher impact on biogeochemical cycles than previously recognized. Additionally, our results demonstrate the central role of soil physical properties in controlling GHG emissions under fertilization treatments, advocating for a proper evaluation when local-to-global afforestation initiatives are designed. Furthermore, this research

emphasizes the necessity of developing tailored management practices adjusted to different soil types to mitigate adverse effects of fertilization while optimizing tree growth and enhancing ecosystem carbon sequestration capacity.

4.6 References

Abdalla, M., Osborne, B., Lanigan, G., Forristal, D., Williams, M., Smith, P. and Jones, M.B. (2013). Conservation tillage systems: a review of its consequences for greenhouse gas emissions. *Soil Use and Management*, 29, 199-209, doi:10.1111/sum.12030.

Amelung, W., Bossio, D., de Vries, W., *et al.* (2020). Towards a global-scale soil climate mitigation strategy. *Nature communication*, 11, 5427, doi:10.1038/s41467-020-18887-7.

Ameray, A., Bergeron, Y., Valeria, O., *et al.* (2021). Forest Carbon Management: A Review of Silvicultural Practices and Management Strategies Across Boreal, Temperate and Tropical Forests. *Current Forestry Reports*, 7, 245–266, doi:10.1007/s40725-021-00151-w.

Aronson, E., Helliker, B. (2010). Methane flux in non-wetland soils in response to nitrogen addition: A meta-analysis. *Ecology*, 91, 3242-3251, doi:10.1890/09-2185.1.

Balster, N.J., Marshall, J.D., (2000). Eight-years responses of light interception, effective leaf area index, and stem wood production in fertilized stands of interior

Douglas-fir (*Pseudotsuga menziesii* var. glauca). *Canadian Journal of Forest Research*, 30, 733-743, doi:10.1139/x00-002.

Barba, J., Poyatos, R. & Vargas, R. (2019). Automated measurements of greenhouse gases fluxes from tree stems and soils: magnitudes, patterns, and drivers. *Scientific Report*, 9, 4005, doi:10.1038/s41598-019-39663-8.

Barton, M.K. (2019). Package MuMIn. https://cran.r-project.org/web/packages/MuMIn/index.html.

Bayer, C., Gomes, J., Costa Beber Vieira, F., Zanatta, J. A., de Cassia Piccolo, M., Dieckov (2012). Methane emission from soil under long-term no-till cropping systems. *Soil and Tillage Research*, 124, 1-7, doi:10.1016/j.still.2012.03.006.

BCMFR, 2007. Enhancing provincial climate monitoring.

BGS, Geology of Britain viewer | British Geological Survey (BGS) (2020).

Beare, M.H., Hendrix, P.F., Cabrera, M.L. and Coleman, D.C. (1994). Aggregate-Protected and Unprotected Organic Matter Pools in Conventional- and No-Tillage Soils. *Soil Science Society of America Journal*, 58, 787-795, doi:10.2136/sssaj1994.03615995005800030021x.

Bellassen, V., Luyssaert, S. (2014). Carbon sequestration: Managing forests in uncertain times. *Nature*, 506, 153–155, doi:10.1038/506153a.

Bergh, J., Nilsson, U., Grip, H., Hedwall, P.O., Lundmark, T. (2008) Effects of frequency of fertilization on production, foliar chemistry and nutrient leaching in young Norway spruce stands in Sweden. *Silva Fennica*, 42, 13.

Wang, X., Bin-feng, S., Hong, Z., Yi-zhong, L., Fei, L. (2016). The effects of nitrogen fertilizer application on methane and nitrous oxide emission/uptake in Chinese croplands. *Journal of Integrative Agriculture*, Volume 15, Issue 2, 440-450, ISSN 2095-3119, doi:10.1016/S2095-3119(15)61063-2Cl.

Bodelier, P.L.E., Laanbroek H.J. (2004). Nitrogen as a regulatory factor of methane oxidation in soils and sediments. *FEMS Microbiology Ecology* 47, Issue 3, 265-277, doi:10.1016/S0168-6496(03)00304-0.

Börjesson, G., Nohrstedt, H.-Ö. (2000). Fast recovery of atmospheric methane consumption in a Swedish forest soil after single-shot N-fertilization. *Forest Ecology Management* 134, 6, 83-88, doi:10.1016/S0378-1127(99)00249-2.

Borges, B.M., Bordonal, R, Silveira, M.L., Coutinho, E.L.M. (2019). Short-term impacts of high levels of nitrogen fertilization on soil carbon dynamics in a tropical pasture. *Catena*, 174, 413-416, doi:10.1016/j.catena.2018.11.033.

Bowden, R.D., Wurzbacher, S.J., Washko, S.E., Wind, L., Rice, A.M., Coble, A.E., Baldauf, N., Johnson, B., Wang, J.-J., Simpson, M. and Lajtha, K. (2019). Long-term Nitrogen Addition Decreases Organic Matter Decomposition and Increases Forest Soil Carbon. *Soil Science Society of America Journal*, 83, 82-95, doi:10.2136/sssaj2018.08.0293.

Bradwell, J. (2021). Norbury Park: an estate tackling climate change, ISBN:978-1-5272-9734-0. office@harborneoffice.co.uk

Cardoso, A.S., Junqueira, J.B., Reis, R.A., Ruggieri, A.C. (2020). How do greenhouse gas emissions vary with biofertilizer type and soil temperature and soil moisture in a tropical grassland? *Pedosphere*, 30, 607-617, doi:10.1016/S1002-0160(20)60025-X.

Castro, M.S., Steudler, P.A., Melillo, J.M., *et al.* (1992). Exchange of N_2O and CH_4 between the atmosphere and soils in spruce-fir forests in the northeastern United States. *Biogeochemistry*, 18, 119-135, doi:10.1007/BF00003273.

Chapuis-Lardy, L., Wrage, N., Metay, A., Chotte, J.L., and Bernoux, M. (2007). Soils, a sink for N_2O? A review. *Global Change Biology*, 13, 1-17, doi:10.1111/j.1365-2486.2006.01280.x.

Chen C.R., Xu, Z.H., Keay, P., Zhang, S.L. (2005). Total soluble nitrogen in forest soils as determined by persulfate oxidation and by high temperature catalytic oxidation. *Australian Journal of Soil Research*, 43, 515-523, doi:10.1071/SR04132.

Chung, Y., Rabe-Hesketh, S., Dorie, V., *et al.* (2013). A Nondegenerate Penalized Likelihood Estimator for Variance Parameters in Multilevel Models. *Psychometrika*, 78, 685–709, doi:10.1007/s11336-013-9328-2.

Cleveland, C., Townsend, A.R. (2006). Nutrient additions to a tropical rain forest drive substantial soil carbon dioxide loss to the atmosphere. *PNAS* 27, 10316-10321, doi:10.173/pnas.0600989103.

Collier, S.M., Ruark, M.D., Oates, L.G., Jokela, W.E., Dell, C.J. (2014). Measurement of Greenhouse gas flux from agricultural soils using static chambers. *J.Vis.Exp.*, 90, e52110, doi:10.3791/52110.

Conrad, R. (2020). Importance of hydrogenotrophic, aceticlastic and methylotrophic methanogenesis for methane production in terrestrial, aquatic and other anoxic environments: A mini review. *Pedosphere*, 30, Issue 1, 25-39, doi:10.1016/S1002-0160(18)60052-9.

Cornwell, W.K., Weedon, J.T. (2014). Decomposition trajectories of diverse litter types: a model selection analysis. *Methods in Ecology and Evolution*, 5, 173-182, doi:10.1111/2041-210X.12138.

Dalal, R. C., Wang, W., Robertson G., Parton, P., William J. (2003). Nitrous oxide emission from Australian agricultural lands and mitigation options: a review. *Soil Research*, **41**, 165-195, doi:10.1071/SR02064.

Dilustro, J.J., Collins, B., Duncan, L., Crawford, C., (2005). Moisture and soil texture effects on soil CO_2 efflux component in southeastern mixed pine forests. *Forest Ecology and Management*, 204, 87-97, doi: 10.1016/j.foreco.2004.09.001.

Dobbie, K.E., McTaggart, I.P., Smith, K.A. (1999). Nitrous oxide emissions from intensive agricultural systems: Variations between crops and seasons, key driving

variables, and mean emission factors. *Journal of Geophysical Research: Atmospheres*, 104, 26, 891–26,899, doi:10.1029/1999JD900378.

Duan, B., Yu, A., Zhang, H. (2023). Effect of Exogenous Nutrient Addition on Soil Organic Carbon Mineralization and Stabilization. *Agronomy*, 13, doi:10.3390/agronomy13071908.

Fender, A.C., Pfeiffer, B., Gansert, D. *et al* (2012). The inhibiting effect of nitrate fertilization on methane uptake of a temperate forest soil is influenced by labile carbon. *Biology and Fertility of soil*, 48, 621-631, doi:10.1007/s00374-011-0660-3.

Fenn, E., Poth, M.A., Aber, J.D., Baron, J.S., Bormann, B.T., Johnson, D.W., Lemly, A.D., McNulty, S.G., Ryan, D.F., Stottlemyer, R. (1998). Nitrogen excess in North American Ecosystems: predisposing factors, ecosystem responses, and management strategies. *Ecological Applications*, 8, 3, 706-733, doi:10.1890/1051-0761(1998)008[0706:NEINAE]2.0.CO;2.

Fierer, N., Schimel, J.P. (2003). A proposed mechanisms for the pulse in carbon dioxide production commonly observed following the rapid rewetting of a dry soil. *Soil Science Society of America Journal*, 67, 798-805, doi:10.2136/sssaj2003.7980.

Fierer, N., Jackson, R.B. (2006). The diversity and biogeography of soil bacterial communities. *Proceedings of the National Academy of Sciences,* 103, 626-631, doi:10.1073/pnas.0507535103.

Field, C.B., Chapin, S., Matson, P.A., Mooney, H.A. (1992). Responses of Terrestrial Ecosystems to the Changing Atmosphere: A resource-based approach. *Annual review of Ecology and Systematics*, 23, 201-235, doi:10.1146/annurev.es.23.110192.001221.

Forrester, D.I., Tachauer, I.H., Annighoefer, P., Barbeito, I., Pretzsch, H., Ruiz-Peinado, R., Stark, H., Vacchiano, G., Zlatanov, T., Chakraborty, T., Saha, S., Sileshi, G.W. (2017). Generalized biomass and leaf area allometric equations for European tree species incorporating stand structure, tree age, and climate. *Forest Ecology and Management*, 396, 160-175, doi:10.1016/j.foreco.2017.04.011.

Forster, P., Ramaswamy, V., Artaxo, P., Berntsen, T., Betts, R., Fahey, D.W., Haywood, J., Lean, J., Lowe, D.C., Myhre, G., Nganga, J., Prinn, R., Raga, G., Schulz, M., Dorland, R.V. (2007). Changes in atmospheric constituents and in radiative forcing. In: Solomon, S., Climate Change 2007: The Physical Science Basis. Contribution of Working Group I to the Fourth Assessment Report of the Intergovernmental Panel on Climate Change. Cambridge University Press, Cambridge, UK, pp. 129–234.

Fowler, D., E. Nemitz, P. Misztal, C. Di Marco, U. Skiba, J. Ryder, C. Helfter, N. Cape, S. Owen, J. Dorsey, M. W. Gallagher, M. Coyle, G. Phillips, B. Davison, B. Langford, A. R. MacKenzie, J. Muller, J. Siong, J. A. Pyle, and C. N. Hewitt, 2011. Effects of land use on trace gas emissions and deposition in Borneo: comparing atmosphere-surface exchange over oil palm plantations with a rainforest. *Phil. Trans. Roy. Soc. Lond. B*, 366, 3210-3224, doi:10.1098/rstb.2011.0055.

Frasier, R., Ullah, S., Moore, T. (2010). Nitrous oxide consumption potentials of well-drained forests soils in southern Quebec, Canada. *Geomicrobiology Journal*, 27, 53-60, doi:10.1080/01490450903232199.

Frei, T., Espelta, J.M., Górriz-Mifsud, E., *et al*. (2024). Can natural forest expansion contribute to Europe's restoration policy agenda? And interdisciplinary assessment. *Ambio*, 53, 34-45, doi:10.1007/s13280-023-01924-2.

Fuchs, R., Herold, M., Verburg, P.H., Clevers, J.G.P.W. (2013). A high-resolution and harmonized model approach for reconstructing and analysing historic land changes in Europe. *Biogeosciences*, 10, 1543-1559, doi:10.5194/bg-10-1543-2013.

Gao, W., Yang, H., Kou, L., *et al* (2015). Effects of nitrogen deposition and fertilization on N transformations in forest soils: a review. *Journal of Soils Sediments*, 15, 863-879, doi:10.1007/s11368-015-1064-z.

Griscom, B.W., Adams, J., Ellis, P.W., Houghton, R.A., Lomax, G., Miteva, D.A., Schlesinger, W.H., Schoch, D., Siikamäki, Smith, P., Woodbury, P., Zganjar, C., Blackman, A., Campari, J., Conant, R.T., Delgado C., Elias P., Gopalakrishna, T., Hamsik, M.R., Herrero, M., Kiesecker, J., Landis, E., Laestadius, L., Leavitt, S.M.,

Minnemeyer, S., Polasky, S., Potapov, P., Putz, F.E., Sanderman, J., Silvius, M., Wollenberg, E., Fargione, J. (2017). Natural Climate Solutions. *PNAS*, 114, 44, 11645-11650, doi:10.1073/pnas.1710465114.

Gundersen, P., Christiansen, J., Alberti, G., Uggeman, N., Castaldi, S., Gasche, R., Kitzler, B., Klemedtsson, L., Lobo-Do-vale, R., Moldan, F., Utting, T., Schleppi, P., Weslien, P., Zechmeister-Boltenstern, S. (2012). The response of methane and nitrous oxide fluxes to forest change in Europe. *Biogeoscience*, 9, 14, 3999–4012, doi:10.5194/bg-9-3999-2012, 2012.

Håkansoon, C., Hedwall, P.O., Strömgren, M., Axelsson, M., Bergh, J. (2021). Effects of fertilization on soil CH_4 and N_2O fluxes in young Norway spruce stands. *Forest Ecology and Management*, 499, doi:10.1016/j.foreco.2021.119610.

Harrison-Kirk, T., Beare, M.H., Meenken, E.D., Condron, L.M. (2013). Soil organic matter and texture affect responses to dry/wet cycles: Effects on carbon dioxide and nitrous oxide emissions. *Soil Biology and Biochemistry*, 57, 43-55, doi:10.1016/j.soilbio.2012.10.008.

Hart, K. M., Curioni, G., Blaen, P., Harper, N. J., Miles, P., Lewin, K. F., MacKenzie, A. R. (2019). Characteristics of free air carbon dioxide enrichment of a northern temperate mature forest. *Global Change Biology*, *26*(2), 1023-1037, doi:10.1111/gcb.14786.

He, T., Ding, W., Cheng, X. *et al*. (2024). Meta-analysis shows the impacts of ecological restoration on greenhouse gas emissions. *Nature Communication*, 15, 2668, doi:10.1038/s41467-024-46991-5.

Hedwall, P., Gong, P., Ingerslev, M., Bergh, J. (2014). Fertilization in northern forests – biological, economic, and environmental constraints and possibilities. Scandinavian Journal of Forest Research, 29:4, 301-311, doi:10.1080/02827581.2014.926096.

Houlton, B.Z., Sigman, D.M., Hedin, L.O. (2006). Isotopic evidence for large gaseous nitrogen losses from tropical rainforests. *Proc. Natl. Acad. Sci. U. S. A.*, 103, 685 8745-8750, doi:10.1073/pnas.0510185103.

Hütsch, B.W. (1998). Methane oxidation in arable soil as inhibited by ammonium, nitrite, and organic manure with respect to soil pH. *Biology and Fertility of Soils,* 28, 27-35, doi:10.1007/s003740050459.

Irland, L.C. (2011). Timber productivity Research Gaps for Extensive Forest Management. *Small-scale Forestry*, 10, 389-400, doi:10.1007/s11842-011-9155-1.

IPCC, 2006. IPCC Guidelines for national Greenhouse Gas Inventories. In: Eggleston, S., Buendia, M., Miwa, K., Ngara, T., Tanabe, K. (Eds). IPCC/OECD/IEA/IGES. Hayama, Japan.

IPCC, 2018. Global warming of 1.5˚C. An IPCC special report on the impacts of global warming of 1.5°C above pre-industrial levels and related global greenhouse gas emissions pathways, in the context of strengthening the global response to the threat of climate change, sustainable development, and efforts to eradicate poverty. World Meteorological organization.

IPCC, 2023. Summary for Policymakers. In: Climate change 2023: Synthesis Report. Contribution of Working groups I, II, and III to the Sixth Assessment Report of the Intergovernmental Panel on Climate Change [Core Writing Team, H. Lee and J. Romero (eds.)]. IPCC, Geneva, Switzerland, pp.1-34, doi:10.59327/IPCC/AR6-9789291691647.001.

IPCC, 2021: Climate Change 2021 – the Physical Science Basis. Contribution of Working Group I to the Sixth Assessment Report of the Intergovernmental Panel on Climate Change [Masson-Delmotte, V., Zhai, P., Pirani, A., Connors, S.L., Pean, C., Berger, S., Caud, N., Chen, Y., Goldfarb, L., Gomis, M.I., Huang, M., Leitzell, K., Lonnoy, E., Matthews, J.B.R., Maycock, T.K., Waterfield, T., Yelekci, O, Yu, R., and Zhou, B. (eds.)]. *Cambridge University Press*, Cambridge ,United Kingdom and New York, NY, USA, 2391 pp., doi:10.1017/9781009157896.

Jacinthe, P.A., Lal, R. (2006). Methane oxidation potential of reclaimed grassland soils as affected by management. *Soil Science*, 171, 772-783, doi:10.1097/01.ss.0000209357.53536.43.

Jassal, R.S., Black, A.T., Real, R., Ethier G. (2011). Effect of nitrogen fertilization on soil CH_4 and N_2O fluxes, and soil and bole respiration. *Geoderma*, 162, 182-186, doi:10.1016/j.geoderma.2011.02.002.

Johnson D.W., Curtis P.S. (2001). Effects of forest management on soil C and N storage: meta-analysis. *Forest Ecology and Management*, 140, Issue 2-3, 227-238, doi:10.1016/S0378-1127(00)00282-6.

Kassambara, A., Mundt, F. (2020). Factoextra: Extract and Visualize the Results of Multivariate Data Analyses. R Package Version 1.0.7, https://CRAN.R-project.org/package=factoextra

Keiluweit, M., Gee, K., Denney, A., Fendorf, S. (2018). Anoxic microsites in upland soils dominalty controlled by clay content. *Soil Biology and Biochemistry*, 118, 42-50, doi:10.1016/j.soilbio.2017.12.002.

Krull, E.S., Baldock, J.A., Skjemstad, J.O. (2003). Importance of mechanisms and processes of the stabilisation of soil organic matter for modelling carbon turnover. *Functional Plant Biology*, 30, 207-222, doi:10.1071/FP02085.

Laughlin, R., Stevens, R. (2003). Changes in Composition of Nitrogen 15-Labeled Gases during Storage in Septum-Capped Vials. *Soil Science of Society of America Journal*¸ 67, 540-543, doi:10.2136/sssaj2003.0540.

Lê, S., Josse, J., Husson, F. (2008). FactoMineR: An R Package for Multivariate Analysis. *Journal of Statistical Software*, 25, 1-18, doi:10.18637/jss.v025.i01.

LeBauer, D.S., and Treseder, K.K. (2008). Nitrogen limitation of net primary productivity in terrestrial ecosystems is globally distributed. *Ecology*, 89, 371-379, doi:10.1890/06-2057.1.

Lesmeister, L. and Koschorreck, M. (2017). A closed-chamber method to measure greenhouse gas fluxes from dry aquatic sediments. *Atmospheric Measurement Techniques*, 10, 2377–2382, doi:10.5194/amt-10-2377-2017.

Le Mer, J., Roger, P. (2001). Production, oxidation, emission and consumption of methane by soils: A review. *European Journal of Soil Biology*, Volume 37, Issue 1, 25-50, doi:10.1016/S1164-5563(01)01067-6.

Le Noë, J., Erb, K.H., Matej, S., *et al.* (2021). Altered growth conditions more than reforestation counteracted forest biomass carbon emissions 1990–2020. *Nature Communication*, 12, doi:10.1038/s41467-021-26398-2.

Li, H., Van de Bulcke, J., Wang, X., Gebremikael, M.T., Hagan, J., De Neve, S., Sleutel, S. (2020). Soil texture strongly controls exogenous organic matter mineralization indirectly via moisture upon progressive drying – Evidence from incubation experiments. *Soil Biology and Biochemistry*, 151, doi:10.1016/j.soilbio.2020.108051.

Liu, L., Greaver, T.L. (2009). A review of nitrogen enrichment effects on three biogenic GHGs: the CO_2 sink may be largely offset by stimulated N_2O and CH_4 emission. *Ecology Letters*, 12, 15, doi:10.1111/j.1461-0248.2009.01351.x.

Lüdecke, D. (2018). Ggeffects: Tidy Data Frames of Marginal Effects from Regression Models. *Journal of Open-Source Software*, 3(26), 772, doi:10.21105/joss.00772.

Lüdecke, D. (2023). *sjPlot: Data Visualization for Statistics in Social Science*. R package version 2.8.15, https://CRAN.R-project.org/package=sjPlot

Lundmark, T., Bergh, J., Hofer, P., Lundström, A., Nordin, A., Poudel, B.C., Sathre, R., Taverna, R., Werner, F. (2014). Potential Roles of Swedish Forestry in the Context of Climate Change Mitigation. *Forest*, 22, 5(4), 557- 578, doi:10.3390/f5040557.

MacKenzie, A.R., Krause, S., Hart, K.M., Thomas, R.M., Blaen, P.J., Hamilton, R.L., Curioni, G., Quick, S.E., Kourmouli, A., Hannah, D.M., Comer-Warner, S.A., Brekenfeld, N., Ullah, S., Press, M.C (2021). Water-soil-vegetation-atmosphere research in a temperate deciduous forest catchment, including under elevated CO_2. *Hydrological Processes*, 35:e14096, doi:10.1002/hyp.14096.

MAGIC, Multi-Agency Geographic Information from the Countryside (2008). Dataset and information and download facility https://magic.defra.gov.uk/MagicMap.aspx. Accessed 16 April 2024.

McKinley, D.C., Ryan, M.G., Birdsey, R.A., Giardina, C.P., Harmon, M.E., Heath, L.S., Houghton, R.A., Jackson, R.B., Morrison, J.F., Murray, B.C., Pataki, D.E. and Skog, K.E. (2011), A synthesis of current knowledge on forests and carbon storage in the United States. *Ecological Applications*, 21, 1902-1924, doi:10.1890/10-0697.1.

McMahon, S.M., Parker, G.G., and Miller, D.R. (2010). Evidence for a recent increase in forest growth. *Proceedings of the National Academy of Sciences*, 107(8), 3611-3615, doi:10.1073/pnas.0912376107.

Mitchell, D.C., Castellano, M.J., Sawyer, J.E., Pantoja, J. (2013). Cover crop effects on Nitrous oxide emissions: Role of Mineralizable Carbon. *Soil Science Society of America Journal*, 77, 1765-1773, doi:10.2136/sssaj2013.02.0074.

Mokany, K., Raison, R.J., Prokushkin, A.S. (2006). Critical analysis of root:shoot ratios in terrestrial biomes. *Global Change Biology* 12, 84-96, doi:10.1111/j.1365-2486.2005.001043.x.

Moulin, A., Glenn, A., Tenuta, M., Lobb, D.A., Dunmola, A.S., Yapa, P. (2014). Alternative transformations of nitrous oxide soil flux data to normal distributions. *Canada Journal of Soil Science*, 94, 105-108, doi:10.4141/cjss2013-008.

Nakagawa, S., and Schielzeth, H. (2013). A general and simple method for obtaining R^2 from generalized linear-mixed-effects models. *Methods in Ecology and Evolution*, 4(2), 133-142, doi:10.1111/j.2041-210x.2012.00261.x.

Nohrstedt, H, Ö. (2001). Response of Coniferous Forest Ecosystems on Mineral Soils to Nutrient Additions: A Review of Swedish Experiences. *Scandinavian Journal Forest Research*, 16, 20.

Oertel, C., Matschullat, J., Zurba, K., Zimmermann, F., Erasmi, S. (2016). Greenhouse gas emissions from soils – A review. *Geochemistry,* 76, 3, 327-352, doi:10.1016/j.chemer.2016.04.002.

Palmer, L. (2021). How trees and forests reduce risks from climate change. *Natural Climate Change* 11, 374-377, doi:10.1038/s41558-021-01041-6.

Papen, H., Daum, H., Steinkamp, R., Butterbach-Bahl, K. (2001). N_2O and CH_4-fluxes from soils of a N-limited and N-fertilized spruce forest ecosystem of the temperate zone. *Journal of Applied Botany*, *75*, 159-16.

Petterson, F., Högbom, L. (2004). Long-term growth effects following forest nitrogen fertilization in *Pinus sylvestris* and *Picea abies* stands in Sweden. *Scandinavian Journal Forest Research*, 19, 339-447, doi:10.1080/02827580410030136.

Poudel, B.C., Sathre, R., Bergh, J., Gustavsson, L., Lundström, A., and Hyvönen, R. (2012). Potential effects of intensive forestry on biomass production and total carbon balance in north-central Sweden. *Environmental Science & Policy*, 15(1), 106-124, doi:10.1016/j.envsci.2011.09.005.

Reichenbach, M., Fiener, P., Garland, G., Griepentrog, M., Six, J., and Doetterl, S. (2021). The role of geochemistry in organic carbon stabilization against microbial decomposition in tropical rainforest soils. *SOIL*, 7, 453–475, doi:10.5194/soil-7-453-2021.

Rodrigues, C.I.D., Brito, L.M., Nunes, L.J.R. (2023). Soil Carbon Sequestration in the Context of Climate Change Mitigation: A Review. *Soil Systems*, *7*, 64, doi:10.3390/soilsystems7030064.

Rowe, E.C., Healey, J.R., Edwards-Jones, G., Hills, J., Howells, M., Jones, D.L. (2006). Fertilizer application during primary succession changes the structure of plant and herbivore communities. *Biological Conservation*, 13, 510-522, doi:10.1016/j.biocon.2006.02.023.

Rütting, T., Björsne, A.-K., Weslien, P., Kasimir, Å., Klemedtsson, L. (2021). Low Nitrous Oxide Emissions in a Boreal Spruce Forest Soil, Despite Long-Term Fertilization. *Frontiers in Forests and Global Change* 4, 2624-893X, doi:10.3389/ffgc.2021.710574.

Ryzak, M., Bieganoski, A. (2011). Methodological aspects for determining soil particle-size distribution using the laser diffraction method. *Pflanzenernähr*, Bodenk. 174, 624-633, doi:10.1002/jpln.201000255=.

Sahrawat, K.L. (2008). Factors Affecting Nitrification in Soils. Communications in Soil Science and Plant Analysis, 39, 9-10, 1436-1446, doi:10.1080/00103620802004235.

Schlesinger, W.H., Bernhardt, E.S. (2000). Biogeochemistry: an analysis of global change. Fourth edition. London, UK, Academic Press.

Sgouridis, F., Ullah, S. (2015). Relative Magnitude and Controls of in Situ N_2 and N_2O fluxes due to denitrification in natural and seminatural terrestrial ecosystems using (15)N tracers. *Environmental Science Technology*, 14, 49(24), 14110-9, doi:10.1021/acs.est.5b03513.

Six, J., Ogle, S.M., Breidt, F.J., Conant, R.T., Mosier, A.R., Paustian, K. (2004). The potential to mitigate global warming with no-tillage management is only realized when practices in the long term. *Global Change Biology*, 10, 155-160, doi:10.1111/j.1529-8817.2003.00730.x.

Skiba, U., Jones, S.K., Dragosits, U., Drewer, J., Fowler, D., Rees, R.M., Pappa, V.A., Cardenas, L., Chadwick, D., Yamulki, S., Manning A.J. (2012). UK emissions of the greenhouse gas nitrous oxide. *Philosophical Transactions of the Royal Society B.*, 367, 1175-1185, doi:10.1098/rstb.2011.0356.

Shrestha, R.K., Strahm, B.D. & Sucre, E.B. (2015). Greenhouse gas emissions in response to nitrogen fertilization in managed forest ecosystems. *New Forests* 46, 167–193, doi:10.1007/s11056-014-9454-4.

Siljanen, H.M., Welti, N., Voigt, C. *et al* (2020). Atmospheric impact of nitrous oxide uptake by boreal forest soils can be comparable to that of methane uptake. *Plant Soil*, 454, 121–138, doi:10.1007/s11104-020-04638-6.

Smith, K.A., Dobbie, K.E., Ball, B.C., Bakken, L.R., Sitaula, B.K., Hansen, S., Brumme, R., Borken, W., Christensen, S., Priemé, A., Fowler, D., Macdonald, J.A., Skiba, U., Klemedtsson, L., Kasimir-Klemedtsson, A., Degórska, A. and Orlanski, P. (2000), Oxidation of atmospheric methane in Northern European soils, comparison with other ecosystems, and uncertainties in the global terrestrial sink. Global Change Biology, 6, 791-803, doi:10.146/j.1365-2486.2000.00356.x.

Snyder, C.S., Bruulsema, T.W., Jensen, T.L., Fixen, P.E. (2009). Review of greenhouse gas emissions.

Soil Science Division Staff (2017). Soil survey manual. USDA Handbook 18. Government Printing Office, Washington, D.C.

Suwanwaree, P. and Robertson, G.P. (2005). Methane Oxidation in Forest, Successional, and No-till Agricultural Ecosystems. *Soil Science Society of America Journal*., 69, 1722-1729, doi:10.2136/sssaj2004.0223.

Tamm, C.O. (1991). Nitrogen in Terrestrial Ecosystems: Question of Productivity, Vegetational Changes and Ecosystem Stability. Springer-Verlag, Berlin.

Topp, E., Patty, E. (1997). Soils as sources and sinks for atmospheric methane. *Canadian Journal of Soil Science*, 77, 167-177, doi:10.4141/S96-107.

Ontl, T.A., Janowiak, M.K., Swanston, C.W., Daley, J., Handler, S., Cornett, M., Hagenbuch, S., Handrick, C., Mccarthy L., Patch N. (2020). Forest Management for Carbon Sequestration and Climate Adaptation. *Journal of Forestry*, Volume 118, Issue 1, 86-101, doi:10.1093/jofore/fvz062.

Ullah, S., Frasier R., King, L., Picotte-Anderson, N., Moore, T.R. (2008). Potential fluxes of N_2O and CH_4 from soils of three forest types in Eastern Canada. *Soil Biology and Biochemistry*, 40, 986-994, doi:10.106/j.soilbio.2007.11.019

Ullah, S., Frasier, R., Pelletier, L., Moore, T.R. (2009). Greenhouse gas fluxes from boreal forest soils during the snow-free period in Quebec, Canada. *Canadian Journal of Forest Research*, 39(3), 666-680, doi:10.1139/X08-209.

Ullah, S., & Moore, T. R. (2011). Biogeochemical controls on methane, nitrous oxide, and carbon dioxide fluxes from deciduous forest soils in eastern Canada. *Journal of Geophysical Research*, 116, G03010, doi:10.1029/2010jg001525.

Venterea, R.T., Burger, M., Spokas, K.A. (2005). Nitrogen oxide and methane emissions under varying tillage and fertilizer management. *Journal of Environmental Quality*, 9, 34(5), 1467-77, doi:10.2134/jeq2005.0018.

Wang, R., Sun, Q., Wang, Y., Liu, Q., Du, L., Zhao, M., Gao, X., Hu, Y., Guo, S. (2016). Temperature sensitivity of soil respiration: Synthetic effects of nitrogen and phosphorous fertilization on Chinese Loess Plateau. *Science of Total Environment*, 574, 1665-1673, doi:10.1016/j.scitotenv.2016.09.001.

Wang, C., Amon, B., Schulz, K., Mehdi, B. (2021). Factors that influence Nitrous Oxide Emissions from Agricultural soils as well as their representation in simulation models: A review. *Agronomy*, 11, 770, doi:10.3390/agronomy11040770.

Wang, L., Xin, J., Nai, H., Zheng, X. (2021). Effects of different fertilizer applications on nitrogen leaching losses and the responses in soil microbial community structure. *Environmental Technology & Innovation*, 23, doi:10.1016/j.eti.2021.101608.

Wei, Z., Lin, C., Xu, C., Xiong, D., Liu, X., Chen, S., Lin, T., Yang, Y. (2022). Soil respiration in planted and naturally regenerated *Castanopis carelesii* forests during Three Years Post-Establishment. *Forests*, 13, 932, doi:10.3390/f13060931.

Yu, L., Zhang, Q., Ye, T., Wenjuan, S., Clemens, S., Tingting, L., Wen, Z. (2022). Global variations and drivers of nitrous oxide emissions from forests and grasslands. *Frontiers in Soil Science*, 16, doi:10.3389/fsoil.2022.1094177.

Zhang, X., Ward, B.B., Sigman, D.M. (2020). Global Nitrogen Cycle: Critical Enzymes, Organisms, and Processes for Nitrogen Budgets, and Dynamics. *Chemical Reviews*, 120, 12, 5308-5351, doi:10.1021/acs.chemrev.9b00613.

Zhang, J., Cavallari, J.M., Fang, S.C., Weisskopf, M.G., Lin, X., Mittleman, M.A., Christiani, D.C. (2017). Application of linear mixed-effects model with LASSO to identify metal components associated with cardiac autonomic responses among welders: a repeated measures study. *Occupational & Environmental Medicine*, 74, 810-815, doi:10.1136/oemed-2016-104067.

Zhang, W., Mo, J., Yu, G., (2008). Emissions of nitrous oxide from three tropical forests in Southern China in response to simulated nitrogen deposition. *Plant Soil*, 306, 221–236, doi:10.1007/s11104-008-9575-7.

Zheng, M., Zhu, P., Zheng, J. *et al.* (2021). Effects of soil texture and nitrogen fertilisation on soil bacterial community structure and nitrogen uptake in flue-cured tobacco. *Scientific Report*, 11, 22643, doi:10.1038/s41598-021-01957-1.

Zuur, A.F., Ieno, E.N. & Elpick, C.S. (2010). A protocol for data exploration to avoid common statistical problems. *Methods Ecology and Evolution*, 1, 3-14, doi:10.1111/j.2041-210X.2009.00001.x.

4.7 Appendix

4-S1: irrigation and fertilization scheme

The diagram below 4-S1 details the irrigation system. Agricultural run-off water is collected from a reservoir located northwest of the main experimental site, pumped through a main station, and supplemented with a commercial soluble fertilizer (NPK 18:18:18 and micronutrients). The liquid fertilizer is prepared by mixing 1 kg of

powdered fertilizer with 100 Lt of water, with a 1:10 ratio. The injection rate of the prepared liquid fertilizer is 0.08% per litre. The water is then delivered across the fertilized sites by above-ground pumps via the drip-irrigation systems, which features drip holes spaced 50 cm with a flow rate of 1 Lt/hr. For greenhouse gas (GHG) measurements, soil collars are placed beneath the drip-holes according to a W sampling strategy to capture the heterogeneity of the fertilized sites.

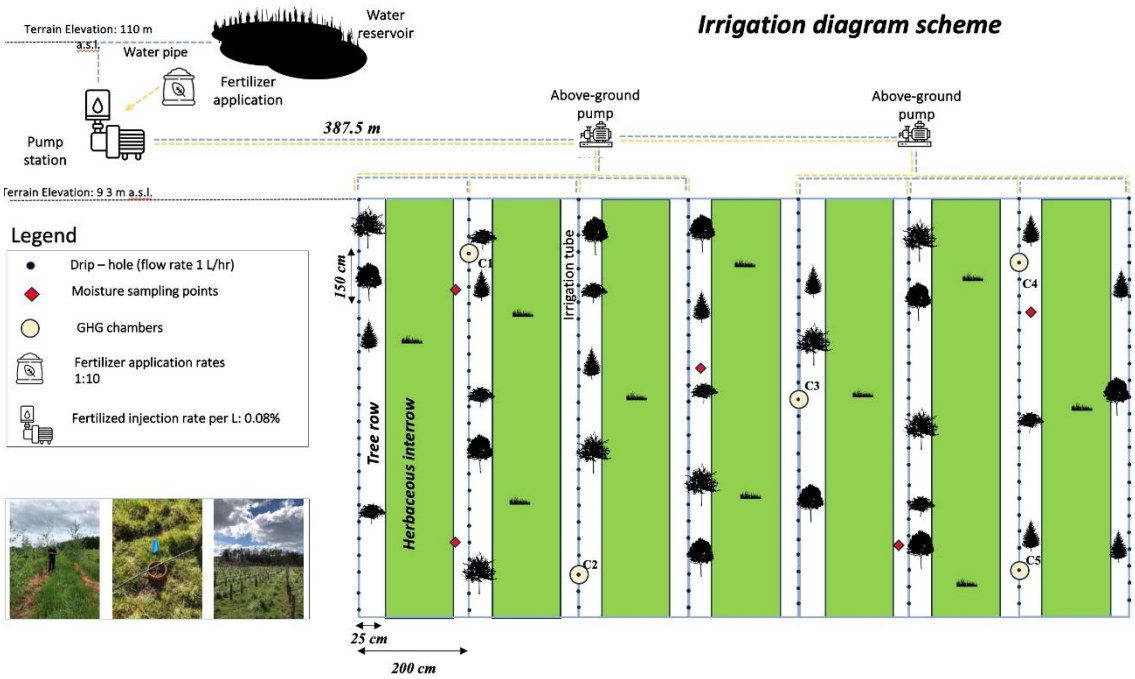

4-S2: hand-made top GHG chamber

A custom-made upper chamber section was employed to close the soil collars. It consists of a cylindrical PVC tube equipped with an internal gasket and a cover lid featured with a 5-cm plastic tube with a three-way Luer lock valve, used as sampling port. To ensure an airtight seal between the cover lid and the cylindrical PVC tube, modelling clay (Pebeo Gedeo Non-Firing Clay) was used to pack the lid in place. This sealing material was chosen for its moldability, inertness, and practicality (Lesmeister & Koschorreck, 2017). The average volume of the chambers was 4.2 L, and the average volume-to-area ratio of the chamber was 14 cm. The chambers were covered

with reflective foil to reduce temperature increases within the chamber headspaces during the incubation period (Ullah & Moore, 2011).

4-S3: GHG samples collection, storage, and analysis.

All gas samples were collected in 12 mL borosilicate glass vials with butyl rubber septa (Exetainer vial; Labco Ltd., High Wycombe, United Kingdom), transferred to the laboratory, and analysed within 8 weeks, assuming that no significant change in gas concentration occurred (Laughlin & Stevens, 2003). The concentrations of N_2O, CO_2, and CH_4 gases were determined using a gas chromatograph (7890A GC Agilent Technologies Ltd., Cheshire, UK) equipped with an election capture detector (ECD) and a flame ionization detector (FID). The GC was fitted with a methanizer, which converts CO_2 in the samples to CH_4 for detection by the FID.

4-S4: Data cleaning

Due to the well-known high variability of GHG emissions in space and time, all GHG flux rates were examined visually for outlier detection. Subsequently, all GHG fluxes with values falling outside the range of ± 3 standard deviations from the mean were considered outliers and excluded from the analysis. According to this procedure, CH_4 fluxes in zones SFt1, SFt2, SFt3, SCt, and LCt for 2022-10-18 were removed. CH_4 fluxes for chamber 1 in zone SFt3 on 2022-07-15 and 2023-02-27, as well as chamber SFt1 in zone SFt3 on 2022-11-15 were also removed.

4-S5: Global Warming Potential – Overall sources (Microbial and Root Respiration)

Under fertilized conditions, the aggregate Global Warming Potential (GWP) was 13.44 t ha^{-1} CO_2-eqv for sandy loam and 12.2 t ha^{-1} CO_2-eqv for loam soil (Figure 4-S5.1. A). After accounting for tree carbon offset, the net aggregate GWP decreased to 10 t ha^{-1} CO_2-eqv for loam and 10.4 t ha^{-1} CO_2-eqv for sandy loam soils, representing an offset potential of 22% and 18%, respectively (Figure 4-S5.1.B). When compared to the GWP from microbial respiration only (Figure 4.9), the aggregate GWP under fertilized conditions was 26.6% higher in loam and 32.8% higher in sandy loam. Additionally,

under intermediate conditions, GWP was 32.7% higher in loam and 37.4% higher in sandy loam, while under control conditions, GWP increased by 29.8% in loam and 28.7% in sandy loam compared to the estimated GWP for microbial respiration.

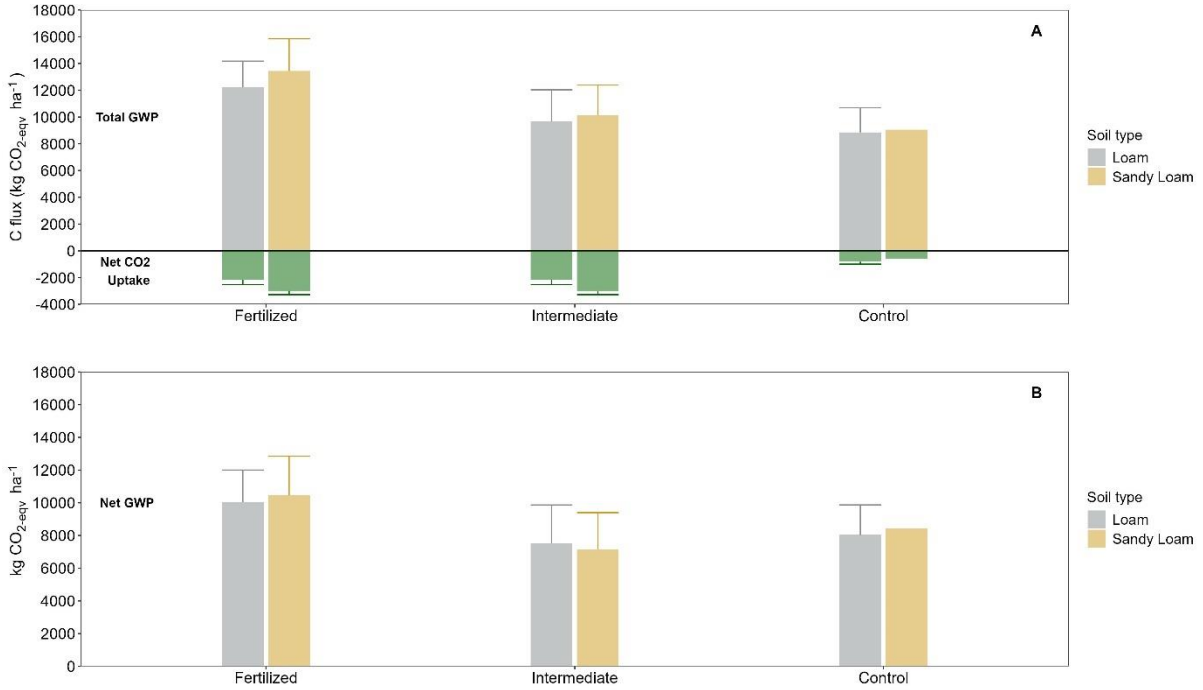

4-S5.1: Aggregate Global warming potential (GWP) and net CO_2 uptake (GCU) in Loam (grey) and Sandy Loam (brown) soils for different treatments: Fertilized, Intermediate, and Control. Panel A illustrates the GWP calculated in kg CO_2-eqv ha^{-1} for both soil types compared to the respective NCU (green) in kg ha^{-1} for the three treatments, with error bars indicating the standard errors of the mean (SEM). Panel B depicts the net GWP in kg CO_2-eqv ha^{-1} with errors bars representing the standard error of the mean (SEM).

4-S6: Soil samples methodology for $NO3^-$, $NH4^+$, DOC, DN, pH, and CEC analysis

For soil texture analysis, the initial phase involves the digestion of 1 gr of soil subsamples using a solution of 30% hydrogen peroxide (H_2O_2) followed by subsequent chemical dispersion in sodium hexametaphosphate ($(NaPO_3)_6$). Parameters for the Mastersizer 2000 were determined based on Ryzak and Bieganoswky (2011) to ensure reliable soil texture measurements. On the other hand, for chemical analyses soil samples (0-15 cm) collected monthly along the irrigation line in all plots next to each collar were transported to the laboratory, and then stored

at 6 ºC overnight. Soil samples were manually homogenised and passed through a sieve with a 2 mm mesh size. A 2 g subsample of fresh soil was then weighed into a 50 mL Falcon tube (Fisher Scientific) for analysis of K_2SO_4-extractable NO_3^- and NH_4^+ contents. After adding 10 mL of 0.5M K_2SO_4 solution to the samples (1:5 ratio), they were gently shaken for 2 hours and centrifuged at 300 rpm for 5 minutes before being filtered through a 0.45 µm PES syringe filter (Starlab LTD., UK). The filtered samples were frozen until the NO_3^- and NH_4^+ concentrations were determined using a continuous flow spectrophotometric analyzer (San++, Skalar Instruments; Breda, The Netherlands). As the mineral nitrogen concentrations were determined, a minimum of three blank samples were analysed alongside the samples to correct background influences during instrument run and limit of detection determination for the individual batch. Total organic carbon (DOC) as non-purgeable organic carbon and total dissolved nitrogen (DN) content in the 0-15 cm soil samples were assessed using a Shimadzu TOC-L analyzer (Shimadzu Corporation; Kyoto, Japan). The analysis utilised the same 0.5M K_2SO_4 soil extracts used for measuring mineral nitrogen. Before conducting measurements, these samples were diluted tenfold to minimise salt precipitation on the Pt/Al_2O_3 catalyst surface (Chen et al., 2005). Soil pH and soil cation exchange capacity (CEC) were measured in the laboratory using a 1:10 ratio of soil to deionized water. An extensive soil sampling and analysis campaign conducted in March 2022 determined the initial physico-chemical soil conditions for each zone before the fertilization and irrigation period began. The results are reported in Table 4-S6.1.

Table 4-S6.1: detailed measurements of pH, soil cation exchange capacity (CEC), extractable nitrate NO_3^--N), extractable ammonium ($NH4^+$-N), carbon and nitrogen ratio (C:N), and organic matter (OM) for each studied zone in March 2022, two months before the start of the fertilization treatment. Values are reported as means ± standard deviations.

Zone	pH	CEC (cmol/kg)	NO_3^--N (µg/gr)	NH_4^+-N (µg/gr)	C:N	OM (%)
Lft1	6.96 (± 0.30)	29.78 (± 9.32)	17.54 (± 4.30	7.58 (± 5.7	8.72 (± 1.32)	3.6 (± 0.5)
LFt2	7.02 (± 0.70)	40.13 (± 17.49)	18.36 (± 5.22)	4.81 (± 1.98)	8.94 (± 1.66)	4.3 (± 0.6)

LFt3	6.86 (± 0.22)	30.12 (± 7.90)	20.26 (± 6.91)	5.86 (± 3.13)	8.84 (± 0.9)	3.5 (± 0.4)
LCt	6.90 (± 0.34)	30.18 (± 6.21)	23.7 (± 4.25)	15.01 (± 3.35)	6.9 (± 0.70)	3.5 (± 0.6)
SFt1	6.80 (± 0.32)	24.42 (± 5.4)	9.24 (± 4.3)	3.85 (± 1.20)	9.66 (± 0.73)	2.4 (± 0.4)
SFt2	7.00 (± 0.66)	20.59 (± 5.2)	5.05 (± 1.36)	2.93 (± 1.69)	10.02 (± 1.04)	1.8 (± 0.2)
Sft3	6.91 (± 0.76)	19.25 (± 6.32)	5.08 (± 1.37)	2.64 (± 1.24)	9.29 (± 1.08)	2.1 (± 0.3)
SCt	6.57 (± 0.21)	22.06 (± 4.35)	9.07 (± 4.20)	2.80 (± 0.82)	8.5 (± 0.71)	2.2 (± 0.4)

4-S7: Linear mixed models, variables selection process

Fixed effects	Symbol	Factors
Precipitation	Pr	Climatic
Cumulative precipitation over 4 days	Pr4	Climatic
Air Temperature	TAir	Climatic
pH	pH	Edaphic
Soil Temperature	Tsoil	Edaphic
Nitrate	NO_3^-	Edaphic
Ammonia	NH_4^+	Edaphic
Carbon Nitrogen Ratio	CN	Edaphic
Dissolved Organic Carbon	DOC	Edaphic
Irrigation	Irr	Site Management
Cumulative Irrigation over 4 days	Irr4	Site Management
Fertilization	Fert	Site Management
Forest Type	Forest Type	Site Management

To address multicollinearity, we initially excluded potential predictor variables for which Pearson's correlation coefficients were greater than 0.8. Subsequently, we calculated the Variance Inflation Factor (VIF) for the remaining predictor variables, and we removed those with values greater than 2 (Zuur et al., 2010; Barba et al., 2019). Given the still high dimensionality of our dataset, we then employed the Lasso regression technique to identify the most relevant covariances. The Lasso regression applies a L1 penalty, which encourages sparsity in the model by shrinking coefficients and thereby reducing excessive complexity (Zhang et al., 2017).

4-S8: Computation and visualization of Linear mixed model results

We computed the marginal and conditional R^2 for the selected models using *r.squaredGLMM* from the *MuMIn* package (Barton, 2019). They represent the variance explained by the fixed effects and both fixed and random effects, respectively (Nakagawa & Schielzeth, 2013). Model results were printed using *tab_mode*l from the *sjPlot* package (Lüdecke, 2023), and *ggpredict* from the *ggeffects* package (Lüdecke, 2018).

4-S9: Temporal dynamics of $NH4^+$, $NO3^-$, and WFPS

As illustrated in the figure below, the application of NH_4^+-based fertilizer in October 2022, along with increased WFPS (panel A) creating anaerobic conditions, led to a decrease in the nitrification process. The resulting higher levels of NH_4^+ inhibited the activity of methane monooxygenase (MMO) driving net positive soil CH_4 fluxes.

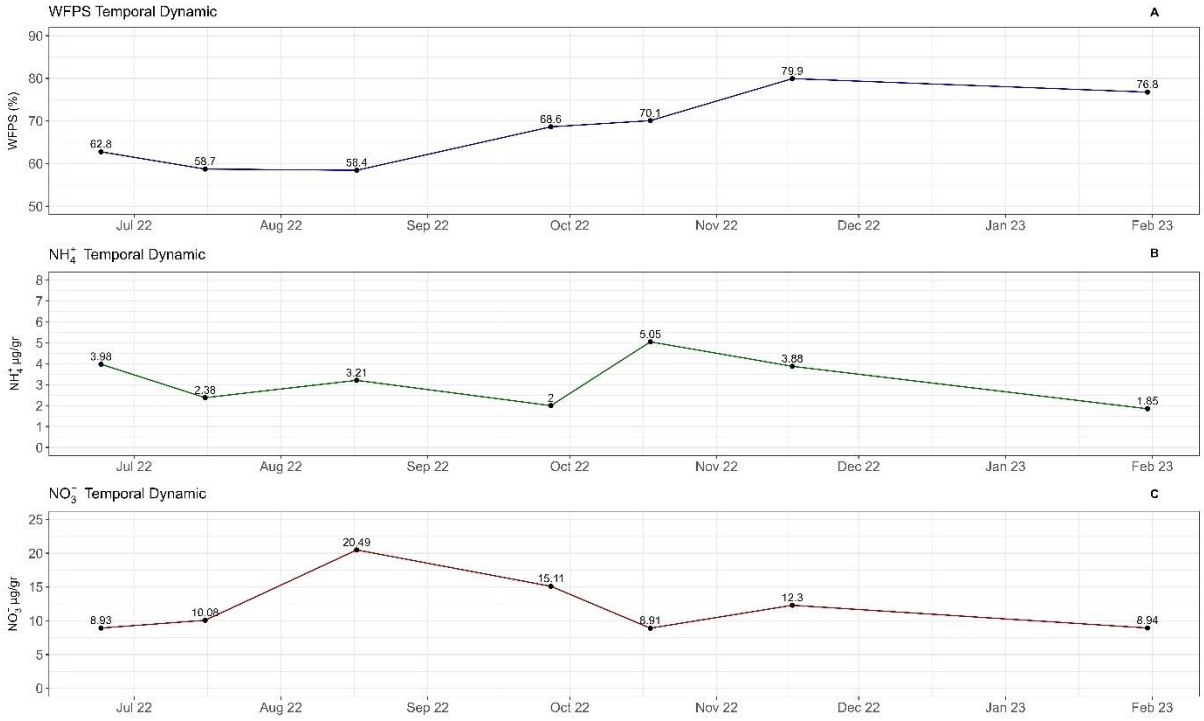

Chapter Four Summary

This chapter evaluates the greenhouse gas (GHG) emissions response to irrigation and fertilization aimed at increasing forest productivity on recently afforested agricultural land. The combined application of 180 kg ha^{-1} of N-based fertilized and irrigation results in significant alterations of carbon dioxide (CO_2), nitrous oxide (N_2O), and methane (CH_4) fluxes across sandy loam and loamy soil types. Principal component analysis was used to disentangle the relationship between GHG emissions, soil properties, and climatic conditions, while linear mixed models were employed to identify the key factors driving the increased emissions of GHGs. Fertilizer applications primarily influenced CO_2 emissions, whereas N_2O fluxes were positively linked to the irrigation regime. Remarkably, the emission factors (EF) observed in this study significantly exceeded those outlined by the IPCC guidelines for agricultural and forest lands, registering values of 3.9% and 2.1%, respectively, for sandy loam and loamy soils. Moreover, there was a clear alteration in the capacity of soils to act as CH_4 sinks, with a clear transition towards CH_4 positive fluxes. Consequently, the total Global Warming Potential (GWP) was significantly influenced by the application of fertilizer through the irrigation system, with a 34% and 32% increase compared to control zones. Despite the tree growth increase under fertilized conditions, as also evidenced in Chapter Three, the potential for offsetting emissions was only partially realized, ultimately resulting in a net positive contribution to GHG emissions. The insufficient evaluation of site and management practices played a crucial role in altering the overall carbon balance of the forest plantation systems, rendering the initiative ineffective in mitigating climate change. Further discussions are provided in Chapter Five, in which all result chapters are concluded.

Chapter Five

Conclusion and Future Perspectives

The main aim of this thesis was to enhance the understanding of managing mixed-species plantations in the face of climate change and investigate alternative silvicultural methods designed to enhance forest productivity and carbon storage while mitigating potential constraints due to abiotic factors and environmental stressors. Each presented results chapter contributed to the advancement of knowledge in particular aspects of mixed-forest plantations, showing how a comprehensive framework for their management is much needed. The research objectives focus on how a young mixed forest plantation responds to drought conditions and the effects of intensive fertilization and irrigation practices on the growth of trees and soil greenhouse gas emissions (GHG). The purpose of this chapter is to illustrate how the results chapters address these research objectives and, finally, to make recommendations for future research that will build on the findings reported in this thesis.

5.1 Research objective 1: Impact of drought on a juvenile mixed forest plantation.

The first research objective was addressed by the analysis of the change in hydrological functions of a newly planted mixed forest plantation in Chapter Two. The presented study focuses mainly on the comparison of the soil moisture dynamics between a juvenile forest plantation and a mature forest ecosystem over a period of five years. Rarely afforestation initiatives are investigated at an appropriate time scale, and this research provided the opportunity to improve our understanding of the drivers

that may influence changes in soil hydrological processes during the establishment and growth of a forest. The main results indicate that following the 2018 drought, the soil moisture dynamics in the juvenile plantation significantly changed, resembling those observed in mature forest ecosystems. This distinct transition towards a new hydrological state is probably a result of the inherent adaptive strategies of various tree species, resulting in increased physiological water demand following the drought. In this context, the drought acted as a proper “renewal event”. Viola et al. (2018) introduced this notion, aiming to explain the influence of droughts on the inter-seasonal changes of soil moisture dynamics within the Mediterranean climate. These findings hold significant implications, particularly regarding the potential impact on the successful establishment of newly planted forests in temperate regions that are unaccustomed to such conditions. Given the projected rise in frequency, duration, and intensity of droughts over the next century, as outlined by the 2018 UK climate projection (Met Office, 2018), the study highlights the urgent need for forest management strategies aimed at reducing potential adverse impacts. The additional results regarding the study of the temperature dynamics in the juvenile forest strengthened this point. The asymmetric development of ecological functions due to environmental stressors such as the drought of 2018 can gradually reduce the overall resilience of forest ecosystems, highlighting again the importance of proactive management (Keenan et al., 2015). In conclusion, Chapter Two addressed the initial research objective by analysing the diverse responses of a juvenile and mature forest to a drought event, pointing out the challenges posed by climate change and the necessity for a forward-thinking approach to forest management.

5.2 Research objective 2: Fertirrigation management of a mixed forest plantation, potential and challenges.

Chapter Three focused on the second research objective, examining how the growth and net carbon uptake capacity (GCU) of four-year-old mixed forest plantations were influenced by fertirrigation, a combined application of fertilizer and irrigation.

Fertirrigation has been proposed as a feasible method to mitigate the negative impacts of abiotic stressors like drought on forests while also promoting growth, carbon sequestration, and efficient resource utilization. However, there is currently a lack of a consistent framework for managing mixed forests using this technique. The chapter thus focused on analysing the relationship between fertirrigation, site suitability, and tree growth while also discussing the opportunities and challenges associated with this method. The positive impact of the fertirrigation on tree growth and consequent net carbon uptake (GCU) was remarkable. On the two soils tested, sandy loam and loamy, the GCU increased by 70% and 56%, respectively, compared to the controls. However, the tree growth response to fertirrigation varied across the site.

The application of the Ordinary Kriging (OK) and the Inverse Distance Weighting (IDW) techniques for mapping the spatial distribution of soil moisture allowed the identification of areas where conditions for tree planting were deemed unsuitable. The findings of this chapter revived the discussion about the importance of evaluating site suitability, which is an aspect of afforestation and reforestation initiatives often overlooked. Proper evaluation not only maximize the growth potential of diverse tree species but also ensures careful resource management (Castro et al., 2021).

Erroneous application of fertilizer and irrigation can lead to unexpected outcomes and may cause detrimental environmental effects. Depending on the fertilizer type, nitrate (NO_3^-) leaching into the groundwater, and enhanced nitrous oxide (N_2O) emission, a potent greenhouse gas, represent only a few of the possible negative effects. In conclusion, Chapter Three analyses the potential associated with intensive management of mixed forest plantations during afforestation, highlighting the critical role of proper site assessment.

5.3 Research objective 3: impact of combined irrigation and fertilizer application on soil GHG emissions.

The third research objective was addressed through the analysis of soil greenhouse gas emissions (GHG) in Chapter Four, demonstrating how the integrated approach of irrigation and fertilizer management within the mixed-plantations influenced the biogeochemical cycles. The use of nitrogen-based fertilizer may lead to altered carbon dioxide (CO_2), nitrous oxide (N_2O), and methane (CH_4) emissions, potentially compromising the beneficial trade-off associated with forest growth and the overall carbon sequestration capacity. Thus, this chapter focused on evaluating the effectiveness of an intensively managed mixed forest plantation in mitigating climate change. GHG emissions were tested across the two predominant site soil types: sandy loam and loamy. Results showed enhanced CO_2, N_2O, and CH_4 emissions for both soil types under fertilization compared to control treatments. In particular, the estimated N_2O emission factors (EF) were significantly higher than the default values suggested by the IPCC (2006) for forest and agricultural land. Additionally, the results showed that the combined application of irrigation and fertilizer led to a clear shift for both soil types from acting as CH_4 sinks to sources. As a result, intensive management had a significant impact on the Global Warming Potential (GWP) for sandy loam and loamy soil types. Despite the concurrent increase in tree growth and net carbon uptake (GCU), the potential of forest plantations to offset emissions was only partially realized, indicating a positive contribution to overall GHG emissions. In summary, the third research objective, which focused on the effect of the combined application of fertilizer and irrigation on soil biogeochemical cycles, was evaluated by monitoring GHG emissions across diverse soil conditions. The results highlight the severe environmental consequences of intensive management, particularly when previous land use and site characteristics were not thoroughly considered.

5.4 Overall conclusions

The presented three result chapters showed the challenges associated with managing mixed species plantations in a changing climate, along with the possible benefits and drawbacks derived by targeted silvicultural techniques that aim to increase the overall resilience of the forest system to biotic and abiotic disturbances. Given the crucial role of forest ecosystems, whether natural or planted, in mitigating climate change, there is a pressing need for proactive approaches that may reduce environmental pressures while enhancing productivity and carbon sequestration. Throughout all chapters, the discussion around the concept of “managing the complexity” of a mixed forest plantation emerged as an important component. For instance, Chapter Two showed the intricate response of a young mixed plantation to the effects of a prolonged drought. The strategies that the diverse tree species likely adopted to maintain adequate water and nutrient uptake resulted in a change in the general hydrological dynamics of the young mixed plantation. The marked alteration in the hydrological condition of the young mixed plantation in response to drought is unprecedented in temperate climates, as outlined within the same chapter, representing an important challenge posed by climate change (Rabbai et al., 2023). The additional study of temperature dynamics revealed an asymmetric response in terms of ecological functions, with the young mixed plantation still unable to achieve canopy closure and consequently lacking thermal buffering capacity. These factors combined may increase mixed forest plantation vulnerability, as evidenced by the tree die-off observed during the 2020 survey, which may be directly linked to water stress. Therefore, maintaining the health of forests amidst a changing climate necessitates a clear focus on strategies aimed at reducing vulnerability to increasing water stress. We need to shift our perception from perceiving forests primarily as a water source to acknowledging their need for water support (Grant et al., 2013). Hydrologic modelling reveals that specific management actions could reduce tree mortality due to drought stress (Tague and Band, 2004).

Building on this, Chapter Three investigated the potential for enhanced forest growth through the provision of combined irrigation and fertilization. This silvicultural approach, together with thinning, planting, and selecting adapted tree species, could be part of effective drought-resilience techniques while enhancing forest plantation carbon sequestration capacity. The research results indicated beneficial outcomes from this intensive management approach, with most tree species showing remarkable improved growth in a relatively short period of time. However, management strategies should be tailored to a specific site or landscape. Chapter Three, through the spatial modelling of soil moisture using the Ordinary Kriging and the Inverse Distance Weighting methodologies, pointed out the areas where tree planting would not be ideal.

The excessive waterlogging observed in these areas, likely determined by the interplay between site hydrology and soil characteristics, resulted in negative effects on successful saplings establishment and growth. This approach not only assists in optimising tree planting efforts but also facilitates targeted allocation of resources according to the latest strategies for managing forest plantations (Castro et al., 2021). Persistent application of fertilizer and irrigation in areas characterized by instability may lead to nutrient runoff, groundwater contamination, or altered biogeochemical cycles, exacerbating environmental concerns. Given these challenges, careful selection of tree species, combined with an appropriate the planting design becomes of paramount importance. Pioneer species, such as those from *Betulaceae* family, can adapt to diverse local hydrological conditions and tolerate waterlogging conditions, ensuring the establishment of more resilient forest ecosystems. The inherent ability of certain tree species to withstand challenging conditions, along with their high transpiration rates, can gradually alter the water balance (Landhäusser et al., 2003; Abaker et al., 2018). Over time, this may create improved site conditions, making it possible to introduce late-successional species through successive planting interventions. This adaptive framework not only may enhance tree survival rates optimizing long-term forest productivity but also contribute to achieve broader climate goals. Chapter Four further elaborates on the potential consequences of fertilizer and

irrigation in application at inadequately evaluated sites. Although nitrogen (N) fertilizer application is driven by policies aimed at promoting tree growth and carbon sequestration as strategies to address climate change, its incorrect use can alter the production and consumption of greenhouse gases such as carbon dioxide (CO_2), nitrous oxide (N_2O), and methane (CH_4). This becomes particularly significant when forest plantations are established on former agricultural land that might already be saturated with nitrogen from previous treatment. Findings revealed that integrated application of fertilizer and irrigation enhanced CO_2, N_2O, and CH_4 emissions across the site, resulting in a significant increase in global warming potential (GWP). Despite the observed increase in tree growth and carbon sequestration capacity in fertilized conditions, the overall offset potential of mixed forests remains only partially realized, indicating a net positive contribution to GHG emissions.

Overall, the three assessed aspects of mixed-forest plantations have increased our understanding of the potential and challenges associated with their management. Findings highlight the importance of predicting the future trajectory of newly planted forests in the face of climate change, as well as the critical need to implement sustainable management approaches.

5.5 Future perspectives

Given that this study is one of the first to highlight the impact of droughts on the hydrological processes of planted mixed forest in temperate climate, along with proposing a potential silvicultural approach to mitigate risks and improve productivity, there are numerous possible directions for future research. Firstly, Chapter Two has already demonstrated how recent droughts have left a legacy, erasing the memory of the past dynamics of soil moisture (Viola et al., 2008), leading to new hydrological conditions characterized by reduced water storage in shallow soil. This unexpectedly early transition to a distinct phase of the young mixed plantation may result in lower survival rates across trees, with consequent failure of the afforestation scheme

proposed. Thus, further discussion on potential mechanisms that young trees may adapt to survive dry stress as well as forest management methods that might be employed during these severe external perturbations is crucial. Despite measurements of tree growth across the plantation obtained by the survey in 2020 and 2021, there is still a lack of ecophysiological data that might help to explain the complex interaction between droughts, the legacy of soil hydrology, and tree growth responses. Analysis of tree rings to evaluate annual growth declines and subsequent recoveries, alongside the long-term monitoring of soil moisture, could bridge this gap in ecophysiological data (Ovenden et al., 2021; DeSoto et al., 2020). In addition to growth variations, leaf intrinsic water use efficiency (iWUE), estimated by measuring the carbon isotope composition of tree rings, may offer insights on the functional response of plants to dry stress (Baoming et al., 2015; Ripullone et al., 2004). This approach would enable a comprehensive assessment of how forest plantations, and diverse tree species have responded to the recent drought, providing valuable information for future forest design and management. Chapter Three, on the other hand, emphasize the crucial significance of site assessment in determining the efficacy of a mixed forest plantation, particularly when examining the integrated use of fertilizer and irrigation. The spatial distribution of site soil moisture was modelled using a comprehensive dataset acquired through significant and labour-intensive collection efforts. This can represent an initial step for more advanced data collection techniques involving, for instance, the use of synthetic aperture radar mounted on Unmanned Aerial *Vehicles* (UAVs), or satellite images that may offer a practical solution for soil moisture monitoring. The main challenges associated with remote sensing analysis include the depth of the measurements (Feldman et al., 2023; Kerr et al., 2010), spatial resolution, and the variability of soil moisture over time and space. The inclusion of ground soil moisture data would allow for the validation and calibration of aerial-derived estimates, improving the overall accuracy of the measurements (Babaeian et al., 2019). Moreover, since remote sensing technology targets near-surface soil moisture, integrating data from deeper soil layers would provide insights into the hydrological connection between the surface and the rootzone. Such information would serve as a valuable resource for landowners, enabling them to make well-

informed decisions regarding the design and management of plantation forests integrated into site- and landscape-scale systems. This approach would enhance the sustainability of the plantation forests by optimizing responses in suitable conditions and promoting diversification and increased biodiversity (correct tree species selection, herbal layers, pollinators, and so on) in areas where current systems have demonstrated instability or environmental harm due to intensive fertilization. Finally, results from Chapter Four, which assessed the GHG emissions resulting from the combined application of irrigation and fertilization could potentially suggest two different research lines. To completely address the influence of the impact of fertilizer application, additional study on nitrate (NO_3^-) leaching would be required. Given the high hydrological connection observed between the surface and the rootzone at the research site, further investigation into NO_3^- pathways would be essential for defining the correct management strategies. Additionally, building on the insights gained from Chapter Three regarding soil moisture pattern distribution, analysing GHG hotspots could help in identifying targeted fertilization approaches aimed at increasing wise resource use.

5.6 Final Remarks

The main purpose of this thesis was to advance our understanding of managing mixed-species forest plantations in the context of climate change while investigating silviculture tools designed to reduce vulnerability and enhance overall forest productivity and carbon storage. The main findings of the thesis highlight the challenge posed by climate change-induced drought on the success of afforestation through mixed forest plantation due to significant alteration of hydrological processes and the potential offered by irrigation and fertilization in the increased resilience and growth of the mixed-plantation forest. However, the thesis emphasizes the crucial role of proper site selection and management, as missteps in these areas could lead to unexpected outcomes such as decreased forest growth and increased greenhouse gas emissions.

Once more, the thesis stresses the urgency for a comprehensive framework for managing mixed-forest plantations, which would provide guidance to landowners towards fostering healthier, more productive, and sustainable forests.

5.7 References

Babeian, E., Sadeghi, M., Jones, S.B., Montzka, C., Vereecken, H., & Tuller, M. (2019). Ground, proximal, and satellite remote sensing of soil moisture. *Reviews of Geophysics*, 57, 530-616, doi:10.1029/2018RG000618

Baoming, D., Zheng, J., Ji, H., Zhu, Y., Yuan, J., Wen, J., Kang, H., Liu, C., (2021). Stable carbon isotope used to estimate water use efficiency can effectively indicate seasonal variation in leaf stoichiometry. *Ecological Indicators*, 121, doi:10.1016/j.ecolind.2020.107250.

Castro, J., Morales, F., Navarro, F.B., Löf, M., Vacchiano, G., Alcaraz-Segura, D., (2021). Precision restoration: a necessary approach to foster forest recovery in the 21st century. *Restoration Ecology*, 29: e13421, doi:10.1111/rec.13421.

DeSoto, L., Cailleret, M., Sterck, F. *et al.* (2020). Low growth resilience to drought is related to future mortality risk in trees. *Nature Communications*, 11, 545, doi:10.1038/s41467-020-14300-5

Feldman, A.F., Gianotti, D.J.S., Dong, J., Akbar, R., Crow, W.T., McColl, K.A., Konings, A.G., Nippert, J.B., Tumber-Dávila, S.J., Holbrook, N.M., Rockwell, F.E., Scott, R.L., Reichel, R.H., Chatterjee, A., Joiner, J., Poulter, B., Entekhabi, D., (2023). Remotely sensed soil moisture can capture dynamics relevant to plant water uptake. *Water Resources Research*, 59, e2022WR033814, doi:10.1029/2022WR033814

Grant, G.E., Tague, C.L., and Allen, C.D. (2013). Watering the forest for the trees: an emerging priority for managing water in forest landscapes. *Frontiers in Ecology and the Environment*, 11, 314-321, doi:10.1890/120209

IPCC, 2006. IPCC Guidelines for national Greenhouse Gas Inventories. In: Eggleston, S., Buendia, M., Miwa, K., Ngara, T., Tanabe, K. (Eds). IPCC/OECD/IEA/IGES. Hayama, Japan.

Keenan, R., J. (2015). Climate change impacts and adaptation in forest management: a review. *Annals of Forest Science*, 72, 145-167, doi:10.1007/s13595-014-0446-5

Kerr, Y., Waldteufel, P., Wigneron, J.-P., Delwart, S., Cabot, F., Boutin, J., et al. (2010). The SMOS mission: New tool for monitoring key elements of the global water cycle. *Proceedings of the IEEE*, 98(5), 666-687, doi:10.1109/jproc.2010.2043032.

Met Office (2018). UK Climate Projections 2018 (UKCP18). Met office. Website: https://www.metoffice.gov.uk/research/approach/collaboration/ukcp. Accessed date: 20/01/2024.

Ovenden T.S., Perks, M.P., Clarke, T-K., Mencuccini, M., Jump, A.S. (2021). Life after recovery: Increased resolution of forest resilience assessment sheds new light on post-drought compensatory growth and recovery dynamics. *Journal of Ecology*, 1099, 3157-3170, doi:10.1111/1365-2745.13576

Rabbai, A., Wendt, D.E., Curioni, G., Quick, S.E., MacKenzie, A.R., Hannah, D.M., Kettridge, N., Ullah, S., Hart, K.M., Krause, S., (2023). Soil moisture and temperature dynamics in juvenile and mature forest as a result of tree growth, hydrometeorological forcings, and drought. *Hydrological Processes*, 37(6), e14919, doi:10.1002/hyp.14919.

Ripullone, F., Lauteri, M., Grassi, G., Amato, M., Borghetti, M., 2004. Variation in nitrogen supply changes water-use efficiency of *Pseudotsuga menziesii* and *Populus x euroamericana*; a comparison of three approaches to determine water-use efficiency. *Three Physiology*, 24, 671-679, doi:10.1093/treephys/24.6.671

Tague, C.L., Band, L.E., (2004). RHESSys: Regional Hydro-Ecologic Simulation System – an object-oriented approach to spatially distributed modelling of carbon, water, and nutrient cycling. *Earth Interact*, 8, 1-42, doi:10.1175/1087-3562(2004)8<1:RRHSSO>2.0.CO;2.

Viola, F., Daly, E., Vico, G., Cannarozzo, M., Porporato A., (2008). Transient soil-moisture dynamics and climate change in Mediterranean ecosystems. *Water Resources Research*, 44, 11, doi:10.1029/2007WR006371.